# Introduction to hadronic collisions: theoretical concepts and practical tools for the LHC
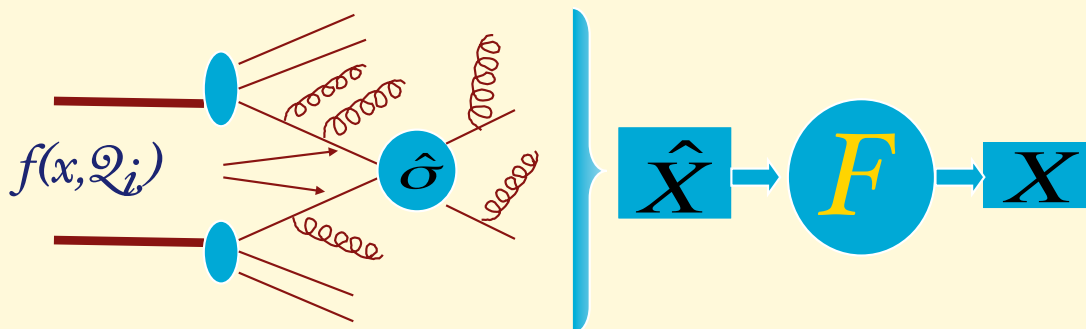
**Michelangelo L. Mangano**
TH Unit, Physics Dept, CERN
michelangelo.mangano@cern.ch

# Contents

- **Lecture I & II:** Define the framework and basic rules
  - Factorization theorem
  - Parton densities
  - Evolution of final states
  - Hard processes

- **Lecture III & IV:** Tools and applications:
  - Monte Carlo codes, virtues and limitations
  - Physics objects relevant to the search of BSM phenomena at the LHC:
    - jets
    - leptons
    - b/c-quark jets
    - W+multijets
    - top quark
  - Example: SUSY searches

# Factorization Theorem

$$\frac{d\sigma}{dX} = \sum_{j,k} \int_{\hat{X}} f_j(x_1, Q_i) \, f_k(x_2, Q_i) \, \frac{d\hat{\sigma}_{jk}(Q_i, Q_f)}{d\hat{X}} \, F(\hat{X} \to X; Q_i, Q_f)$$



$f(x, Q_i)$     $\hat{\sigma}$     $\hat{X}$ → $F$ → $X$

$f_j(x, Q)$ Parton distribution functions (PDF)

$F(\hat{X} \to X; Q_i, Q_f)$

- sum over all initial state histories leading, at the scale Q, to:

$$\vec{p}_j = x \, \vec{P}_{proton}$$

- transition from partonic final state to the hadronic observable (hadronization, fragm. function, jet definition, etc)
- Sum over all histories with $X$ in them

3
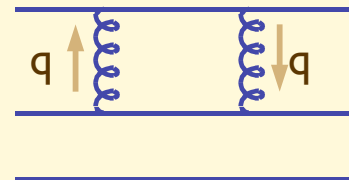
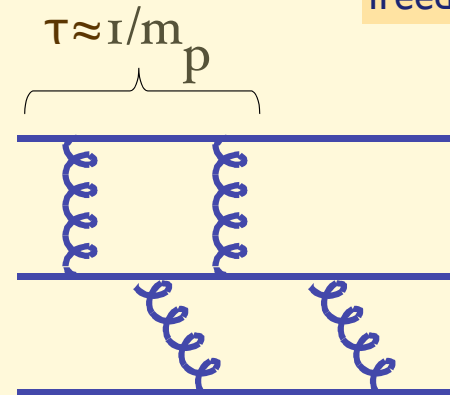# Universality of parton densities and factorization, an intuitive view

1) Exchange of **hard gluons** among quarks inside the proton is suppressed by powers of $(m_p/Q)^2$

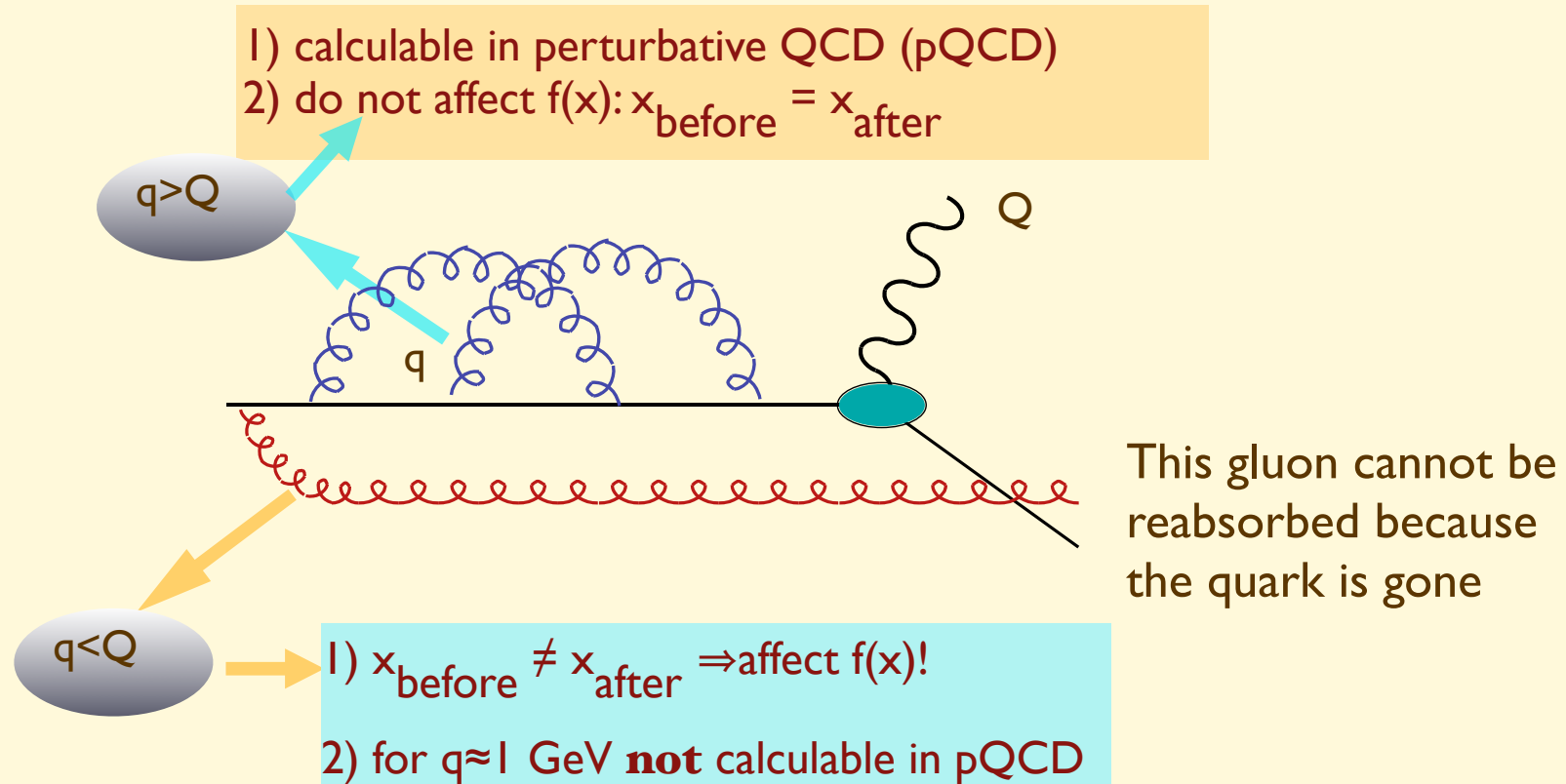$$\underset{\sim}{q>Q} \int_Q^\infty \frac{d^4q}{q^6} \sim \frac{1}{Q^2}$$

Assuming asymptotic freedom!

$\tau \approx 1/m_p$

2) **Typical time-scale of interactions binding the proton** is therefore of $O(1/m_p)$ (in a frame in which the proton has energy E, $\tau = \gamma/m_p = E/m_p^2$)

3) If a hard probe ($Q \gg m_p$) hits the proton, on a time scale $= 1/Q$, there is no time for quarks to negotiate a coherent response. The struck quark receives no feedback from its pals, and acts as a free particle

As a result, to study inclusive processes at large Q it is sufficient to consider the interactions between the external probe and a single parton:

1) calculable in perturbative QCD (pQCD)
2) do not affect f(x): $x_{before} = x_{after}$

q>Q

Q

q

This gluon cannot be reabsorbed because the quark is gone

q<Q

1) $x_{before} \neq x_{after}$ ⇒affect f(x)!

2) for q≈1 GeV **not** calculable in pQCD

However, since τ(q≈1GeV)>>1/Q, the emission of low-virtuality gluons will take place long before the hard collision, and therefore cannot depend on the detailed nature of the hard probe. While it is not calculable in pQCD, f(q<<Q) can be measured using a reference probe, and used elsewhere

➡ **Universality of f(x)**

# Q dependence of parton densities

**Q>μ**

**μ>q**

$x = y\,x_{in}$

$x = x_{in}$

$x_{in}$

$\mu$
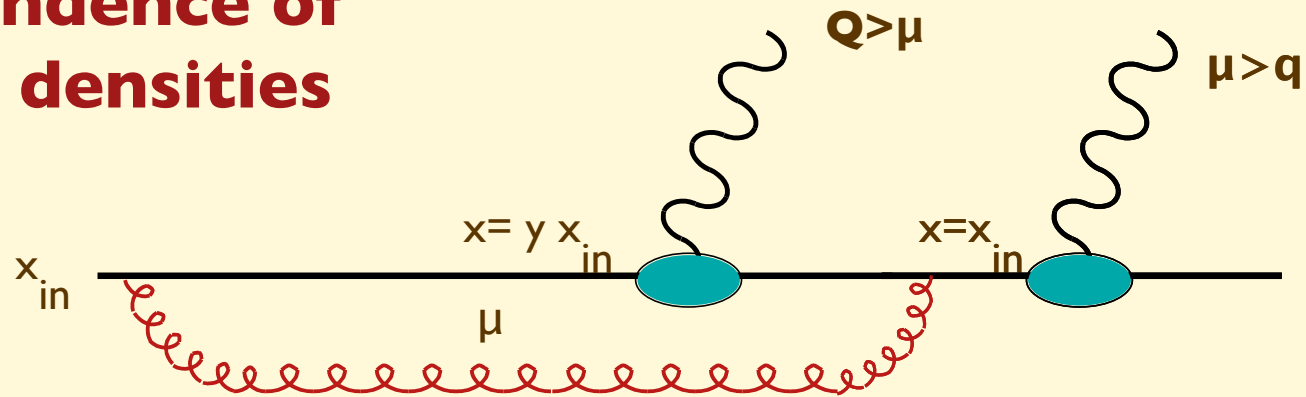
The larger is Q, the more gluons will **not** have time to be reabsorbed

**PDF's depend on Q!**

$$f(x, Q) = f(x, \mu) + \int_x^1 dx_{in}\, f(x_{in}, \mu) \int_\mu^Q dq^2 \int_0^1 dy\, P(y, q^2)\, \delta(x - y x_{in})$$

$$f(x,Q) = f(x,\mu) + \int_x^1 dx_{in}\, f(x_{in},\mu) \int_\mu^Q dq^2 \int_0^1 dy\, P(y,q^2)\, \delta(x - yx_{in})$$

f(x,Q) should be independent of the intermediate scale μ considered:

$$\frac{df(x,Q)}{d\mu^2} = 0 \quad \Rightarrow \quad \frac{df(x,\mu)}{d\mu^2} = \int_x^1 \frac{dy}{y} f(y,\mu)\, P(x/y,\mu^2)$$

One can prove that:

calculable in pQCD

$$P(x,Q^2) = \frac{\alpha_s}{2\pi} \frac{1}{Q^2} P(x)$$

and therefore (Altarelli-Parisi equation):

$$\frac{df(x,\mu)}{d\log\mu^2} = \frac{\alpha_s}{2\pi} \int_x^1 \frac{dy}{y} f(y,\mu)\, P(x/y)$$

More in general, one should consider additional processes which lead to the evolution of partons at high Q ($t=\log Q^2$):

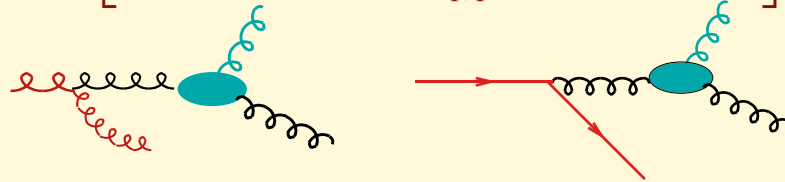$$[g(x)]_+ : \quad \int_0^1 dx\, f(x)\, g(x)_+ \equiv \int_0^1 [f(x) - f(1)]\, g(x)\, dx$$

$$\frac{dq(x,Q)}{dt} = \frac{\alpha_s}{2\pi} \int_x^1 \frac{dy}{y} \left[ q(y,Q)\, P_{qq}(\frac{x}{y}) + g(y,Q)\, P_{qg}(\frac{x}{y}) \right]$$
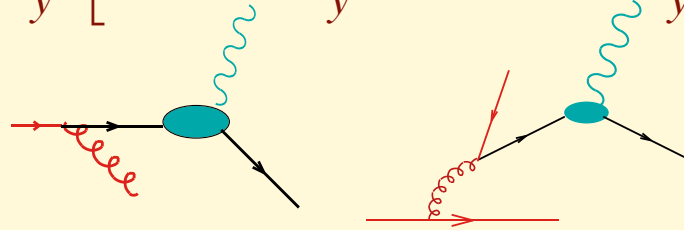


$$P_{qq}(x) = C_F \left( \frac{1+x^2}{1-x} \right)_+$$
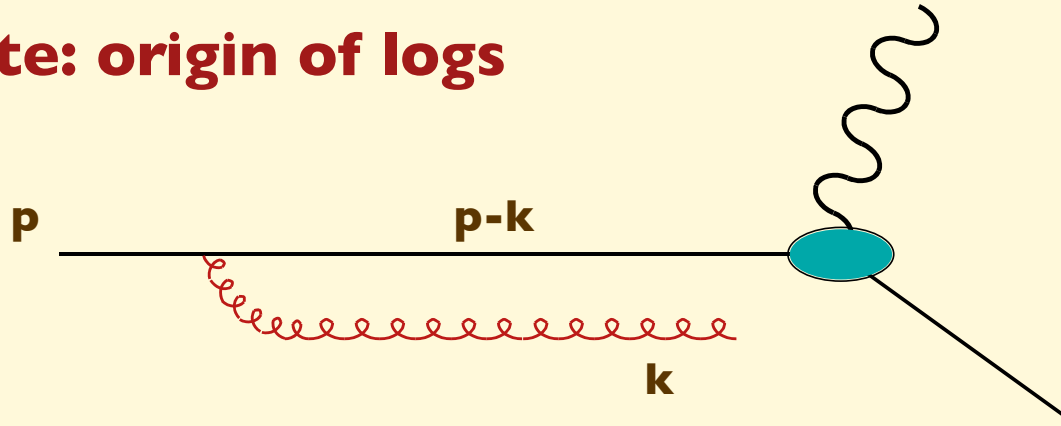
$$P_{qg}(x) = \frac{1}{2} \left[ x^2 + (1-x)^2 \right]$$

$$\frac{dg(x,Q)}{dt} = \frac{\alpha_s}{2\pi} \int_x^1 \frac{dy}{y} \left[ g(y,Q)\, P_{gg}(\frac{x}{y}) + \sum_{q,\bar{q}} q(y,Q)\, P_{gq}(\frac{x}{y}) \right]$$
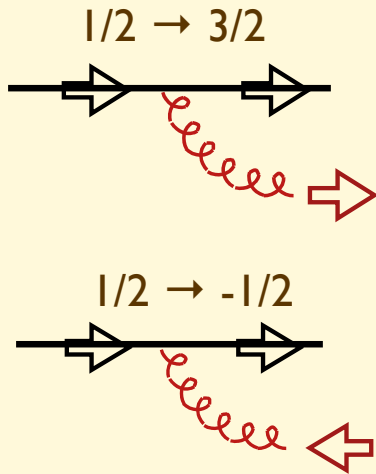


$$P_{gq}(x) = C_F \left( \frac{1+(1-x)^2}{x} \right)$$

$$P_{gg}(x) = 2N_c \left[ \frac{x}{(1-x)_+} + \frac{1-x}{x} + x(1-x) \right] + \delta(1-x) \left( \frac{11N_c - 2n_f}{6} \right)$$

# Note: origin of logs

$$(p - k)^2 = -2\,p^0 k^0 (1 - \cos\theta_{pk})$$

1/2 → 3/2

1/2 → -1/2

Helicity conservation ~ p·k

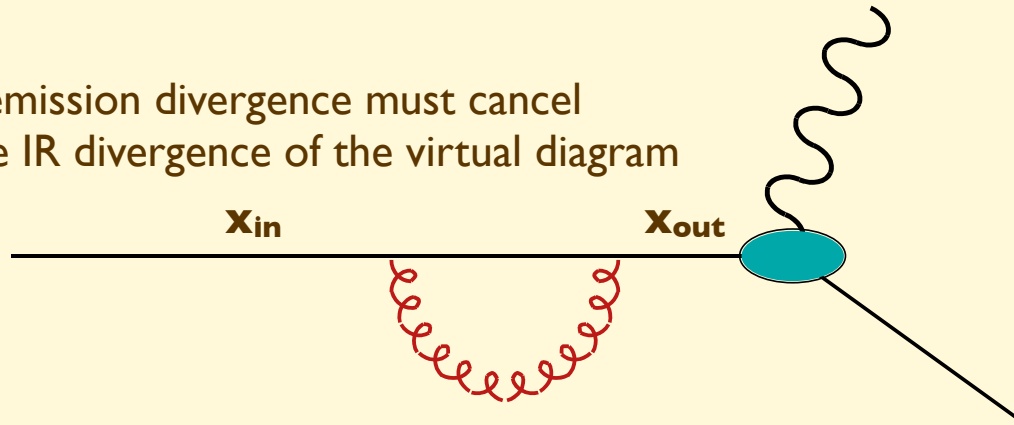$$|M|^2 \sim \left[\frac{1}{(p-k)^2}\right]^2 \qquad \rightarrow \qquad \frac{1}{p^0}\frac{dk^0}{k^0}\frac{d\theta}{\theta}$$

Soft divergence

Collinear divergence

9

Soft emission cannot lead to a physical
divergence, however, since it is not observable

$$k^0 \to 0 \Rightarrow x_{out} = x_{in}$$
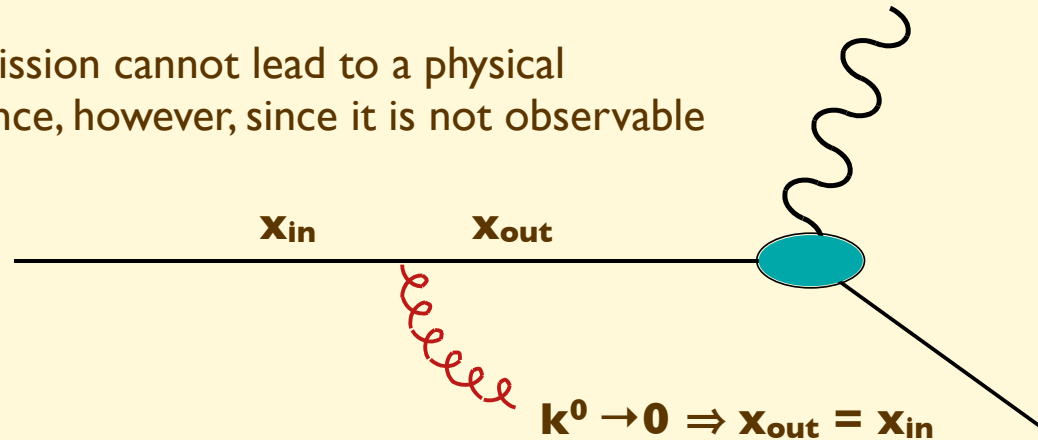
The soft-emission divergence must cancel
against the IR divergence of the virtual diagram

The cancellation cannot take place in the case of
collinear divergence, since $x_{out} \neq x_{in}$, so virtual
and real configurations are not equivalent

Things are different if $p^0 \to 0$. In this case, again, $x_{out} \neq x_{in}$, no virtual-real cancellation takes place, and an extra singularity due to the $1/p^0$ pole appears
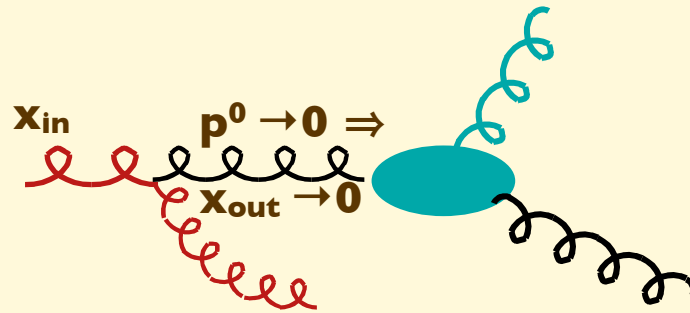


These are called **small-x** logarithms. They give rise to the double-log growth of the number of gluons at small **x** and large **Q**

# Example: charm in the proton
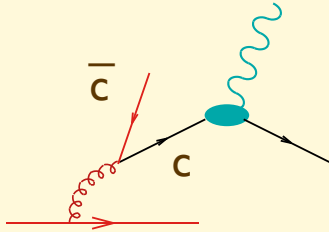
$$\frac{dc(x,Q)}{dt} = \frac{\alpha_s}{2\pi} \int_x^1 \frac{dy}{y} g(y,Q) P_{qg}(\frac{x}{y})$$

Assuming a typical behaviour of the gluon density: $g(x,Q) \sim A/x$

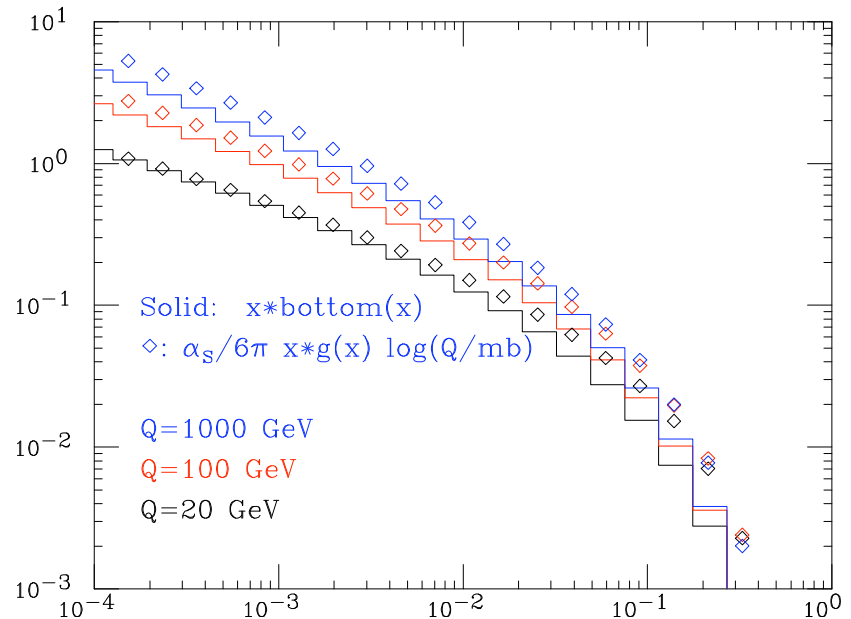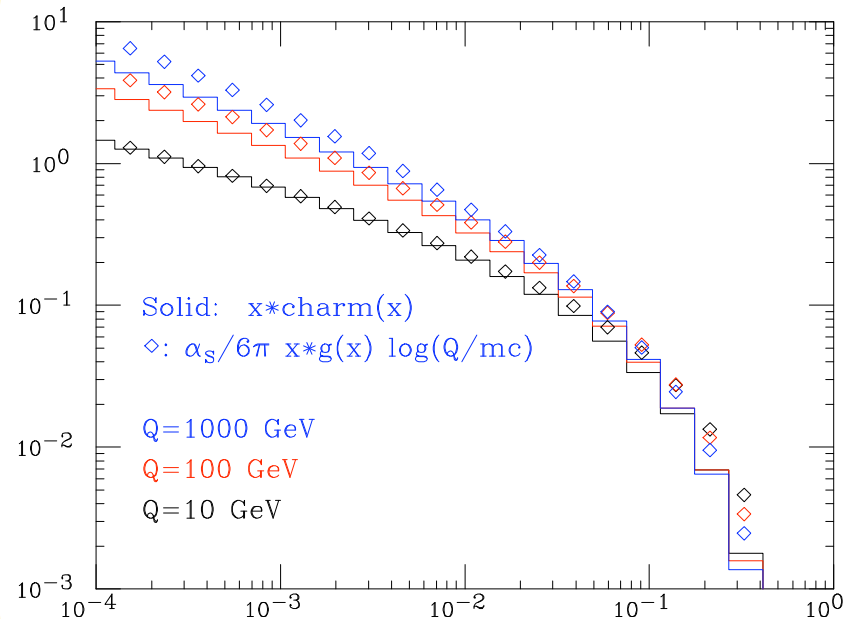and using $\quad P_{qg}(x) = \frac{1}{2}\left[x^2 + (1-x)^2\right]$ we get:

$$\frac{dc(x,Q)}{dt} = \frac{\alpha_s}{2\pi} \int_x^1 \frac{dy}{y} g(x/y,Q) P_{qg}(y) = \frac{\alpha_s}{2\pi} \int_x^1 dy \frac{A}{x} \frac{1}{2}[y^2 + (1-y)^2] = \frac{\alpha_s}{6\pi} \frac{A}{x}$$

and therefore:

$$c(x,Q) \sim \frac{\alpha_s}{6\pi} \log(\frac{Q^2}{m_c^2}) \, g(x,Q)$$

Corrections to this simple formula will arise due to the Q dependence of g(x) and of $\alpha$s

# Numerical example



Solid: $x*charm(x)$
$\diamond$: $\alpha_S/6\pi\ x*g(x)\ \log(Q/mc)$

Q=1000 GeV
Q=100 GeV
Q=10 GeV

Solid: $x*bottom(x)$
$\diamond$: $\alpha_S/6\pi\ x*g(x)\ \log(Q/mb)$
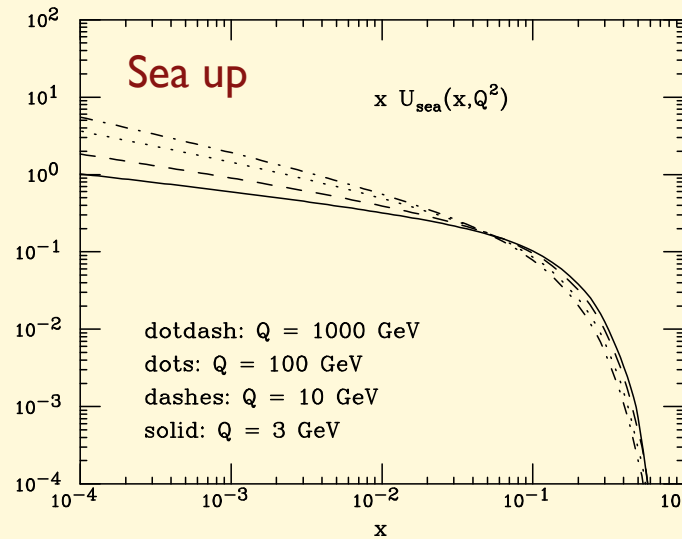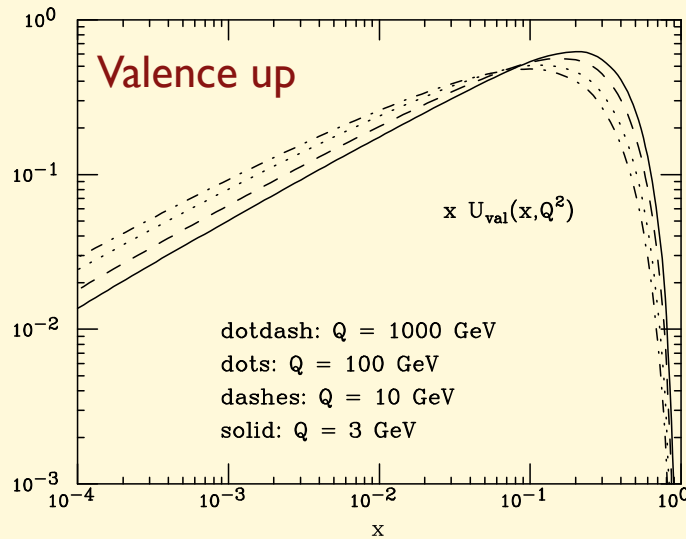
Q=1000 GeV
Q=100 GeV
Q=20 GeV

Excellent agreement, given the simplicity of the approximation!
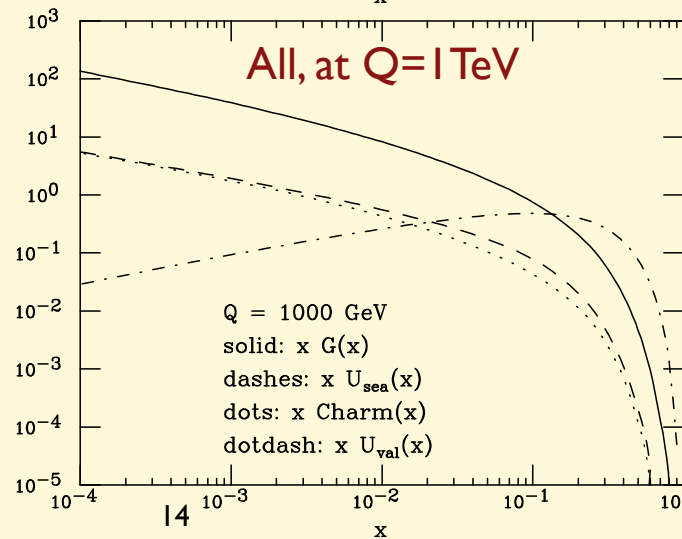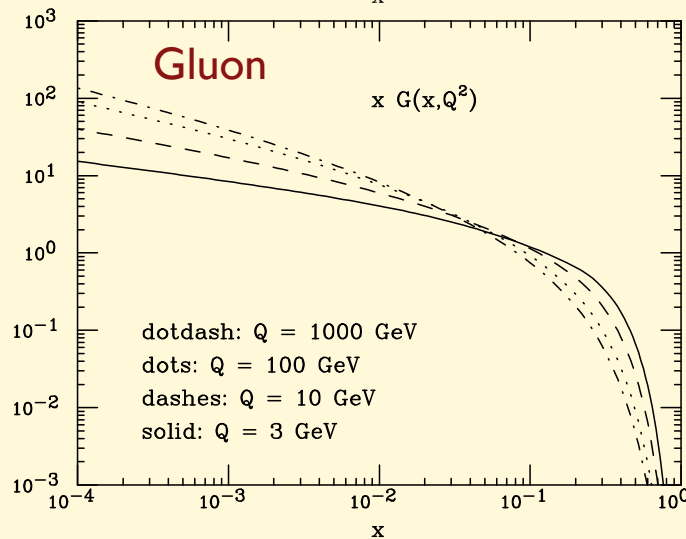
Can be improved by tuning the argument of the log (threshold onset), including a better parameterization of g(x), etc....

More about heavy quarks in the proton in Lecture 4 ......

13

# Examples of PDFs and their evolution



Valence up — $x\,U_{val}(x,Q^2)$

dotdash: Q = 1000 GeV
dots: Q = 100 GeV
dashes: Q = 10 GeV
solid: Q = 3 GeV

Sea up — $x\,U_{sea}(x,Q^2)$

dotdash: Q = 1000 GeV
dots: Q = 100 GeV
dashes: Q = 10 GeV
solid: Q = 3 GeV

Note:
sea ≈10% glue

Gluon — $x\,G(x,Q^2)$

dotdash: Q = 1000 GeV
dots: Q = 100 GeV
dashes: Q = 10 GeV
solid: Q = 3 GeV

All, at Q=1TeV

Q = 1000 GeV
solid: x G(x)
dashes: x $U_{sea}(x)$
dots: x Charm(x)
dotdash: x $U_{val}(x)$

Note:
charm≈up at
high Q

# PDF uncertainties

Green bands represent the convolution of theoretical and experimental systematics in the determination of PDFs
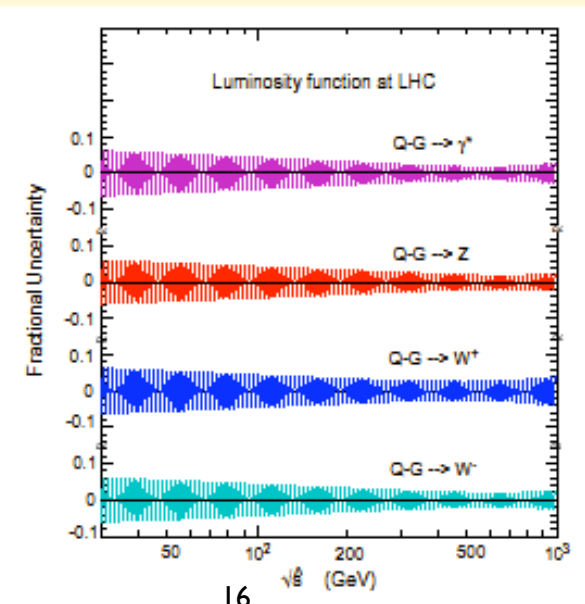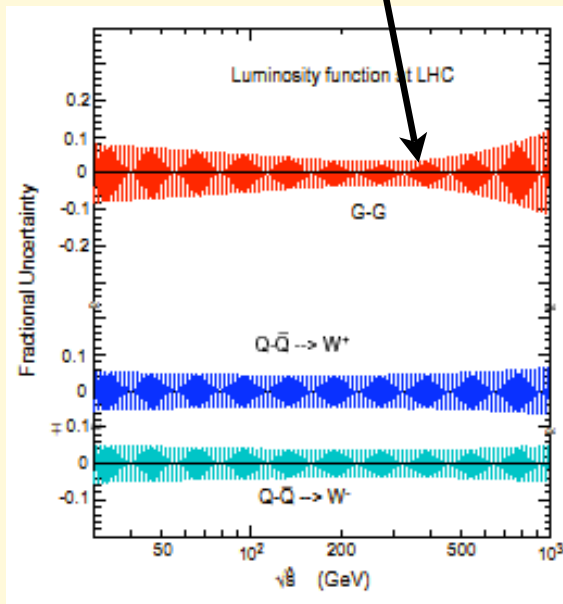


up at Q=3.16 GeV



gluon at Q=3.16 GeV
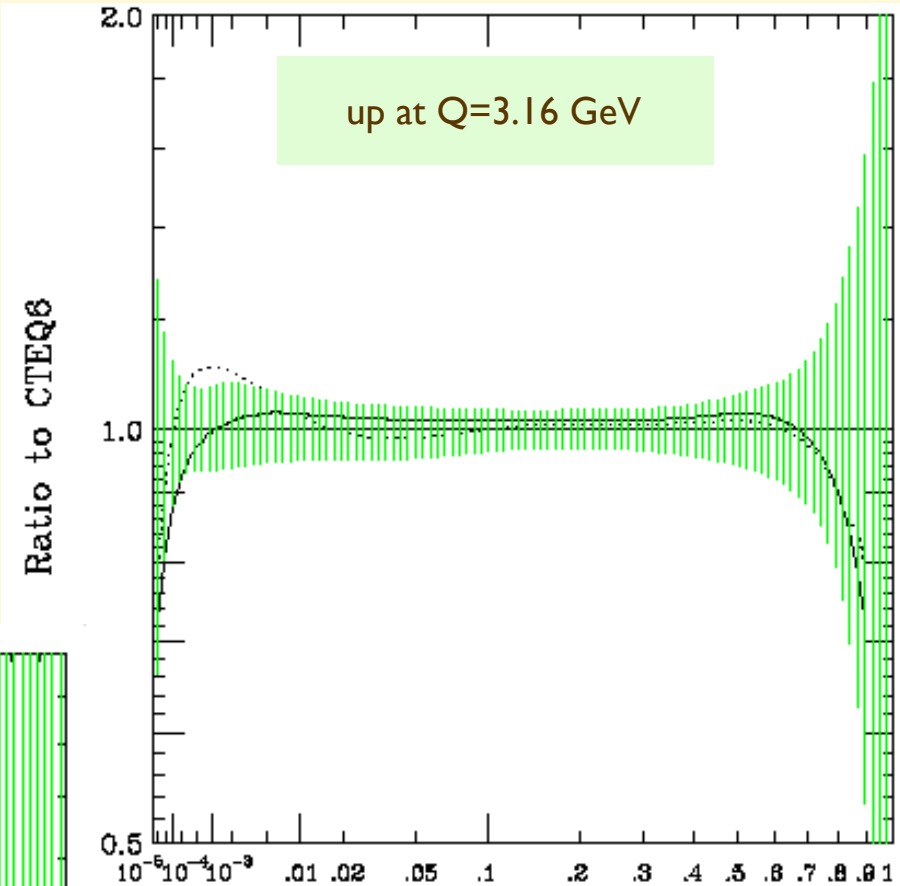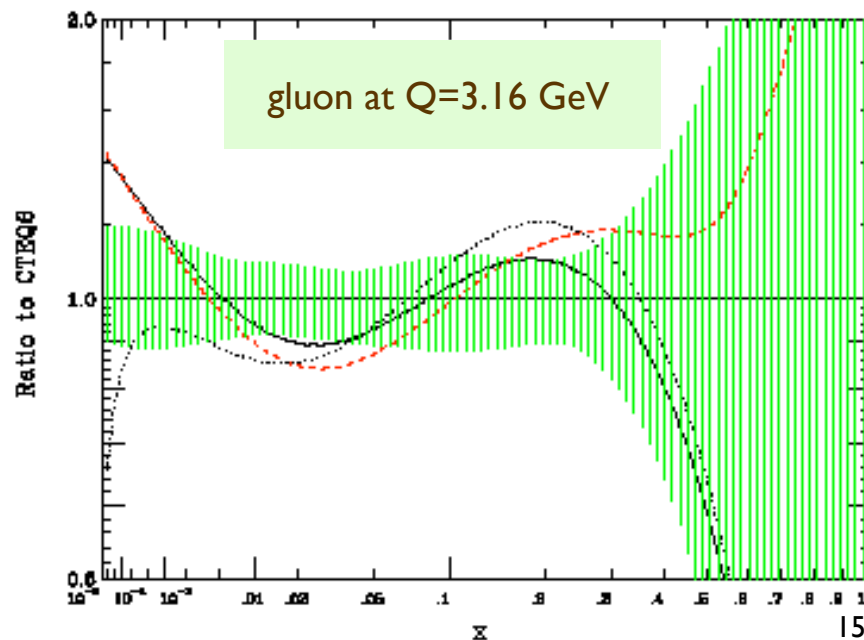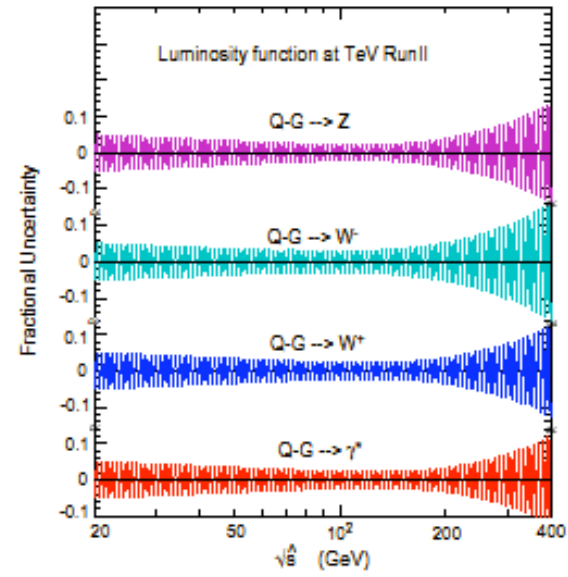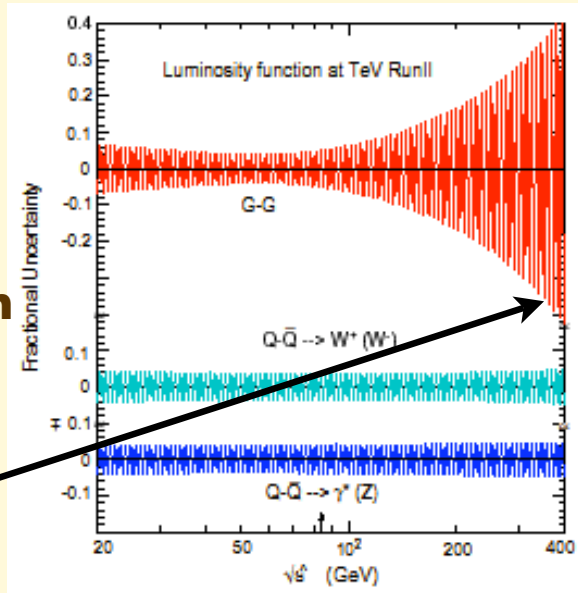
Proton PDFs known to 10-20% for $10^{-3}<x<0.3$, with uncertainties getting smaller at larger Q

15

# PDF luminosity uncertainties

**At the Tevatron**

tt production, smaller uncertainty at the LHC!

**At the LHC**

**Example: Drell-Yan processes**

q

q̄

$W \to \ell\nu$

$Z \to \ell^+\ell^-$
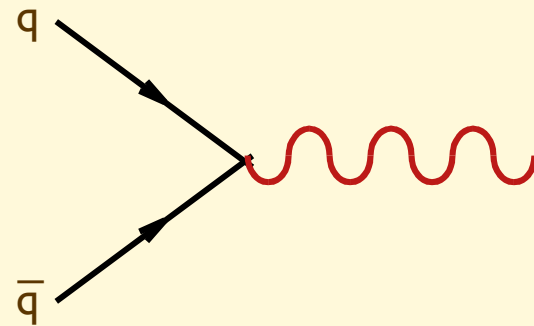
**Properties/Goals of the measurement**:

- Clean final state (no hadrons from the hard process)

- Tests of QCD: σ(W,Z) known up to NNLO (2-loops)

- Measure m(W) ( ➥ constrain m(H))

- constrain PDFs (e.g. $f_{up}(x)/f_{down}(x)$)

- search for new gauge bosons: $q\bar{q} \to W', Z'$

- Probe contact interactions: $q\bar{q}\ell^+\ell^-$

# Some useful relations and definitions

Rapidity: $\quad y = \dfrac{1}{2}\log\dfrac{E_W + p_W^z}{E_W - p_W^z}$
$\qquad\qquad$ Pseudorapidity: $\quad \eta = -\log(\tan\dfrac{\theta}{2})$

where:
$$\tan\theta = \frac{p_T}{p^z} \quad\text{and}\quad p_T = \sqrt{p_x^2 + p_y^2}$$

**Exercise**: prove that for a massless particle rapidity=pseudorapidity:

**Exercise**: using $\quad \tau = \dfrac{\hat{s}}{S} = x_1 x_2 \quad$ and

$$\begin{cases} E_W = (x_1 + x_2)\,E_{\text{beam}} \\ p_W^z = (x_1 - x_2)\,E_{\text{beam}} \end{cases} \Rightarrow y = \frac{1}{2}\log\frac{x_1}{x_2}$$

prove the following relations:

$$x_{1.2} = \sqrt{\tau}\,e^{\pm y} \quad dx_1\,dx_2 = dy\,d\tau$$

$$dy = \frac{dx_1}{x_1} \qquad d\tau\,\delta(\hat{s} - m_W^2) = \frac{1}{S}$$

# LO Cross-section calculation

$$\sigma(pp \to W) = \sum_{q,q'} \int dx_1 dx_2 \, f_q(x_1, Q) \, f_{\bar{q}'}(x_2, Q) \, \frac{1}{2\hat{s}} \int d[PS] \, \overline{\sum_{spin,col}} |M(q\bar{q}' \to W)|^2$$

where:

$$\overline{\sum_{spin,col}} |M(q\bar{q}' \to W)|^2 = \frac{1}{3}\frac{1}{4} 8 g_W^2 |V_{qq'}|^2 \hat{s} = \frac{2}{3}\frac{G_F m_W^2}{\sqrt{2}} |V_{qq'}|^2 \hat{s}$$

$$d[PS] = \frac{d^3 p_W}{(2\pi)^3 p_W^0} (2\pi)^4 \delta^4(P_{in} - p_W)$$

$$= 2\pi \, d^4 p_W \, \delta(p_W^2 - m_W^2) \, \delta^4(P_{in} - p_W) = 2\pi \, \delta(\hat{s} - m_W^2)$$

leading to:

$$\sigma(pp \to W) = \sum_{ij} \frac{\pi A_{ij}}{m_W^2} \, \tau \int_\tau^1 \frac{dx}{x} f_i(x, Q) f_j(\frac{\tau}{x}, Q) \equiv \sum_{ij} \frac{\pi A_{ij}}{m_W^2} \, \tau L_{ij}(\tau)$$

where:

$$\frac{\pi A_{u\bar{d}}}{m_W^2} = 6.5 \text{nb} \quad \text{and} \quad \tau = \frac{m_W^2}{S}$$

19

# Exercise: Study the function τL(τ)

Assume, for example, that
$$f(x) \sim \frac{1}{x^{1+\delta}}, \quad 0 < \delta < 1$$

Then:
$$L(\tau) = \int_\tau^1 \frac{dx}{x} \frac{1}{x^{1+\delta}} \left(\frac{x}{\tau}\right)^{1+\delta} = \frac{1}{\tau^{1+\delta}} \log\left(\frac{1}{\tau}\right)$$

and:
$$\sigma_W = \sigma_W^0 \left(\frac{S}{m_W^2}\right)^\delta \log\left(\frac{S}{m_W^2}\right)$$

Therefore the W cross-section grows at least logarithmically with the hadronic CM energy. This is a typical behavior of cross-sections for production of fixed-mass objects in hadronic collisions, contrary to the case of e+e- collisions, where cross-sections tend to decrease with CM energy.

Note also the following relation, which allows the measurement of the total width of the W boson from the determination of the leptonic rates of W and Z bosons,

$$\Gamma_W = \frac{N(e^+e^-)}{N(e^\pm\nu)} \left(\frac{\sigma_{W^\pm}}{\sigma_Z}\right) \left(\frac{\Gamma_{e\nu}^W}{\Gamma_{e^+e^-}^Z}\right) \Gamma_Z$$

LHC data

20  theory

LEP/SLC

# Introduction to hadronic collisions: theoretical concepts and practical tools for the LHC

## Lecture 2

*Weizmann Institute & Technion Institute*
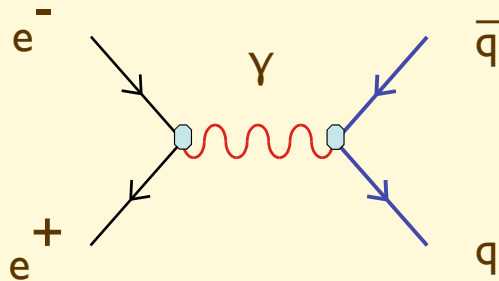*Dec 27 2006 -Jan 1 2007*

**Michelangelo L. Mangano**
TH Unit, Physics Dept, CERN
michelangelo.mangano@cern.ch

# Evolution of hadronic final states

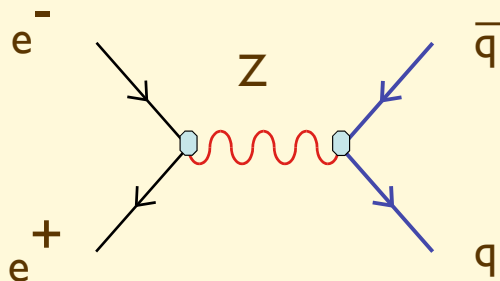Asymptotic freedom implies that at $E_{CM} \gg 1$ GeV

$$\sigma(e^+ e^- \rightarrow \text{hadrons}) \longleftrightarrow \sigma(e^+ e^- \rightarrow \text{quarks/gluons})$$
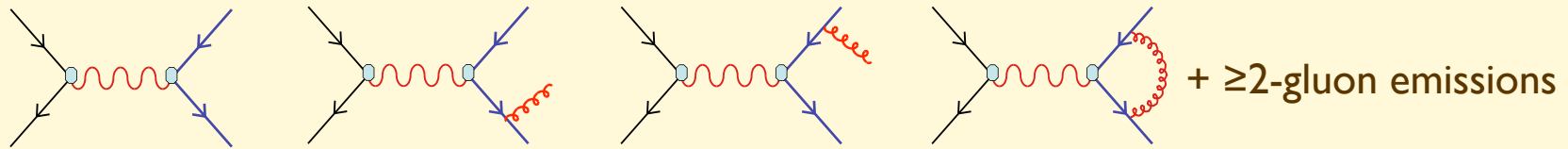
At the Leading Order (LO) in PT:

$$\sigma_0(e^+ e^- \rightarrow q\bar{q}) = \frac{4\pi\alpha^2}{9s} N_c \sum_{f=u,d,...} e_{q_f}^2$$

$$\frac{\sigma_0(e^+ e^- \rightarrow q\bar{q})}{\sigma_0(e^+ e^- \rightarrow \mu^+\mu^-)} = N_c \sum_{f=u,d,...} e_{q_f}^2$$

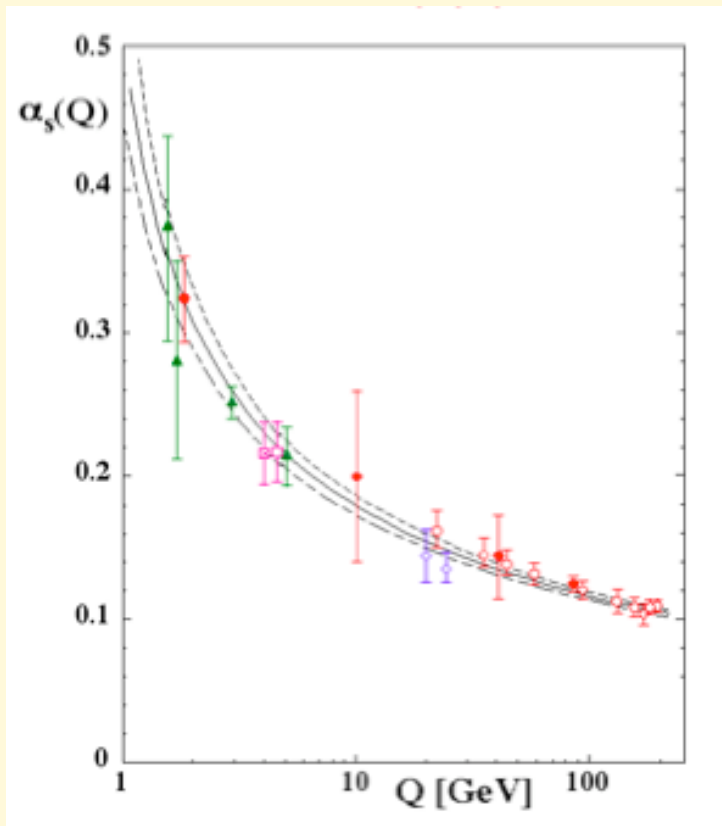$$\frac{\sigma_0(e^+ e^- \rightarrow Z \rightarrow q\bar{q})}{\sigma_0(e^+ e^- \rightarrow Z \rightarrow \mu^+\mu^-)} = N_c \frac{\sum_{f=u,d,...} \left(v_{q_f}^2 + a_{q_f}^2\right)}{\left(v_\mu^2 + a_\mu^2\right)}$$

2

# Adding higher-order perturbative terms:



+ ≥2-gluon emissions

$$\sigma_1(e^+e^- \to q\bar{q}(g)) = \sigma_0(e^+e^- \to q\bar{q}) \left( 1 + \frac{\alpha_s(E_{CM})}{\pi} + O(\alpha_s^2) \right)$$

O(3%) at $M_Z$



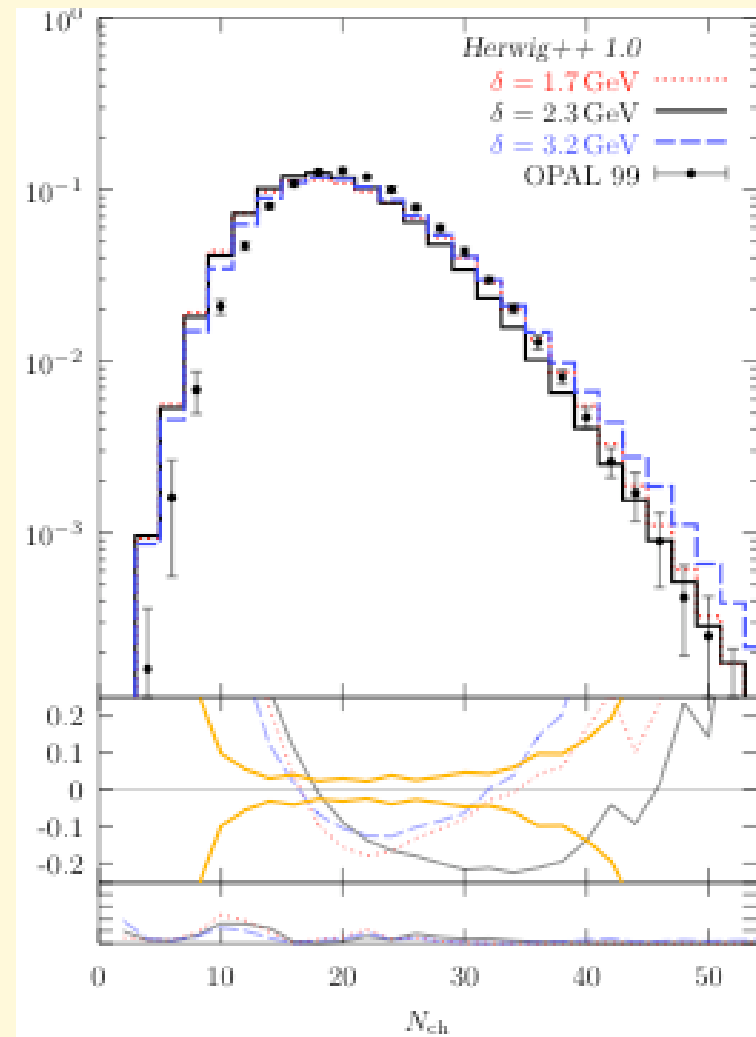Excellent agreement with data,
**provided $N_c=3$**
Extraction of αs consistent with the Q
evolution predicted by QCD

3

However, the final states contain a large number of particles, not 2 or 3 as apparently predicted by the perturbative calculation.
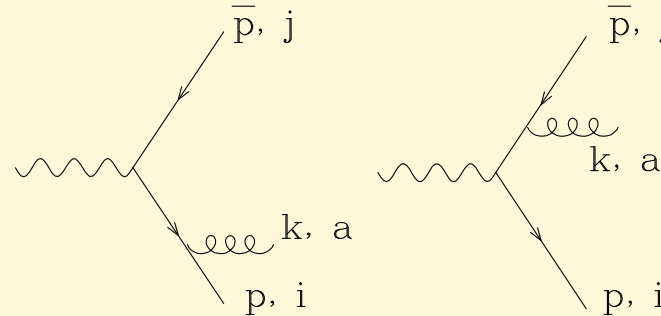
Experimental multiplicity distribution

$\langle n_{charged} \rangle = 20.9$

**What's going on??**

# Soft gluon emission



$$A = \bar{u}(p)\epsilon(k)(ig)\frac{-i}{\not{p}+\not{k}}\Gamma^\mu v(\bar{p})\,\lambda^a_{ij} + \bar{u}(p)\Gamma^\mu\frac{i}{\not{\bar{p}}+\not{k}}(ig)\epsilon(k)v(\bar{p})\,\lambda^a_{ij}$$

$$= \left[\frac{g}{2p\cdot k}\bar{u}(p)\epsilon(k)(\not{p}+\not{k})\Gamma^\mu v(\bar{p}) - \frac{g}{2\bar{p}\cdot k}\bar{u}(p)\Gamma^\mu(\not{\bar{p}}+\not{k})\epsilon(k)v(\bar{p})\right]\lambda^a_{ij}$$

p·k = p$_0$ k$_0$ (1-cosθ)⟹ singularities for collinear (cosθ→1) or soft (k$_0$→0) emission
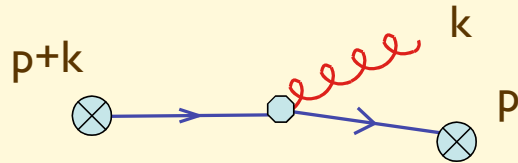
**Collinear emission** does not alter the global structure of the final state, since its preserves its "pencil-like-ness". **Soft emission** at large angle, however, could spoil the structure, and leads to strong interferences between emissions from different legs. So soft emission needs to be studied in more detail.

In the soft (k$_0$→0) limit the amplitude simplifies and factorizes as follows:

$$A_{soft} = g\lambda^a_{ij}\left(\frac{p\cdot\varepsilon}{p\cdot k} - \frac{\bar{p}\cdot\varepsilon}{\bar{p}\cdot k}\right)A_{Born}$$
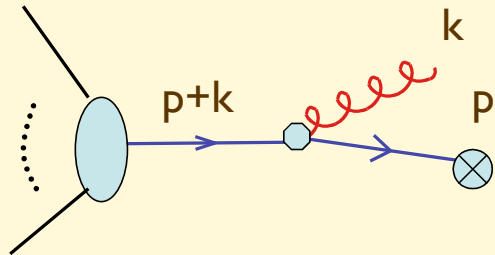
**Factorization:** it is the expression of the independence of long-wavelength (soft) emission on the nature of the hard (short-distance) process.

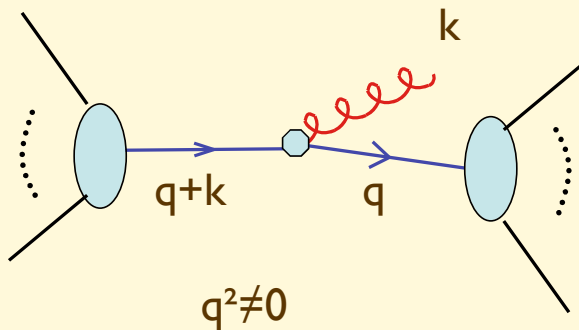# Another simple derivation of soft-gluon emission rules

$$\bar{\psi}(p)\,\gamma_\mu\,\psi(p+k)\,\varepsilon^\mu(k) \quad \stackrel{k\to 0}{\longrightarrow} \quad \bar{\psi}(p)\,\gamma_\mu\,\psi(p)\varepsilon^\mu(k) = 2p\cdot\varepsilon$$

charge current of a free fermion

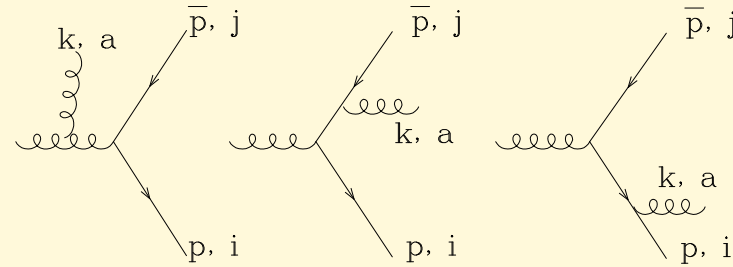$$\frac{1}{\not{p}+\not{k}}\gamma_\mu\psi(p+k)\,\varepsilon^\mu(k) \quad \stackrel{k\to 0}{\longrightarrow}$$

$$\frac{1}{2p\cdot k}\not{p}\gamma_\mu\psi(p)\varepsilon^\mu(k) = \frac{p\cdot\varepsilon}{p\cdot k}$$

$$\frac{1}{\not{q}+\not{k}}\gamma_\mu\frac{1}{\not{q}}\varepsilon^\mu(k) \quad \stackrel{q^2\neq 0,\, k\to 0}{\longrightarrow} \quad \frac{1}{q^2}\not{q}\gamma_\mu\not{q}\frac{1}{q^2}\varepsilon^\mu(k)$$
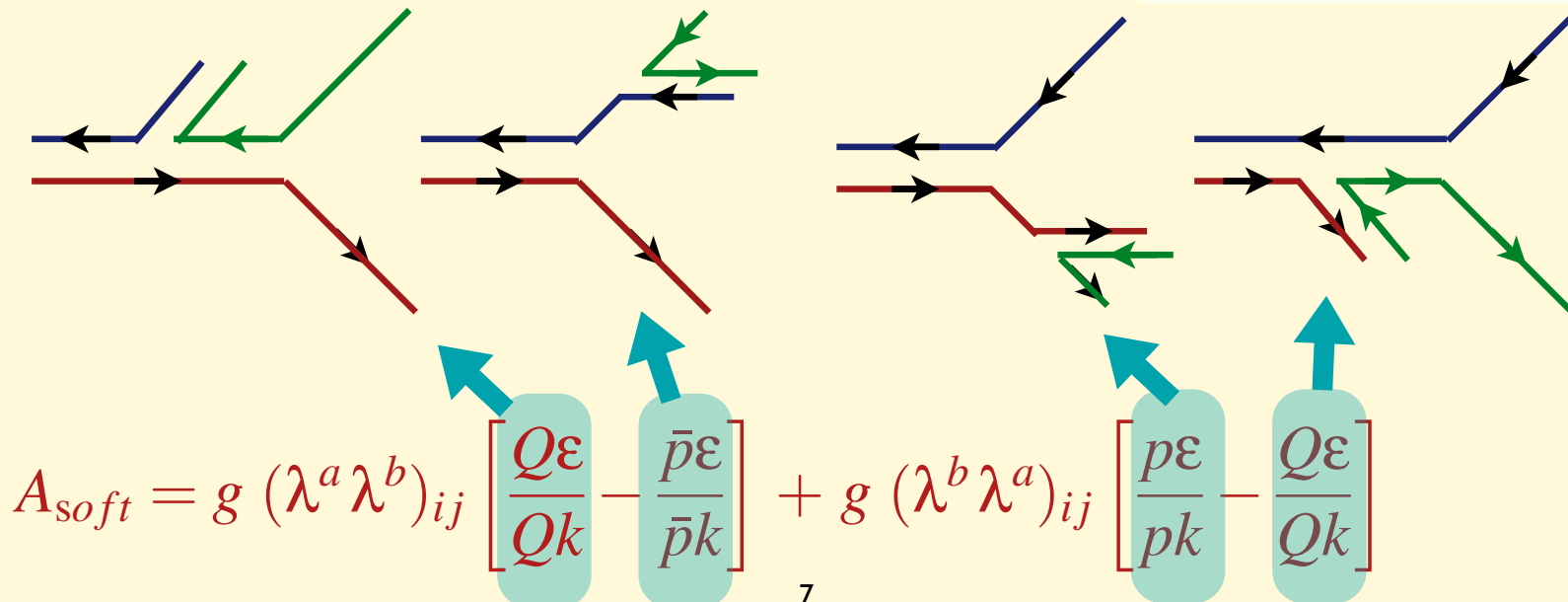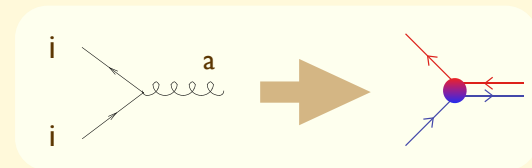
$q^2\neq 0$

=> finite

6

Similar, but more structured, result in the case of a fully coloured process:



$$A_{soft} = g\,(\lambda^a \lambda^b)_{ij} \left[ \frac{Q\varepsilon}{Qk} - \frac{\bar{p}\varepsilon}{\bar{p}k} \right] + g\,(\lambda^b \lambda^a)_{ij} \left[ \frac{p\varepsilon}{pk} - \frac{Q\varepsilon}{Qk} \right]$$

The four terms correspond to the two possible ways colour can flow, and to the two possible emissions for each colour flow:



$$A_{soft} = g\,(\lambda^a \lambda^b)_{ij} \left[ \frac{Q\varepsilon}{Qk} - \frac{\bar{p}\varepsilon}{\bar{p}k} \right] + g\,(\lambda^b \lambda^a)_{ij} \left[ \frac{p\varepsilon}{pk} - \frac{Q\varepsilon}{Qk} \right]$$

7

The interference between the two colour structures

 $\propto (\lambda^a \lambda^b)_{ij}$     $\propto (\lambda^b \lambda^a)_{ij}$

is suppressed by $1/N_c^2$ :

$$\sum_{a,b,i,j} |(\lambda^a \lambda^b)_{ij}|^2 = \sum_{a,b} tr\left(\lambda^a \lambda^b \lambda^b \lambda^a\right) = \frac{N^2-1}{2} C_F = O(N^3)$$

$$\sum_{a,b,i,j} (\lambda^a \lambda^b)_{ij}[(\lambda^b \lambda^a)_{ij}]^* = \sum_{a,b} tr(\lambda^a \lambda^b \lambda^a \lambda^b) = \frac{N^2-1}{2} \underbrace{\left(C_F - \frac{C_A}{2}\right)}_{-\frac{1}{2N}} = O(N)$$

As a result, the emission of a soft gluon can be described, to the leading order in $1/N_c^2$, as the incoherent sum of the emission from the two colour currents

What about the interference between the two diagrams corresponding to the same colour flow? ➡
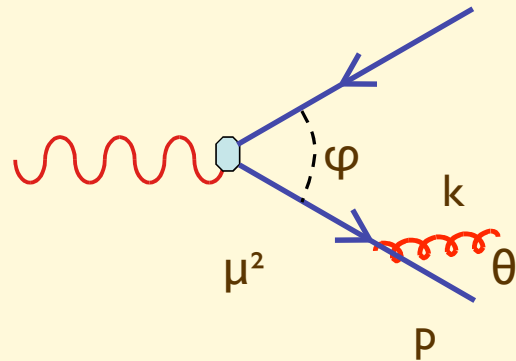
# Angular ordering

$$\left| \begin{matrix} \end{matrix} \right|^2 \;=\; \left| \begin{matrix} \varphi_1 \\ \varphi \end{matrix} \right|^2 \Theta(\varphi-\varphi_1)$$

$$+$$

$$\left| \begin{matrix} \\ \varphi_2 \end{matrix} \right|^2 \Theta(\varphi-\varphi_2)$$

Radiation inside the cones is allowed, and described by the eikonal probability, radiation outside the cones is suppressed and averages to 0 when integrated over the full azimuth
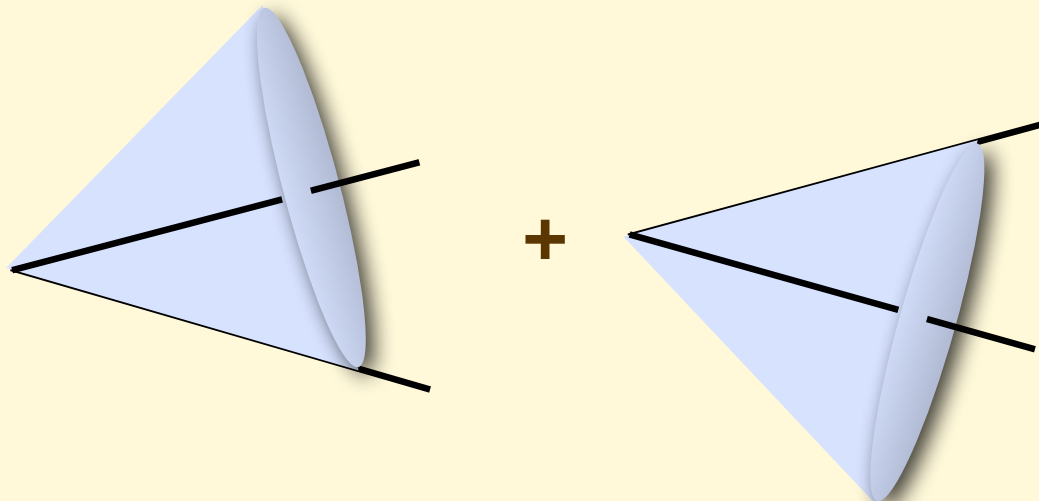
# An intuitive explanation of angular ordering

Lifetime of the virtual intermediate state:

$$\tau < \gamma/\mu = E/\mu^2 = 1 / k_0 \, \theta^2 = 1/k_\perp \theta$$

$$\mu^2 = (p+k)^2 = 2E \, k_0 \, (1-\cos\theta)$$
$$\sim E \, k_0 \, \theta^2 \sim E \, k_\perp \, \theta$$
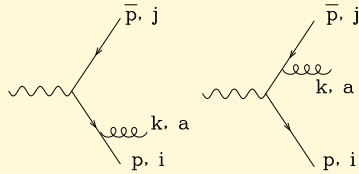
Distance between q and qbar after $\tau$:

$$d = \varphi\tau = (\varphi/\theta) \, 1/k_\perp$$

If the transverse wavelength of the emitted gluon is longer than the separation between q and qbar, the gluon emission is suppressed, because the q qbar system will appear as colour neutral (=> dipole-like emission, suppressed)

Therefore $d > 1/k_\perp$, which implies  $\theta < \varphi$

# The formal proof of angular ordering

$$d\sigma_g = \sum |A_{soft}|^2 \frac{d^3k}{(2\pi)^3 2k^0} \sum |A_0|^2 \frac{-2p^\mu \bar{p}^\nu}{(pk)(\bar{p}k)} g^2 \sum \varepsilon_\mu \varepsilon_\nu^* \frac{d^3k}{(2\pi)^3 2k^0}$$
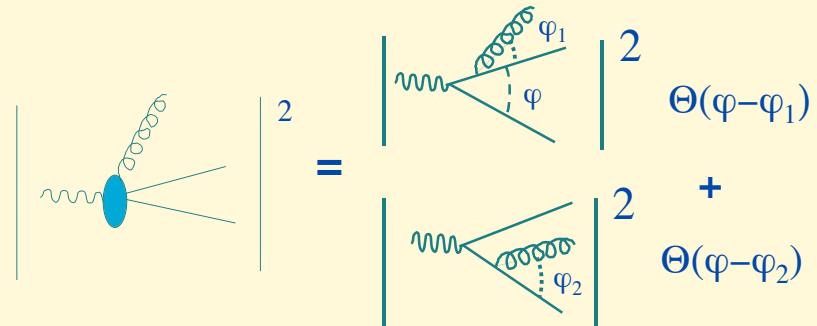
$$= d\sigma_0 \frac{\alpha_s C_F}{\pi} \frac{dk^0}{k^0} \frac{d\phi}{2\pi} \frac{1 - \cos\theta_{ij}}{(1 - \cos\theta_{ik})(1 - \cos\theta_{jk})} d\cos\theta$$

You can easily prove that:

$$\frac{1 - \cos\theta_{ij}}{(1 - \cos\theta_{ik})(1 - \cos\theta_{jk})} = \frac{1}{2}\left[ \frac{\cos\theta_{jk} - \cos\theta_{ij}}{(1 - \cos\theta_{ik})(1 - \cos\theta_{jk})} + \frac{1}{1 - \cos\theta_{ik}} \right] + \frac{1}{2}[i \leftrightarrow j] \equiv W_{(i)} + W_{(j)}$$

where:
$$W_{(i)} \rightarrow finite \ if \ k \parallel j \ (\cos\theta_{jk} \rightarrow 1)$$
$$W_{(j)} \rightarrow finite \ if \ k \parallel i \ (\cos\theta_{ik} \rightarrow 1)$$

The probabilistic interpretation of W(i) and W(j) is a priori spoiled by their non-positivity. However, you can prove that after azimuthal averaging:

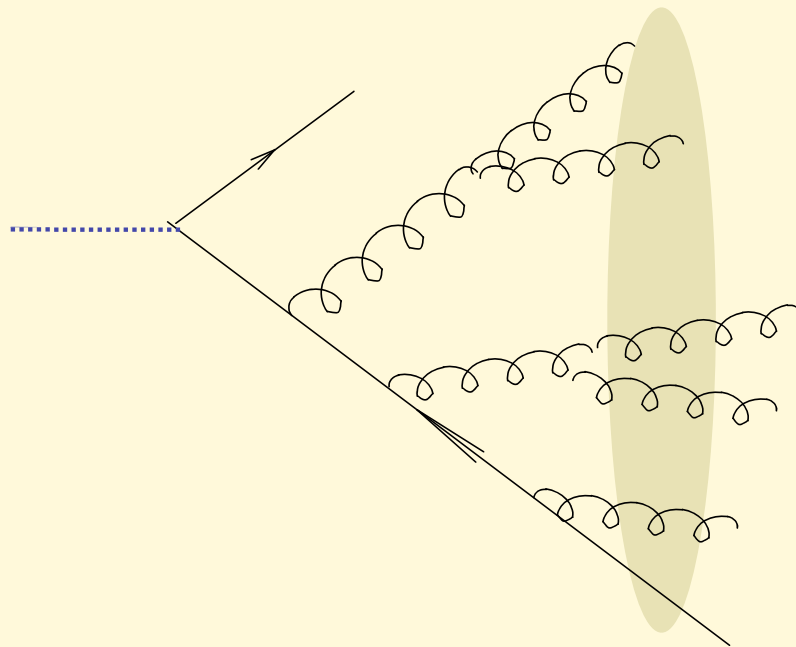$$\int \frac{d\phi}{2\pi} W_{(i)} = \frac{1}{1 - \cos\theta_{ik}} \ \text{if} \ \theta_{ik} < \theta_{ij}, \quad 0 \ \text{otherwise}$$

$$\int \frac{d\phi}{2\pi} W_{(j)} = \frac{1}{1 - \cos\theta_{jk}} \ \text{if} \ \theta_{jk} < \theta_{ij}, \quad 0 \ \text{otherwise}$$

Further branchings will obey angular ordering relative to the new angles. As a result emission angles get smaller and smaller, squeezing the jet
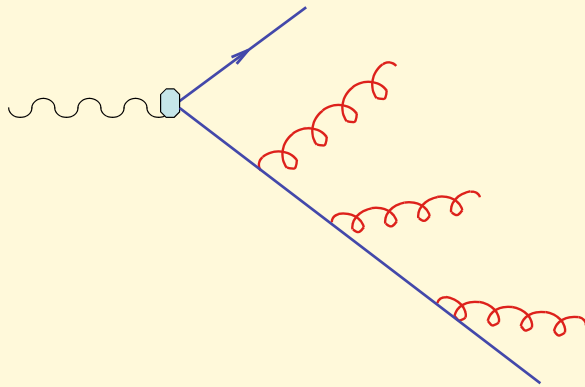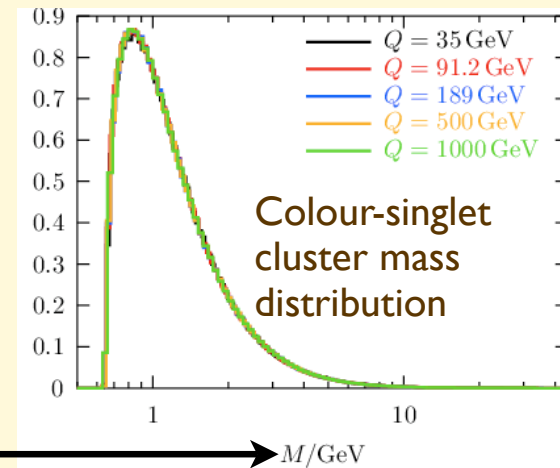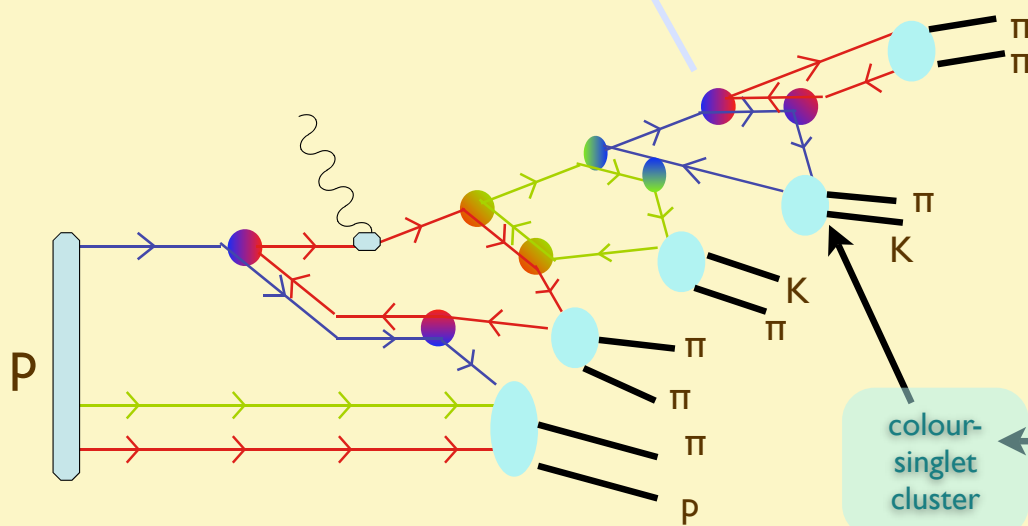
The construction can be iterated to the next emission, with the result that emission angles keep getting smaller and smaller => **jet structure**

Total colour charge of the system is equal to the quark colour charge. Treating the system as the incoherent superposition of N gluons would lead to artificial growth of gluon multiplicity. Angular ordering enforces coherence, and leads to the proper evolution with energy of particle multiplicities.

j

a

i
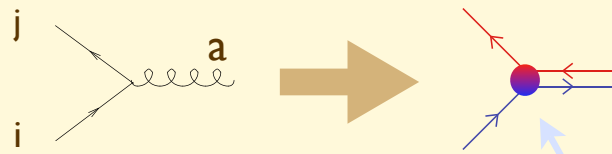
The structure of the perturbative evolution leads naturally to the clustering in phase-space of colour-singlet parton pairs ("preconfinement"). Long-range correlations are strongly suppressed. Hadronization will only act locally, on low-mass colour-singlet clusters.

π
π

π
K

Colour-singlet cluster mass distribution

K
π

π

π

P

π

p

colour-singlet cluster

$Q = 35\,\text{GeV}$
$Q = 91.2\,\text{GeV}$
$Q = 189\,\text{GeV}$
$Q = 500\,\text{GeV}$
$Q = 1000\,\text{GeV}$

$M/\text{GeV}$

Colour is left "behind" by the struck quark. The first soft gluon emitted at large angle will connect to the beam fragments, ensuring that the beam fragments can recombine to form hadrons, and will allow the struck quark to evolve without having to worry about what happens to the proton fragments.
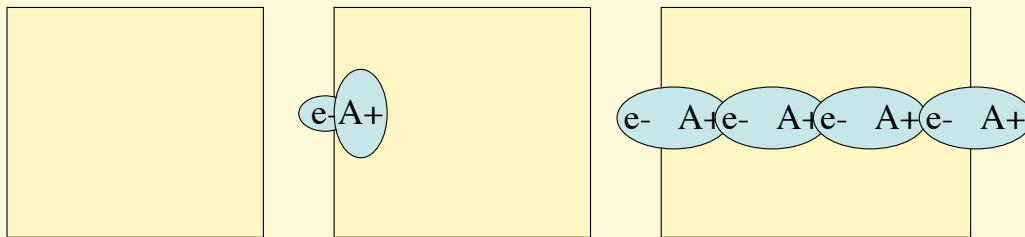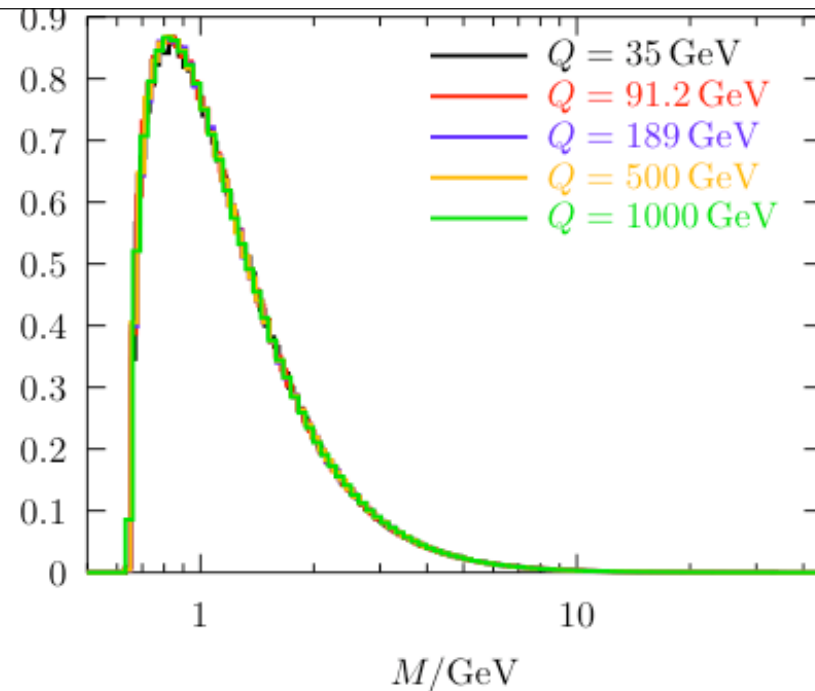
e- A+

e-  A+ e-  A+ e-  A+ e-  A+

13

The existence of high-mass clusters, however rare, is unavoidable, due to IR cutoff which leads to a non-zero probability that no emission takes place. This is particularly true for evolution of massive quarks (as in, e.g. Z→bb or cc). Prescriptions have to be defined to deal with the "evolution" of these clusters. **This has an impact on the z→1 behaviour of fragmentation functions.**

Phenomenologically, this leads to uncertainties, for example, in the background rates for H→γγ (jet→γ).

14

# *Hadronization*

At the end of the perturbative evolution, the final state consists of quarks and gluons, forming, as a result of angular-ordering, low-mass clusters of colour-singlet pairs:
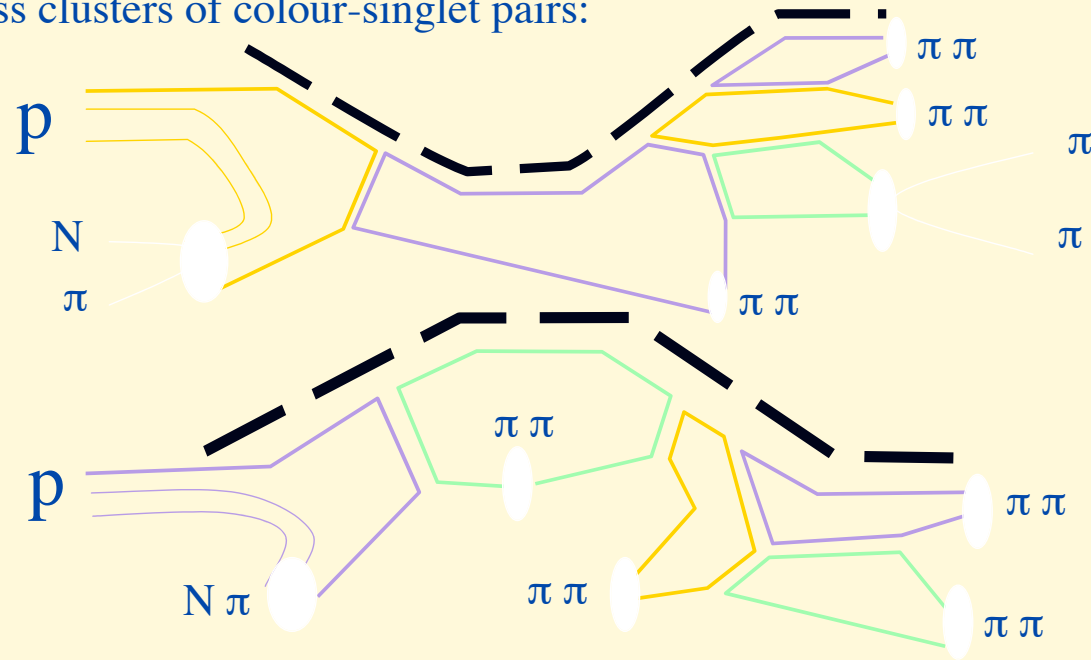
Thanks to the cluster pre-confinement, hadronization is local and independent of the nature of the primary hard process, as well as of the details of how hadronization acts on different clusters. Among other things, one therefore expects:

$$N(pions) = C\ N(gluons),$$
$$C=constant \sim 2$$

# Jets in hadronic collisions
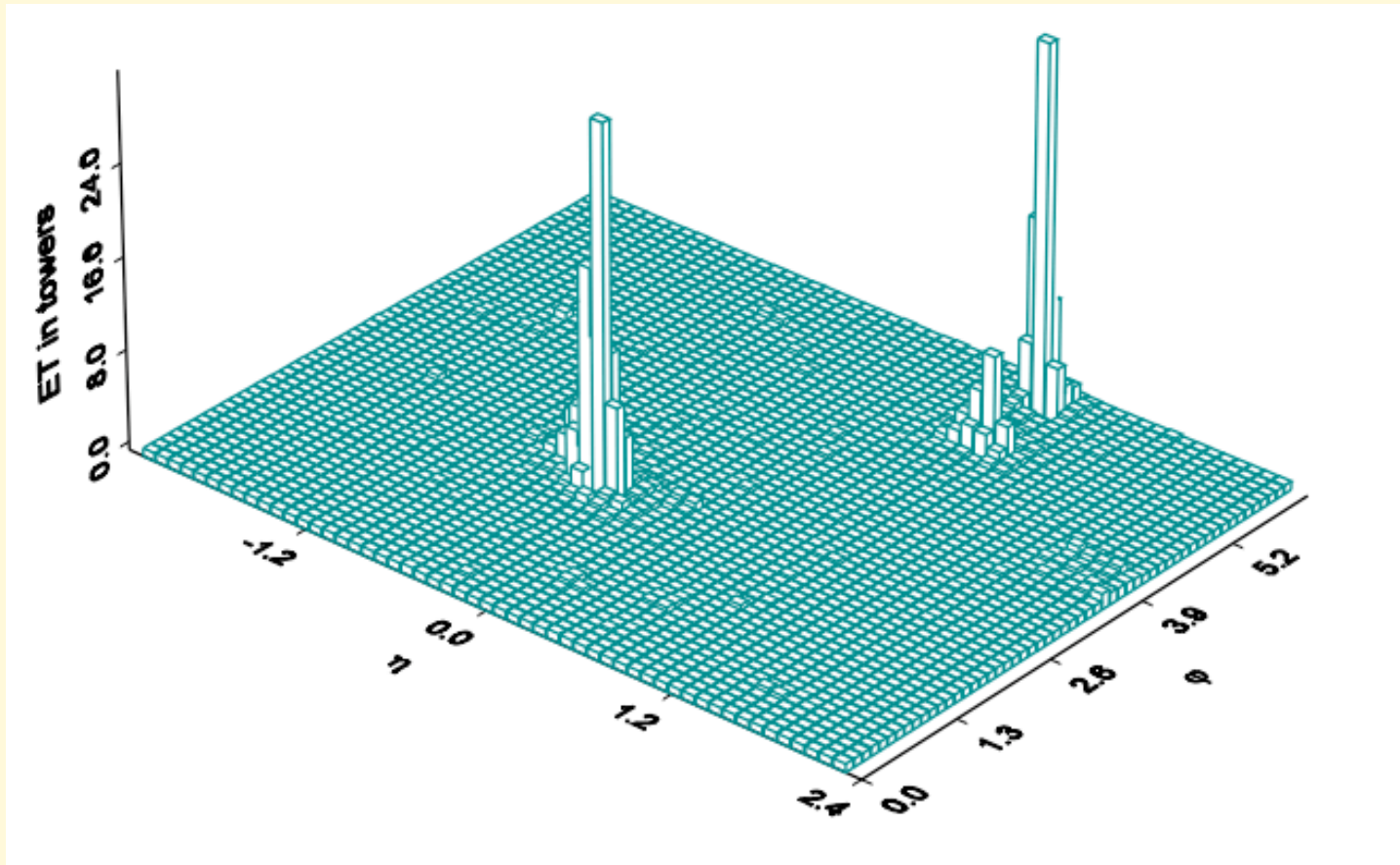
- Inclusive production of jets is the largest component of high-Q phenomena in hadronic collisions
- QCD predictions are known up to NLO accuracy
- Intrinsic theoretical uncertainty (at NLO) is approximately 10%
- Uncertainty due to knowledge of parton densities varies from 5-10% (at low transverse momentum, $p_T$ to 100% (at very high $p_T$, corresponding to high-x gluons)

- Jet are used as probes of the quark structure (possible substructure implies departures from point-like behaviour of cross-section), or as probes of new particles (peaks in the invariant mass distribution of jet pairs)
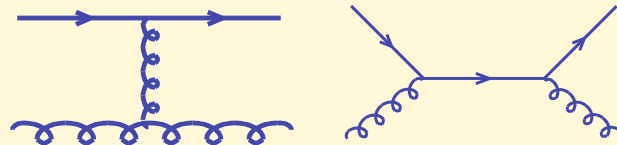
gg→gg

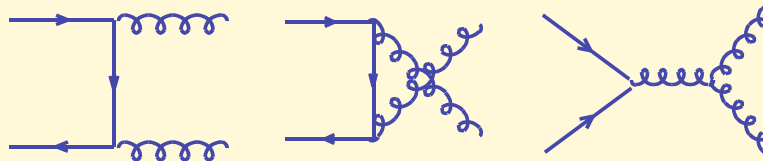2    3      2    4      3    2

1    4      1    3      1    4
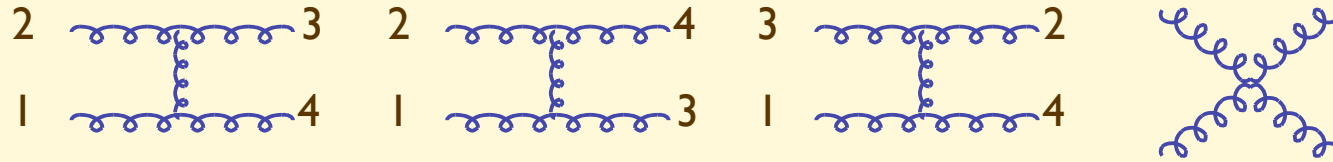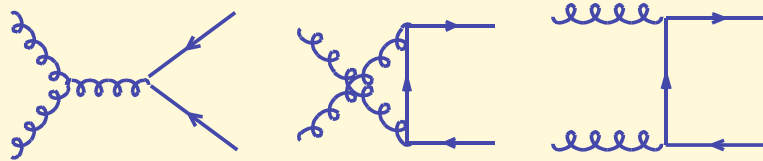
gg→q̄q

qg→qg

q̄q→gg

qq′→qq′

q̄q→qq̄

18
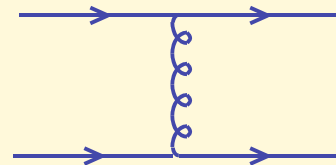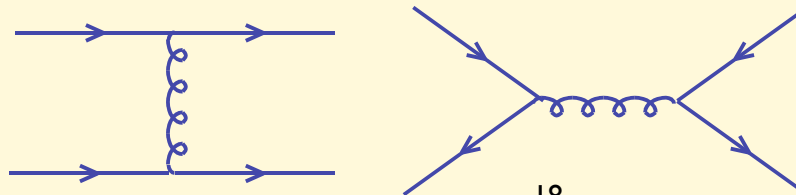
# Phase space and cross-section for LO jet production

$$d[PS] = \frac{d^3p_1}{(2\pi)^2 2p_1^0} \frac{d^3p_2}{(2\pi)^2 2p_2^0} (2\pi)^4 \delta^4(P_{in} - P_{out})\, dx_1\, dx_2$$

(a)    $\delta(E_{in} - E_{out})\, \delta(P_{in}^z - P_{out}^z)\, dx_1\, dx_2 = \dfrac{1}{2E_{beam}^2}$

(b)    $\dfrac{dp^z}{p^0} = dy \equiv d\eta$

$$d[PS] = \frac{1}{4\pi S} p_T\, dp_T\, d\eta_1\, d\eta_2$$

$$\frac{d^3\sigma}{dp_T d\eta_1 d\eta_2} = \frac{p_T}{4\pi S} \sum_{i,j} f_i(x_1) f_j(x_2) \frac{1}{2\hat{s}} \overline{\sum_{kl}} |M(ij \to kl)|^2$$
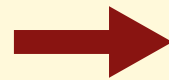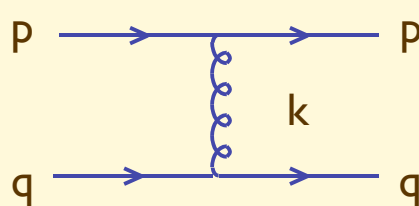
The measurement of pT and rapidities for a dijet final state uniquely determines the parton momenta $x_1$ and $x_2$. Knowledge of the partonic cross-section allows therefore the determination of partonic densities f(x)

# Small-angle jet production, a useful approximation for the determination of the matrix elements and of the cross-section

At small scattering angle, $\quad t = (p_1 - p_3)^2 \sim (1 - \cos\theta) \to 0$

and the $1/t^2$ propagators associated with t-channel gluon exchange dominate the matrix elements for all <u>processes</u>. In this limit it is easy to evaluate the matrix elements. For example:



$$\sim (\lambda^a)_{ij}(\lambda^a)_{kl}(2p_\mu)\frac{1}{t}(2q_\mu) = \frac{2s}{t}(\lambda^a)_{ij}(\lambda^a)_{kl}$$

where we used the fact that, for k=p-p'<<p (small angle scattering),

$$\bar{u}(p')\gamma_\mu u(p) \sim \bar{u}(p)\gamma_\mu u(p) = 2p_\mu$$

Using our colour algebra results, we then get: $\quad \overline{\sum_{col,spin}}|M|^2 = \frac{1}{N_c^2}\frac{N_c^2-1}{4}\frac{4s^2}{t^2}$
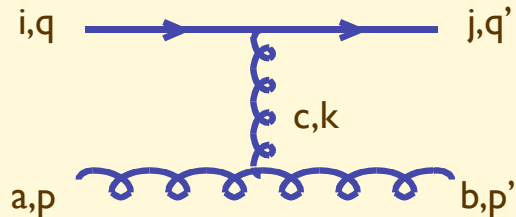
Noting that the result must be symmetric under s↔u exchange, and setting Nc=3, we finally obtain: $\quad \overline{\sum_{col,spin}}|M|^2 = \frac{4}{9}\frac{s^2+u^2}{t^2}$

which turns out to be the exact result!

20

# Quark-gluon and gluon-gluon scattering

We repeat the exercise in the more complex case of qg scattering, assuming the dominance of the t-channel gluon-exchange diagram:



$$\sim f^{abc}\lambda^c_{ij}2p_\mu\frac{1}{t}2q_\mu = 2\frac{s}{t}f^{abc}\lambda^c_{ij}$$

Using the colour algebra results, and enforcing the s↔u symmetry, we get:

$$\overline{\sum_{col,spin}}|M|^2 = \frac{s^2+u^2}{t^2}$$

which differs by only 20% from the exact result

$$\overline{\sum_{col,spin}}|M|^2 = \frac{s^2+u^2}{t^2} - \frac{4}{9}\frac{s^2+u^2}{us}$$

even in the large-angle region, at 90°

In a similar way we obtain for gg scattering (using the t↔u symmetry):

$$\overline{\sum_{col,spin}}|M(gg \to gg)|^2 = \frac{9}{2}\left(\frac{s^2}{t^2}+\frac{s^2}{u^2}\right)$$

compared to the exact result

$$\overline{\sum_{col,spin}}|M(gg \to gg)|^2 = \frac{9}{2}\left(3-\frac{ut}{s^2}-\frac{us}{t^2}-\frac{st}{u^2}\right)$$

with a 20% difference at 90°

21

Note that in the leading 1/t approximation we get the following result:

$$\hat{\sigma}_{gg} : \hat{\sigma}_{qg} : \hat{\sigma}_{qq} = \frac{9}{4} : 1 : \frac{4}{9}$$

where 4/9 = $C_F$ / $C_A$ = [($N^2$-1)/2N] / N is the ratio of the squared colour charges of quarks and gluons

and therefore

$$d\sigma_{jet} = \int dx_1 \, dx_2 \sum_{ij} f_i(x_1) f_j(x_2) \, d\hat{\sigma}_{ij} = \int dx_1 \, dx_2 \sum_{ij} F(x_1) F(x_2) \, d\hat{\sigma}_{gg}$$
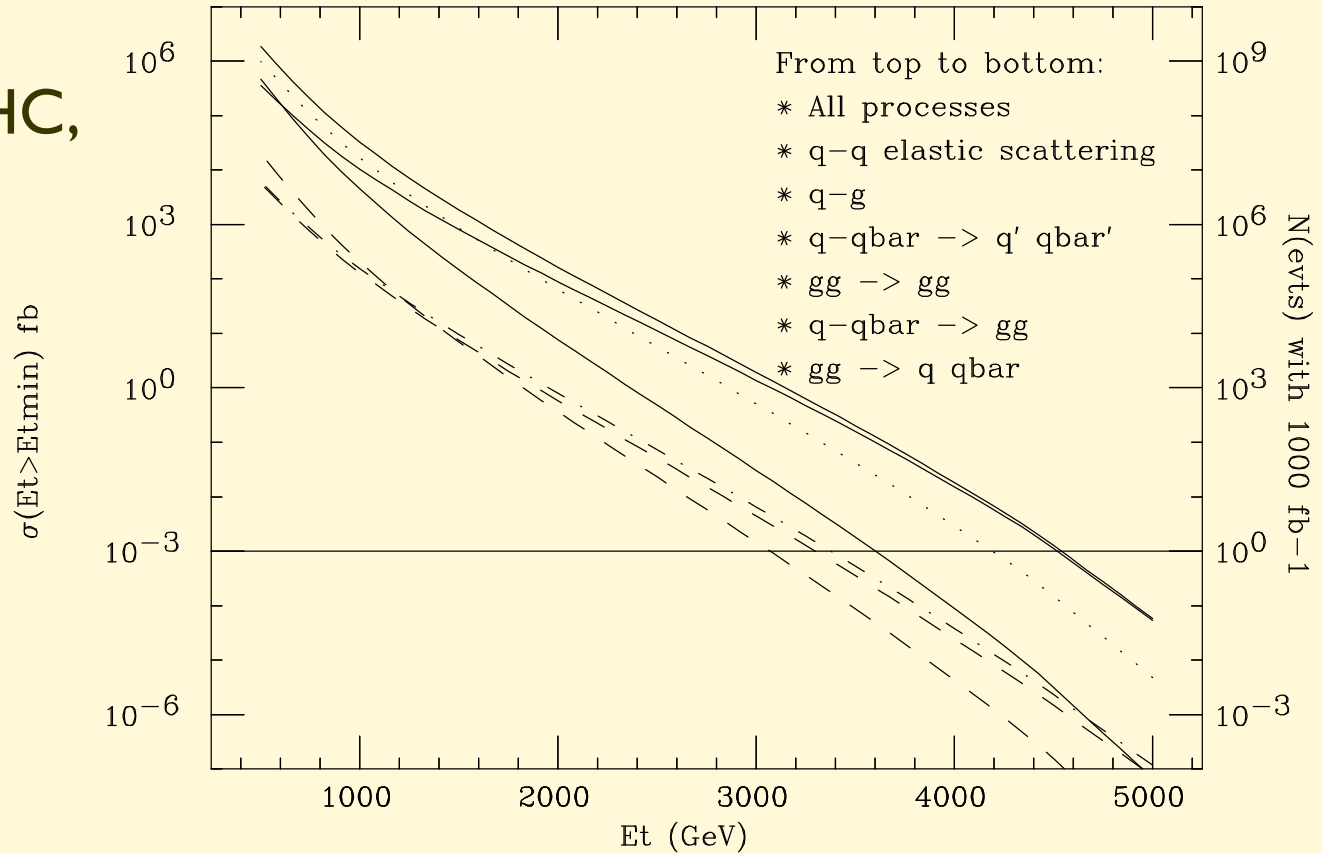
where we defined the `effective parton density' F(x):

$$F(x) = g(x) + \frac{4}{9} \sum_i [q_i(x) + \bar{q}_i(x)]$$

As a result jet data cannot be used to extract separately gluon and quark densities. On the other hand, assuming an accurate knowledge of the quark densities (say from HERA), jet data can help in the determination of the gluon density

| Process | $\dfrac{d\hat{\sigma}}{d\Phi_2}$ | at 90° |
|---|---|---|
| $qq' \to qq'$ | $\frac{4}{9}\dfrac{\hat{s}^2+\hat{u}^2}{\hat{t}^2}$ | 2.22 |
| $qq \to qq$ | $\left[\frac{4}{9}\left(\dfrac{\hat{s}^2+\hat{u}^2}{\hat{t}^2}+\dfrac{\hat{s}^2+\hat{t}^2}{\hat{u}^2}\right)-\dfrac{8}{27}\dfrac{\hat{s}^2}{\hat{u}\hat{t}}\right]$ | 3.26 |
| $q\bar{q} \to q'\bar{q}'$ | $\frac{4}{9}\dfrac{\hat{t}^2+\hat{u}^2}{\hat{s}^2}$ | 0.22 |
| $q\bar{q} \to q\bar{q}$ | $\left[\frac{4}{9}\left(\dfrac{\hat{s}^2+\hat{u}^2}{\hat{t}^2}+\dfrac{\hat{t}^2+\hat{u}^2}{\hat{s}^2}\right)-\dfrac{8}{27}\dfrac{\hat{u}^2}{\hat{s}\hat{t}}\right]$ | 2.59 |
| $q\bar{q} \to gg$ | $\left[\dfrac{32}{27}\dfrac{\hat{t}^2+\hat{u}^2}{\hat{t}\hat{u}}-\dfrac{8}{3}\dfrac{\hat{t}^2+\hat{u}^2}{\hat{s}^2}\right]$ | 1.04 |
| $gg \to q\bar{q}$ | $\left[\dfrac{1}{6}\dfrac{\hat{t}^2+\hat{u}^2}{\hat{t}\hat{u}}-\dfrac{3}{8}\dfrac{\hat{t}^2+\hat{u}^2}{\hat{s}^2}\right]$ | 0.15 |
| $gq \to gq$ | $\left[-\dfrac{4}{9}\dfrac{\hat{s}^2+\hat{u}^2}{\hat{s}\hat{u}}+\dfrac{\hat{u}^2+\hat{s}^2}{\hat{t}^2}\right]$ | 6.11 |
| $gg \to gg$ | $\dfrac{9}{2}\left(3-\dfrac{\hat{t}\hat{u}}{\hat{s}^2}-\dfrac{\hat{s}\hat{u}}{\hat{t}^2}-\dfrac{\hat{s}\hat{t}}{\hat{u}^2}\right)$ | 30.4 |

# Jet production rates at the LHC, subprocess composition

From top to bottom:
* All processes
* q–q elastic scattering
* q–g
* q–qbar –> q' qbar'
* gg –> gg
* q–qbar –> gg
* gg –> q qbar

$\sigma(Et>Etmin)$ fb

N(evts) with 1000 fb-1

Et (GeV)

The presence of a quark substructure would manifest itself via contact interactions (as in Fermi's theory of weak interactions). On one side these new interactions would lead to an increase in cross-section, on the other they would affect the jets' angular distributions. In the dijet CMF, QCD implies Rutherford law, and extra point-like interactions can then be isolated using a fit. With the anticipated statistics of 300 fb-1, limits on the scale of the new interactions in excess of 40 TeV should be reached (to increase to 60 TeV with 3000 fb-1)

24

# Some more kinematics

Prove as an **exercise** that

$$x_{1,2} = \frac{p_T}{E_{beam}} \cosh y^* \, e^{\pm y_b}$$
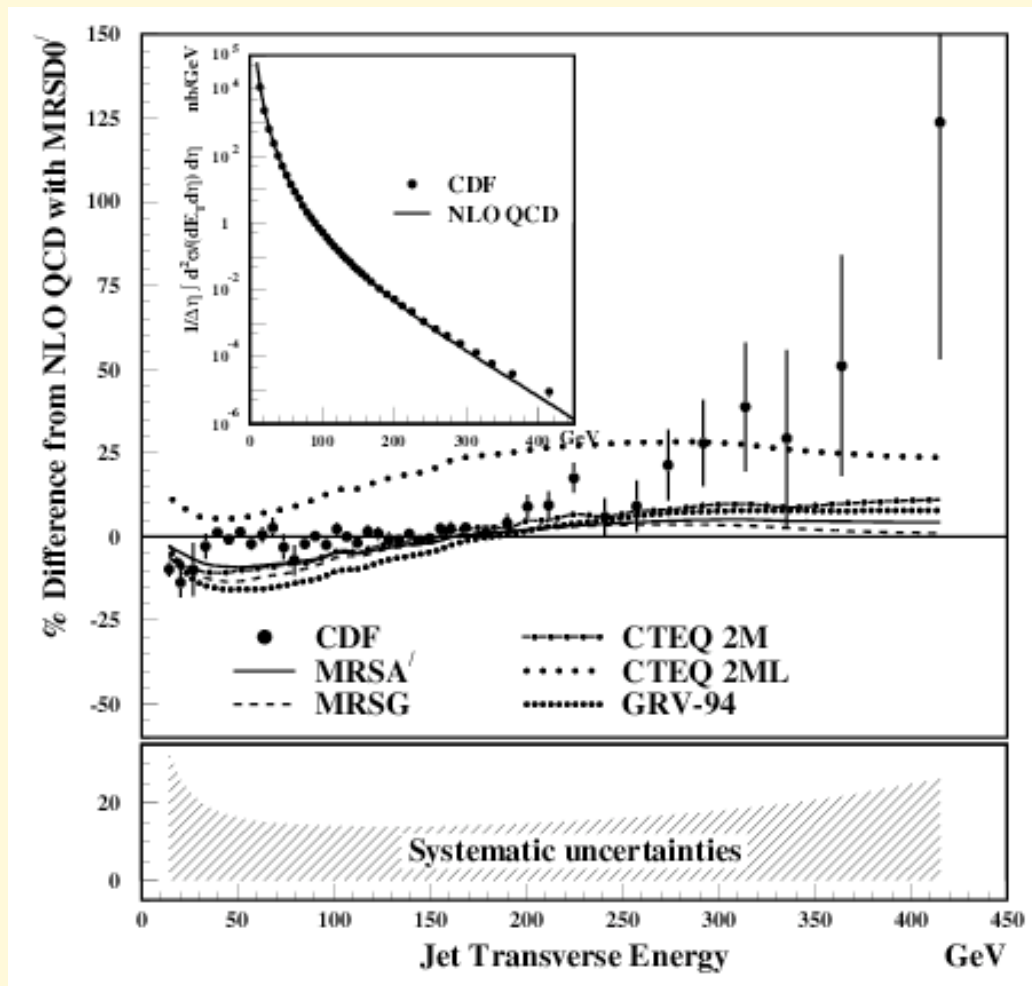
where

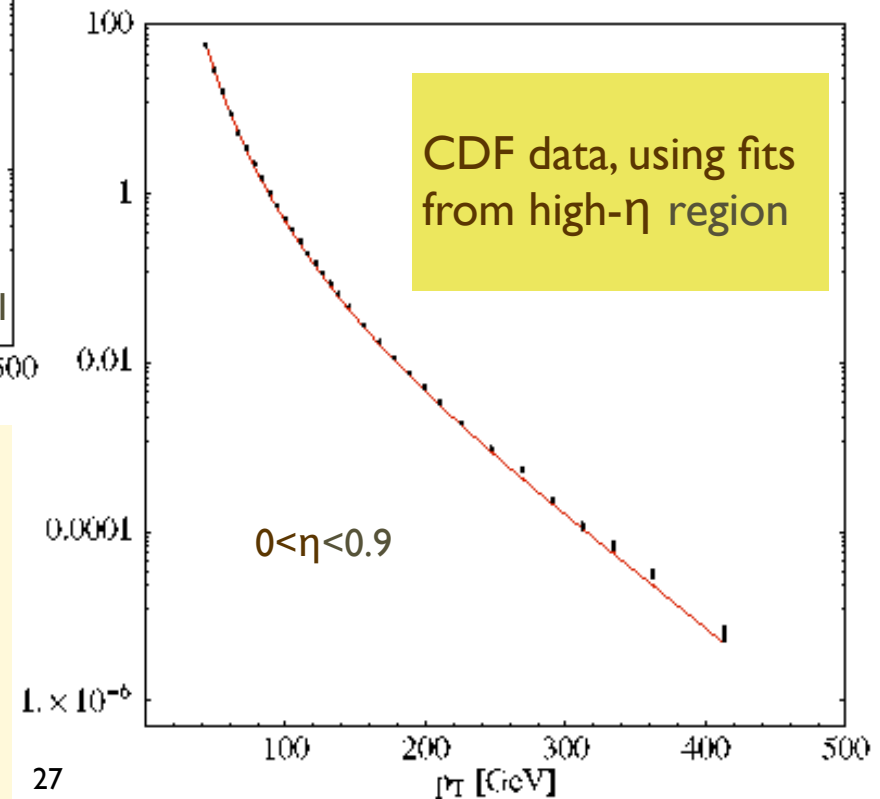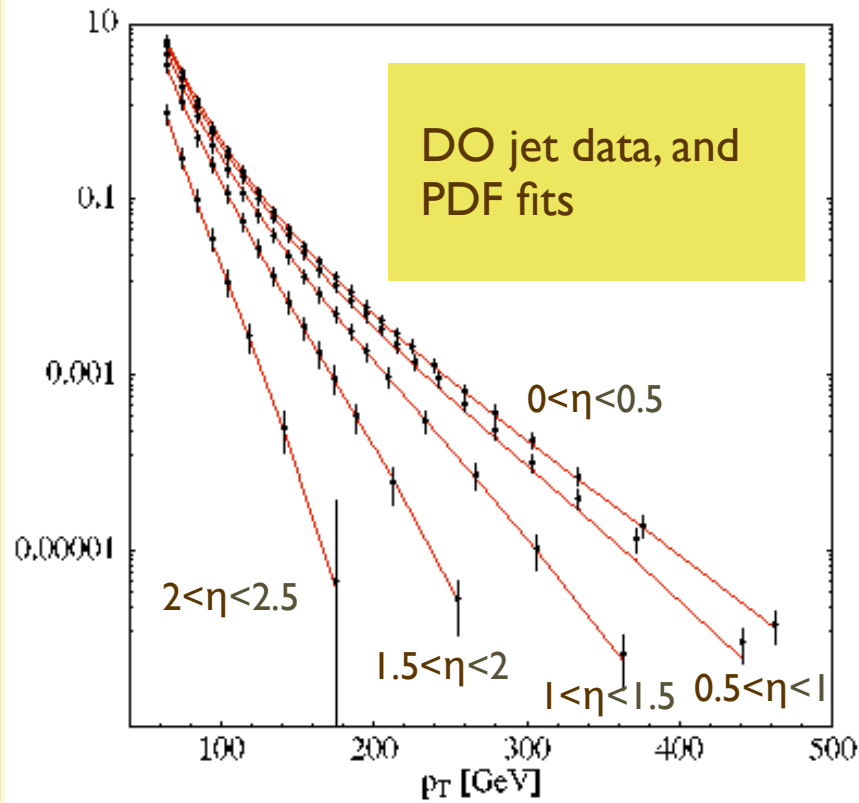$$y^* = \frac{\eta_1 - \eta_2}{2}, \quad y_b = \frac{\eta_1 + \eta_2}{2}$$

We can therefore reach large values of x either by selecting large invariant mass events:

$$\frac{p_T}{E_{beam}} \cosh y^* \equiv \sqrt{\tau} \to 1$$

or by selecting low-mass events, but with large boosts ($y_b$ large) in either positive of negative directions. In this case, we probe large-x with events where possible new physics is absent, thus setting consistent constraints on the behaviour of the cross-section in the high-mass region, which could hide new phenomena.

# Example, at the Tevatron

DO jet data, and PDF fits

0<η<0.5

2<η<2.5

1.5<η<2

1<η<1.5   0.5<η<1

CDF data, using fits from high-η region

0<η<0.9

27

# Introduction to hadronic collisions: theoretical concepts and practical tools for the LHC
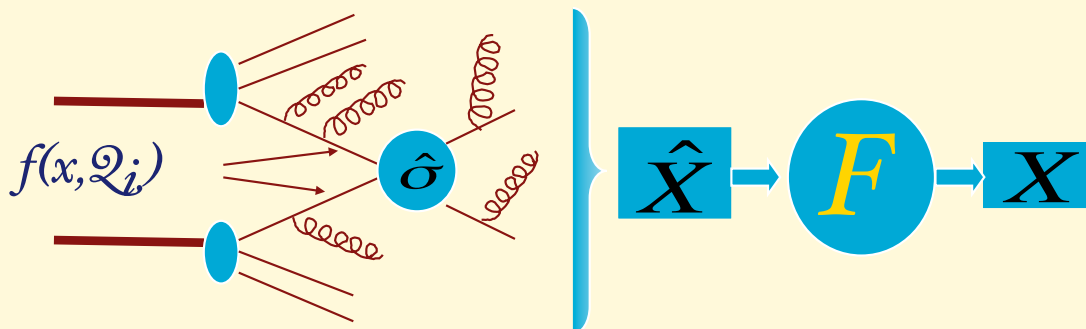
## Lecture 3

*Weizmann Institute & Technion Institute*
*Dec 27 2006 -Jan 1 2007*

**Michelangelo L. Mangano**
TH Unit, Physics Dept, CERN
michelangelo.mangano@cern.ch

# Factorization Theorem

$$\frac{d\sigma}{dX} = \sum_{j,k} \int_{\hat{X}} f_j(x_1, Q_i)\, f_k(x_2, Q_i)\, \frac{d\hat{\sigma}_{jk}(Q_i, Q_f)}{d\hat{X}}\, F(\hat{X} \to X; Q_i, Q_f)$$



$f(x, Q_i)$    $\hat{\sigma}$    $\hat{X}$   $F$   $X$

$f_j(x, Q)$ **Parton distribution functions (PDF)**

$F(\hat{X} \to X; Q_i, Q_f)$

- sum over all initial state histories leading, at the scale Q, to:

$$\vec{p}_j = x\, \vec{P}_{proton}$$

- transition from partonic final state to the hadronic observable (hadronization, fragm. function, jet definition, etc)
- Sum over all histories with $X$ in them

2

- The possible histories of initial and final state, and their relative probabilities, are in principle independent of the hard process (they only depend on the flavours of partons involved and on the scales Q)

- Once an algorithm is developed to describe initial (IS) and final (FS) state evolution, it can be applied to partonic IS and FS arising from the calculation of an arbitrary hard process

- Depending on the extent to which different possible FS and IS histories affect the value of the observable $X$, different realizations of the factorization theorem can be implemented, and 3 different tools developed:

  1. **Cross-section evaluators**
  2. **Parton-level Monte Carlos**
  3. **Shower Monte Carlos**

# 1: Cross-section evaluators

- Only some component of the final state is singled out for the measurement, all the rest being ignored (i.e. integrated over). E.g. $pp \rightarrow e^+ e^- + X$

- No 'events' are 'generated', only cross-sections are evaluated:

$$\sigma\left(pp \rightarrow Z^0\right), \quad \frac{d\sigma}{dM(e^+e^-)\, dy(e^+e^-)}, \quad \dots$$

Experimental selection criteria (e.g. jet definition or acceptance) are applied on parton-level quantities. Provided these are infrared/collinear finite, it therefore doesn't matter what **F(X)** is, as we assume (*fact. theorem*) that:

$$\sum_X F(\hat{X}, X) = 1 \quad \forall \, \hat{X}$$

- Thanks to the inclusiveness of the result, it is `straightforward' to include higher-order corrections, as well as to resum classes of dominant and subdominant logs

4

# State of the art

- NLO available for:

    - jet and heavy quarks production

    - prompt photon production

    - gauge boson pairs

    - most new physics processes (e.g. SUSY)

- NNLO available for:

    - W/Z/DY production $(q\bar{q} \to W)$

    - Higgs production $(gg \to H)$

# 2: **Parton-level** (*aka* matrix-element) **MC's**

- Parton level configurations (i.e. sets of quarks and gluons) are generated, with probability proportional to the respective perturbative M.E.

- Transition function between a final-state parton and the observed object (jet, missing energy, lepton, etc) is unity

- No need to expand $f(x)$ or $F(X)$ in terms of histories, since they all lead to the same observable

- Experimentally, equivalent to assuming

  - perfect jet reconstruction $(P_\mu^{parton} \rightarrow P_\mu^{jet})$

  - linear detector response

# **State of the art**

- W/Z/gamma + N jets (N≤6)
- W/Z/gamma + Q Qbar + N jets (N≤4)
- Q Qbar + N jets (N≤4)
- Q Qbar Q' Q'bar + N jets (N≤2)
- Q Qbar H + N jets (N≤3)
- nW + mZ + kH + N jets (n+m+k+N ≤8, N≤2)
- N jets (N≤8)

Example of complexity of the calculations, for gg-> N gluons:

| Njets | 2 | 3 | 4 | 5 | 6 | 7 | 8 |
|---|---|---|---|---|---|---|---|
| # diag's | 4 | 25 | 220 | 2485 | 34300 | $5 \times 10^5$ | $10^7$ |

For each process, flavour state and colour flow (leading 1/Nc) are calculated on an event-by-event basis, to allow QCD-coherent shower evolution

# 3: Shower Monte Carlos

**Goal:** complete description of the event,
at the level of individual hadrons
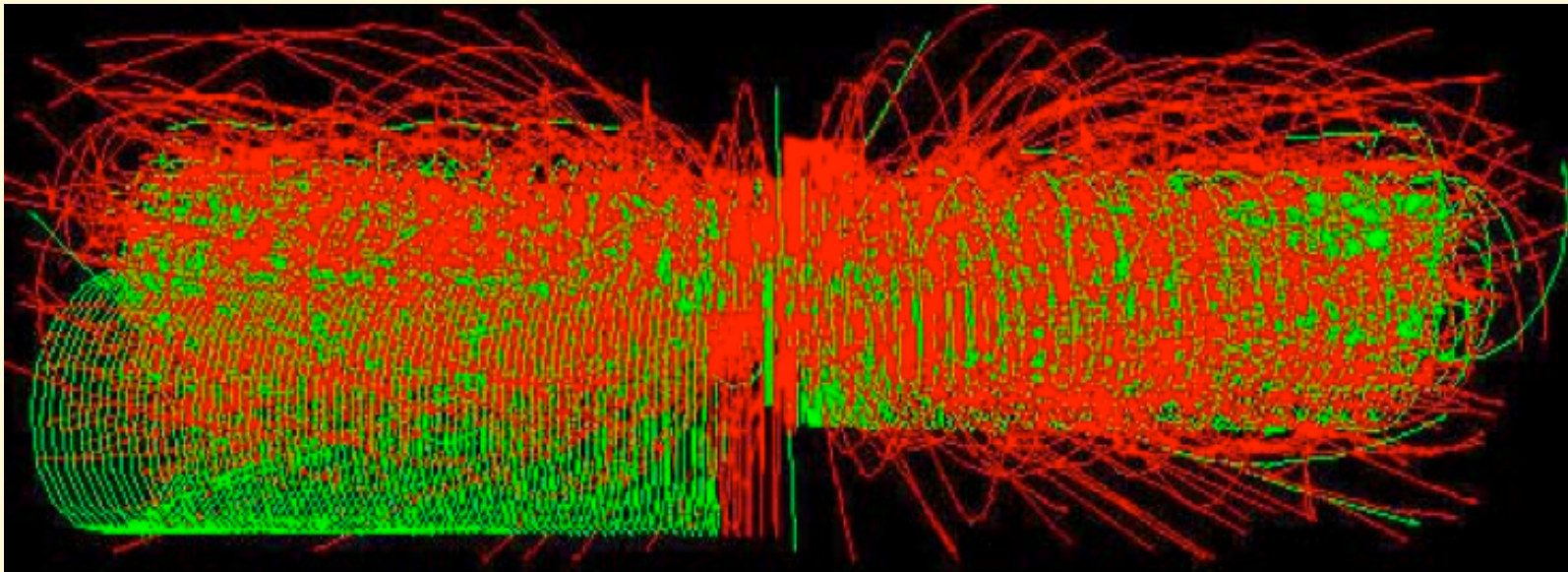
# I: Generate the parton-level hard event
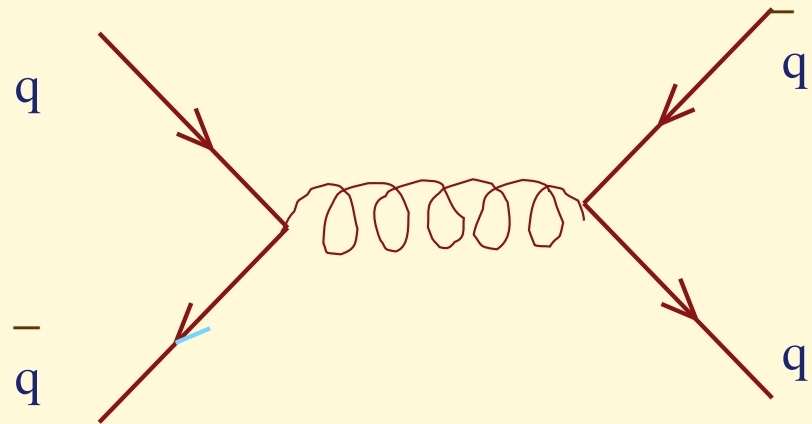
# II: Develop the parton shower

1. Final state

2. Initial state
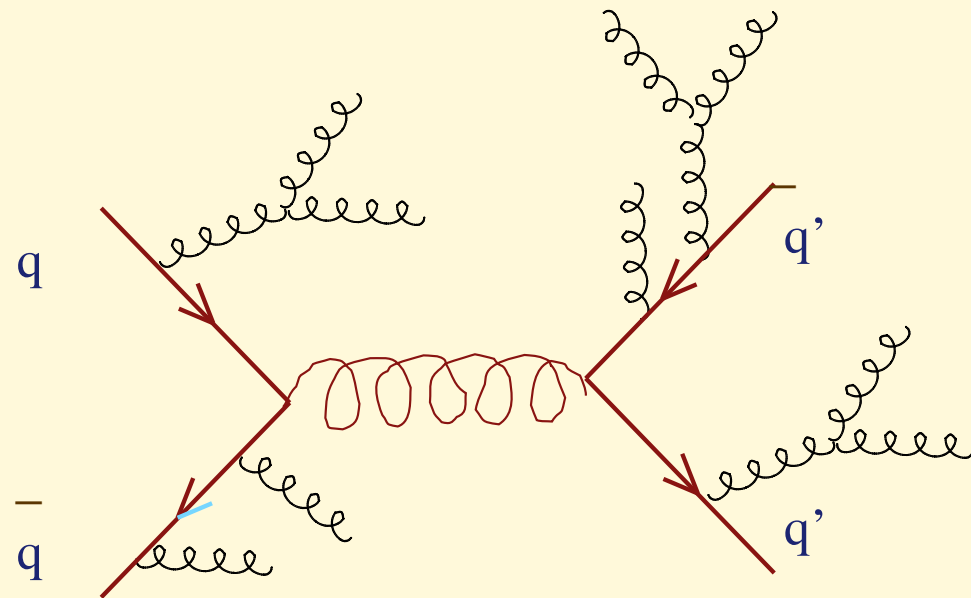
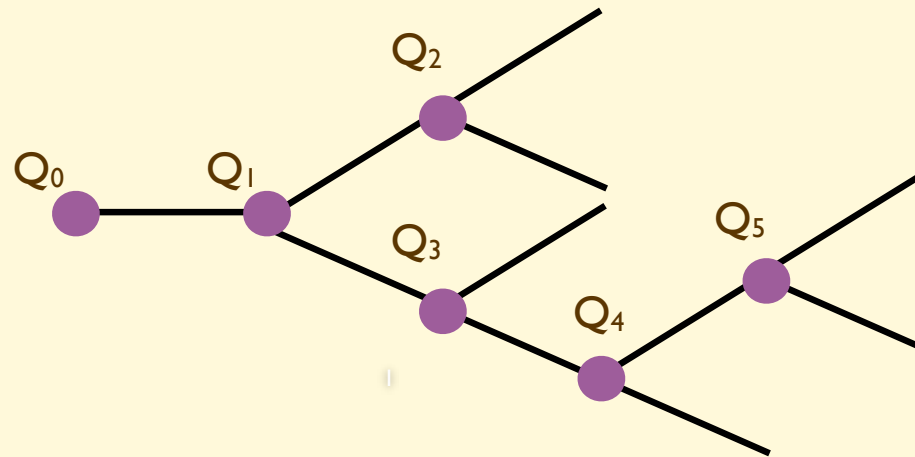# III: Hadronize partons

1. Split gluons into q-qbar pairs

2. Connect colour-singlet pairs

3. Decay the colour-singlet clusters into hadron pairs

**N**

π   π   π   π

π

q

q̄

q'

q'

11
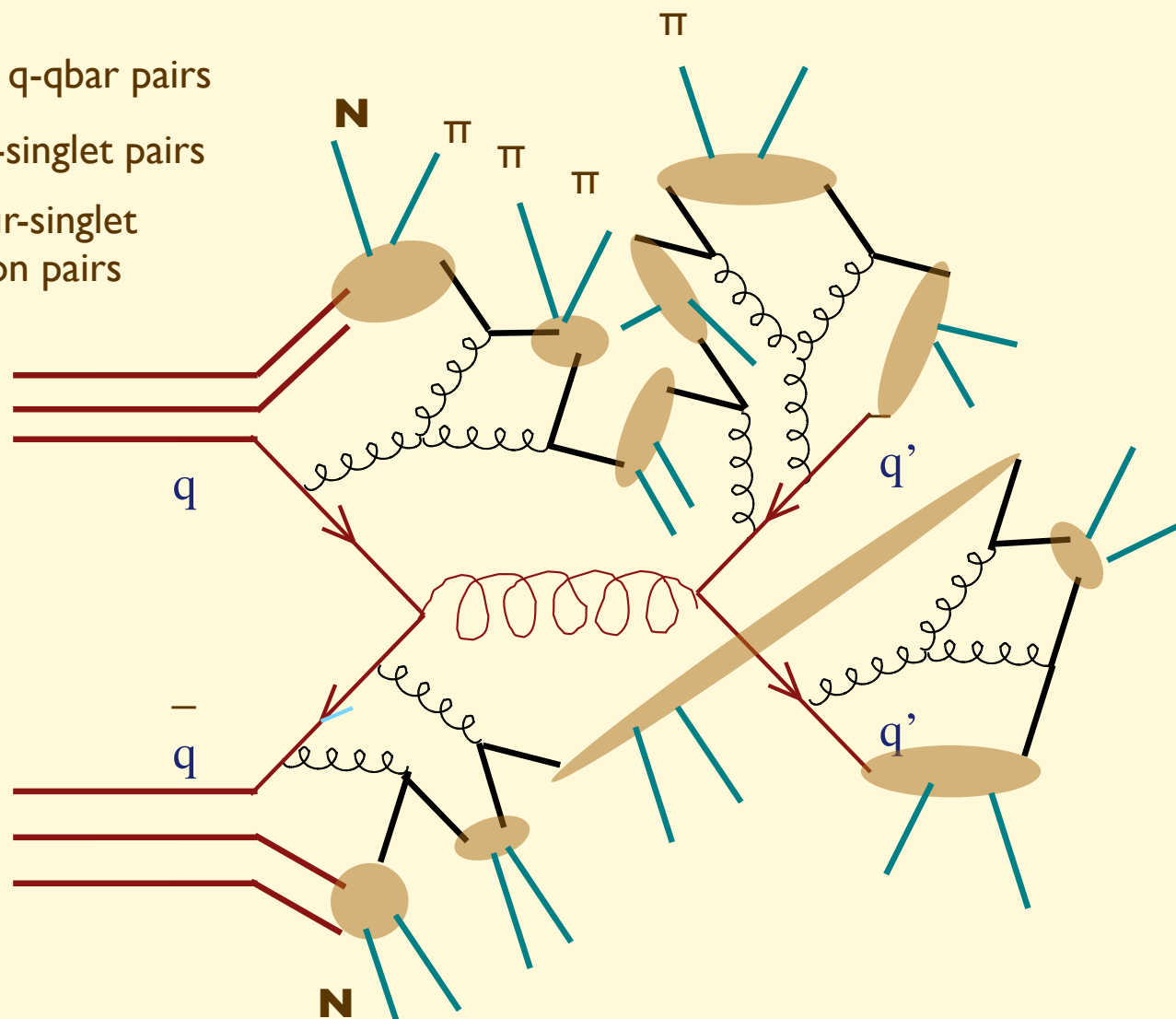
# The shower algorithm

Sequential probabilistic evolution (Markov chain)



The probability of each emission only depends on the state of the splitting parton, and of the daughters. The QCD dynamics is encoded in these splitting probabilities.

The total probability of all possible evolutions is **1** (unitary evolution).
- The shower evolution does not change the event rate inherited from the parton level, matrix element computation.
- No K-factors from the shower, even though the shower describes higher-order corrections to the leading-order process

# Single emission
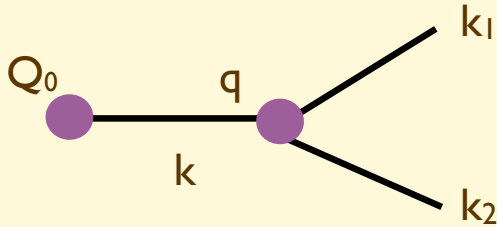


$$\frac{d\mathrm{Prob}(Q_0 \to q^2)}{dq^2\, dz\, d\phi} = P_0 \frac{\alpha_s(\mu)}{2\pi}\frac{1}{q^2}P(z)$$

$P_0 \Rightarrow \int d\,\mathrm{Prob} = 1$

**$q^2 \approx$** virtuality scale of the branching:

- **$(k_1 + k_2)^2$**
- **$k_1 \cdot k_2$**
- **$k_\perp^2$**

- **....**

**$\phi$** = azimuth

**z=P($k_2$)/P(k)$\approx$** energy/momentum fraction carried by one of the two partons after splitting

- **P=$k^0$**
- **P=$k^{/\!/}$**
- **P=$k^{/\!/} + k^0$**
- **...**

**$\mu$ = f(z,q)**

While at leading-logarithmic order (LL) all choices of evolution variables and of scale for αs are equivalent, specific choices can lead to improved description of NLL effects and allow a more accurate and easy-to-implement inclusion of angular-ordering constraints and mass effects, as well as to a better merging of multijet ME's with the shower
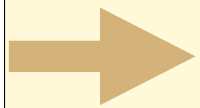
# Multiple emission
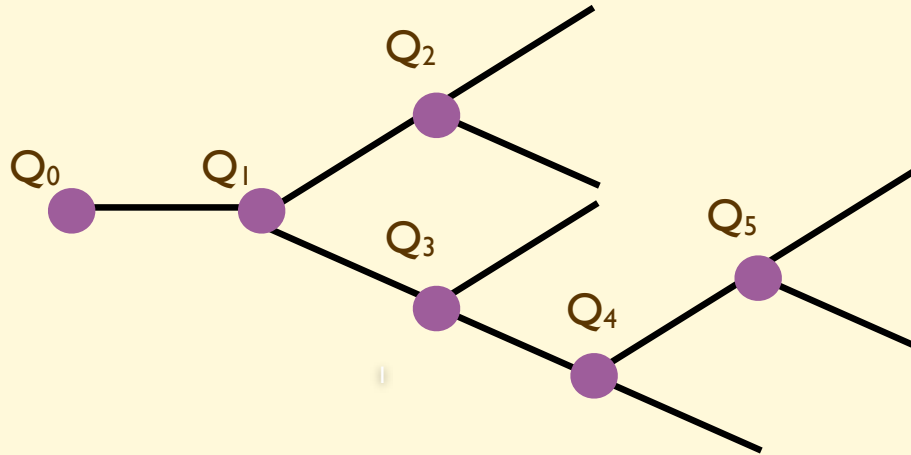


$$\text{Prob}(Q_0 \to Q_1) = P_0 \frac{\alpha_s}{2\pi} \int_{Q_1}^{Q_0} \frac{dq^2}{q^2} dz P(z) d\phi$$

$$\text{Prob}(Q_0 \to Q_1 \to Q_2) = P_0 \frac{\alpha_s}{2\pi} \int_{Q_1}^{Q_0} \frac{dq^2}{q^2} dz P(z) d\phi \frac{\alpha_s}{2\pi} \int_{Q_2}^{Q_1} \frac{dq^2}{q^2} dz P(z) d\phi$$

$$\sim P_0 \frac{1}{2!} [\frac{\alpha_s}{2\pi} \int_{Q_1}^{Q_0} \frac{dq^2}{q^2} dz P(z) d\phi]^2$$

$$\text{Prob}(Q_0 \to X) = P_0 \times \sum \frac{1}{n!} [\frac{\alpha_s}{2\pi} \int_{\Lambda}^{Q_0} \frac{dq^2}{q^2} dz P(z) d\phi]^n = 1 \qquad \Lambda = \text{infrared cutoff}$$
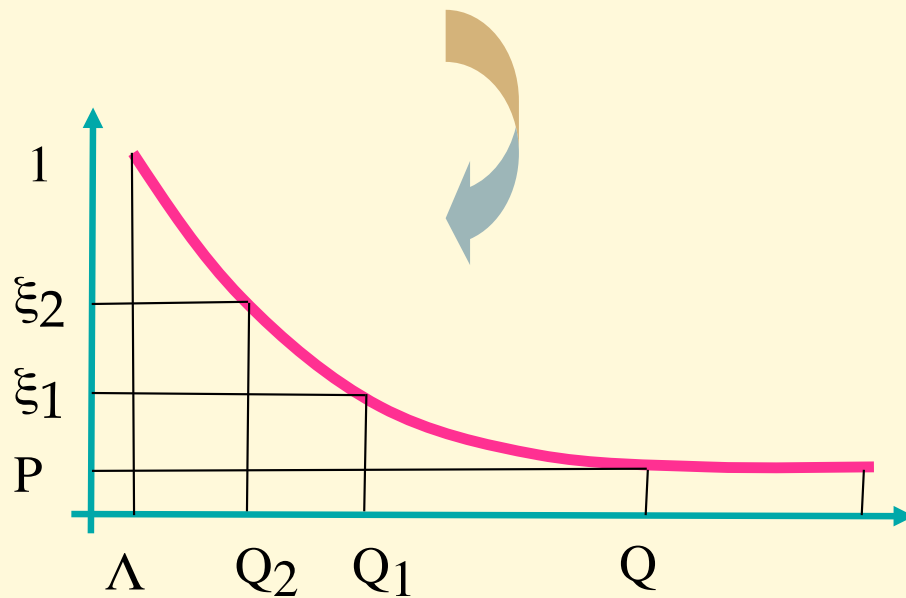
$$P_0 = \exp\{-\frac{\alpha_s}{2\pi} \int_{\Lambda}^{Q_0} \frac{dq^2}{q^2} dz P(z) d\phi\}$$

$P_0$ = Sudakov form factor
~ probability of no emission
between the scale $Q_0$ and $\Lambda$

14

# Generation of splittings

$$P(Q,\Lambda) = exp\left[-\int_\Lambda^Q \frac{dq^2}{q^2}\frac{\alpha_s(q)}{2\pi}P(z)dz\right]$$
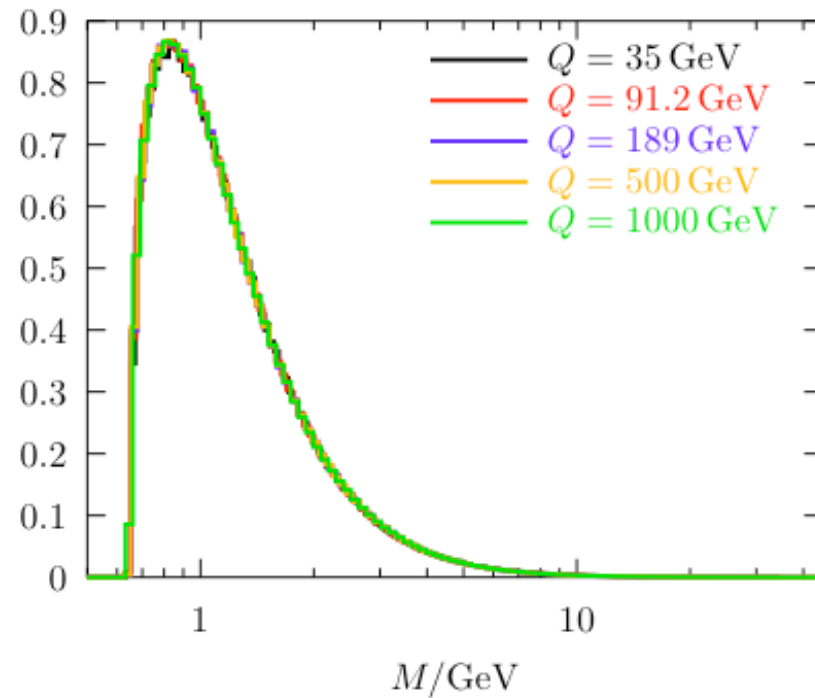
prob. of no radiation between Q and Λ

1. Generate $0 < \xi_1 < 1$

2. If $\xi_1 < P(Q,\Lambda) \Rightarrow$ no radiation, q' goes directly on-shell at scale Λ≈GeV

3. Else
   1. calculate $Q_1$ such that $P(Q_1,\Lambda) = \xi_1$
   2. emission at scale $Q_1$:

   $Q_1$

4. Select z according to P(z)

5. Reconstruct the full kinematics of the splitting

6. Go back to 1) and reiterate, until shower stops in 2). At each step the probability of emission gets smaller and smaller

1

$\xi_2$

$\xi_1$

P

Λ    $Q_2$   $Q_1$       Q

The existence of high-mass clusters, however rare, is unavoidable, due to IR cutoff which leads to a non-zero probability that no emission takes place. This is particularly true for evolution of massive quarks (as in, e.g. Z→bb or cc). Prescriptions have to be defined to deal with the "evolution" of these clusters. **This has an impact on the z→1 behaviour of fragmentation functions.**

Phenomenologically, this leads to uncertainties, for example, in the background rates for H→γγ (jet→γ).

**This approach is extremely successful in describing the properties of hadronic final states!**

**Ex: Particle multiplicities:**

**Table 2:** Multiplicities per event at 91.2 GeV. We show results from Herwig++ with the implementation of the old cluster hadronization model (Old Model) and the new model (Herwig++), and from HERWIG 6.5 shower and hadronization (Fortran). Parameter values used are given in table 1. Experiments are Aleph(A), Delphi(D), L3(L), Opal(O), Mk2(M) and SLD(S). The ∗ indicates a prediction that differs from the measured value by more than three standard deviations.

| Particle | Experiment | Measured | Old Model | Herwig++ | Fortran |
|---|---|---|---|---|---|
| All Charged | M,A,D,L,O | $20.924 \pm 0.117$ | 20.22* | 20.814 | 20.532* |
| $\gamma$ | A,O | $21.27 \pm 0.6$ | 23.03 | 22.67 | 20.74 |
| $\pi^0$ | A,D,L,O | $9.59 \pm 0.33$ | 10.27 | 10.08 | 9.88 |
| $\rho(770)^0$ | A,D | $1.295 \pm 0.125$ | 1.235 | 1.316 | 1.07 |
| $\pi^\pm$ | A,O | $17.04 \pm 0.25$ | 16.30 | 16.95 | 16.74 |
| $\rho(770)^\pm$ | O | $2.4 \pm 0.43$ | 1.99 | 2.14 | 2.06 |
| $\eta$ | A,L,O | $0.956 \pm 0.049$ | 0.886 | 0.893 | 0.669* |
| $\omega(782)$ | A,L,O | $1.083 \pm 0.088$ | 0.859 | 0.916 | 1.044 |
| $\eta'(958)$ | A,L,O | $0.152 \pm 0.03$ | 0.13 | 0.136 | 0.106 |
| $K^0$ | S,A,D,L,O | $2.027 \pm 0.025$ | 2.121* | 2.062 | 2.026 |
| $K^*(892)^0$ | A,D,O | $0.761 \pm 0.032$ | 0.667 | 0.681 | 0.583* |
| $K^*(1430)^0$ | D,O | $0.106 \pm 0.06$ | 0.065 | 0.079 | 0.072 |
| $K^\pm$ | A,D,O | $2.319 \pm 0.079$ | 2.335 | 2.286 | 2.250 |
| $K^*(892)^\pm$ | A,D,O | $0.731 \pm 0.058$ | 0.637 | 0.657 | 0.578 |
| $\phi(1020)$ | A,D,O | $0.097 \pm 0.007$ | 0.107 | 0.114 | 0.134* |
| $p$ | A,D,O | $0.991 \pm 0.054$ | 0.981 | 0.947 | 1.027 |
| $\Delta^{++}$ | D,O | $0.088 \pm 0.034$ | 0.185 | 0.092 | 0.209* |
| $\Sigma^-$ | O | $0.083 \pm 0.011$ | 0.063 | 0.071 | 0.071 |
| $\Lambda$ | A,D,L,O | $0.373 \pm 0.008$ | 0.325* | 0.384 | 0.347* |
| $\Sigma^0$ | A,D,O | $0.074 \pm 0.009$ | 0.078 | 0.091 | 0.063 |
| $\Sigma^+$ | O | $0.099 \pm 0.015$ | 0.067 | 0.077 | 0.088 |
| $\Sigma(1385)^\pm$ | A,D,O | $0.0471 \pm 0.0046$ | 0.057 | 0.0312* | 0.061* |
| $\Xi^-$ | A,D,O | $0.0262 \pm 0.001$ | 0.024 | 0.0286 | 0.029 |
| $\Xi(1530)^0$ | A,D,O | $0.0058 \pm 0.001$ | 0.026* | 0.0288* | 0.009* |
| $\Omega^-$ | A,D,O | $0.00125 \pm 0.00024$ | 0.001 | 0.00144 | 0.0009 |
| $f_2(1270)$ | D,L,O | $0.168 \pm 0.021$ | 0.113 | 0.150 | 0.173 |
| $f_2'(1525)$ | D | $0.02 \pm 0.008$ | 0.003 | 0.012 | 0.012 |
| $D^\pm$ | A,D,O | $0.184 \pm 0.018$ | 0.322* | 0.319* | 0.283* |
| $D^*(2010)^\pm$ | A,D,O | $0.182 \pm 0.009$ | 0.168 | 0.180 | 0.151* |
| $D^0$ | A,D,O | $0.473 \pm 0.026$ | 0.625* | 0.570* | 0.501 |
| $D_s^\pm$ | A,O | $0.129 \pm 0.013$ | 0.218* | 0.195* | 0.127 |
| $D_s^{*\pm}$ | O | $0.096 \pm 0.046$ | 0.082 | 0.066 | 0.043 |
| $J/\Psi$ | A,D,L,O | $0.00544 \pm 0.00029$ | 0.006 | 0.00361* | 0.002* |
| $\Lambda_c^+$ | D,O | $0.077 \pm 0.016$ | 0.006* | 0.023* | 0.001* |
| $\Psi'(3685)$ | D,L,O | $0.00229 \pm 0.00041$ | 0.001* | 0.00178 | 0.0008* |

17

# Ex: Energy distributions

(Winter, Krauss, Soff,
 hep-ph/0311085)



## Charged particle scaled momentum distribution

cm energy = 91.2 GeV

Experimental data
○ OPAL
▼ DELPHI
✕ SLD

uds only

MC simulations

**PYTHIA-6.1**

**HERWIG-6.1**

**SHERPA preliminary**

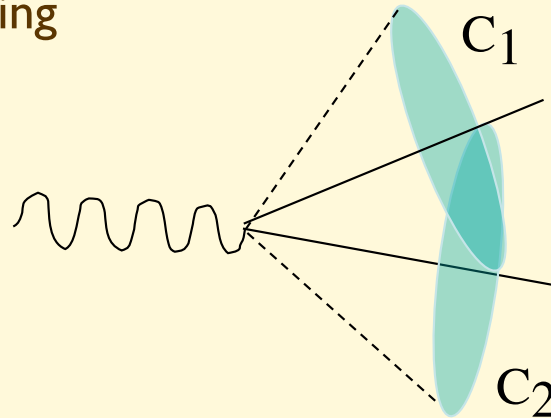mean: 0.0616581     mean: 0.0637626     mean: 0.0605735

$x_p^{uds}$
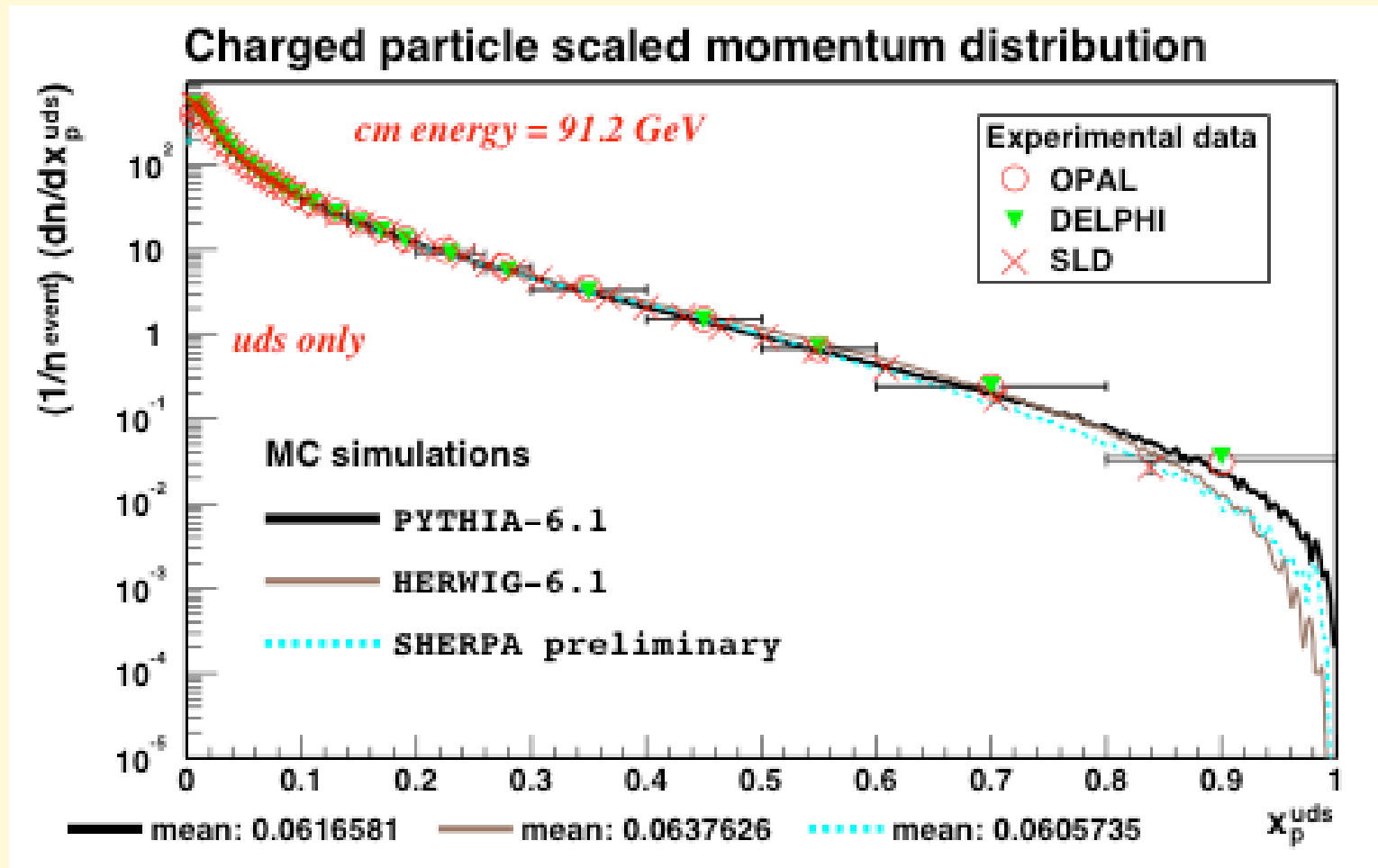
## Ex: Transverse momenta w.r.t. thrust axis:
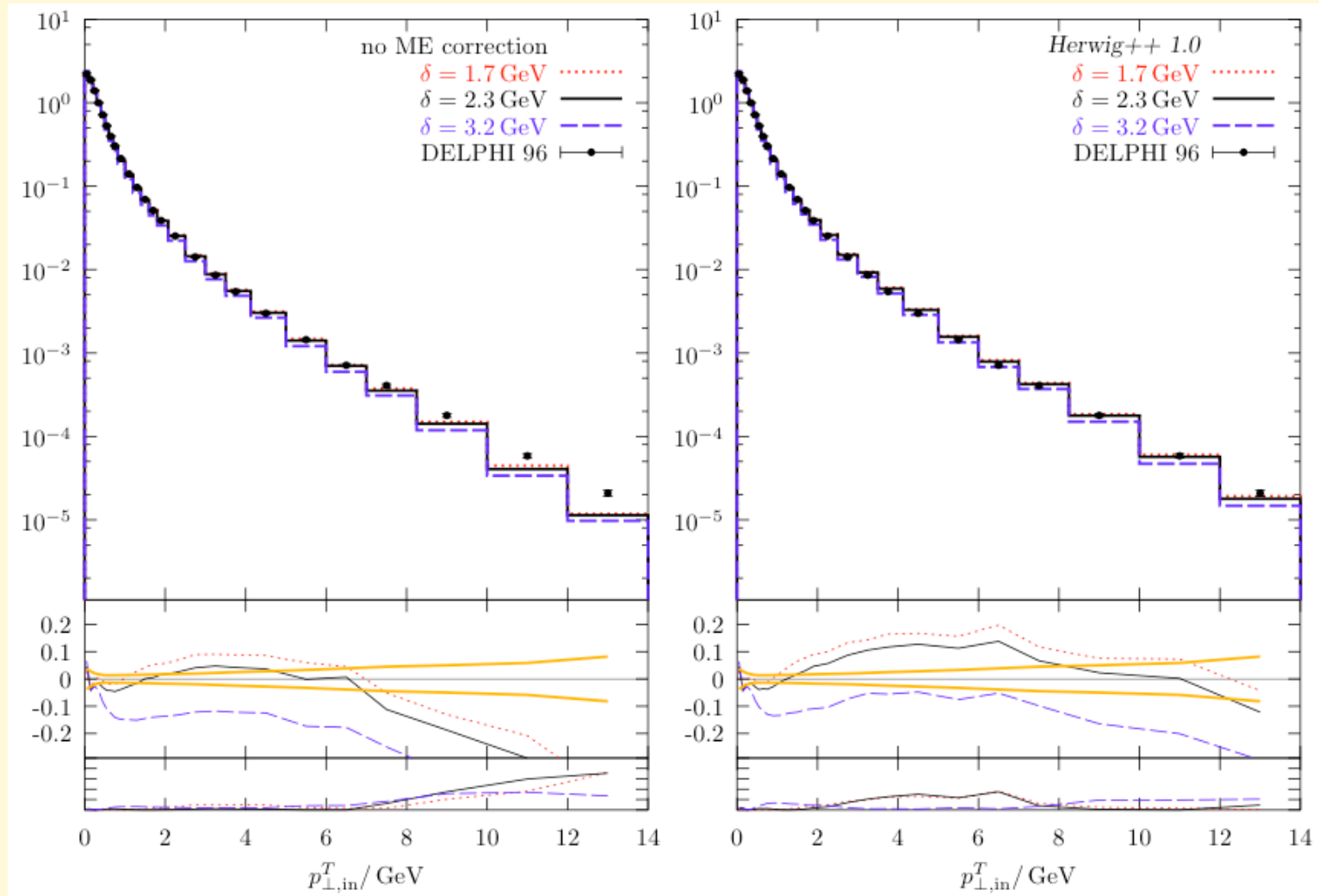
# Main limitation of shower approach:

Because of angular ordering



➡️ **no emission outside $C_1 \oplus C_2$:**

- lack of hard, large-angle emission
- poor description of multijet events

➡️ **incoherent emission inside $C_1 \oplus C_2$:**

- loss of accuracy for intrajet radiation

# Example



Z+ N jet, LHC, pT>30 GeV
Integrated pT rate of N−th jet
solid: Alpgen → Exact, LO matrix element estimate
dashes: Herwig ↘ Shower MC result

N=1
N=2
N=3
N=4

21
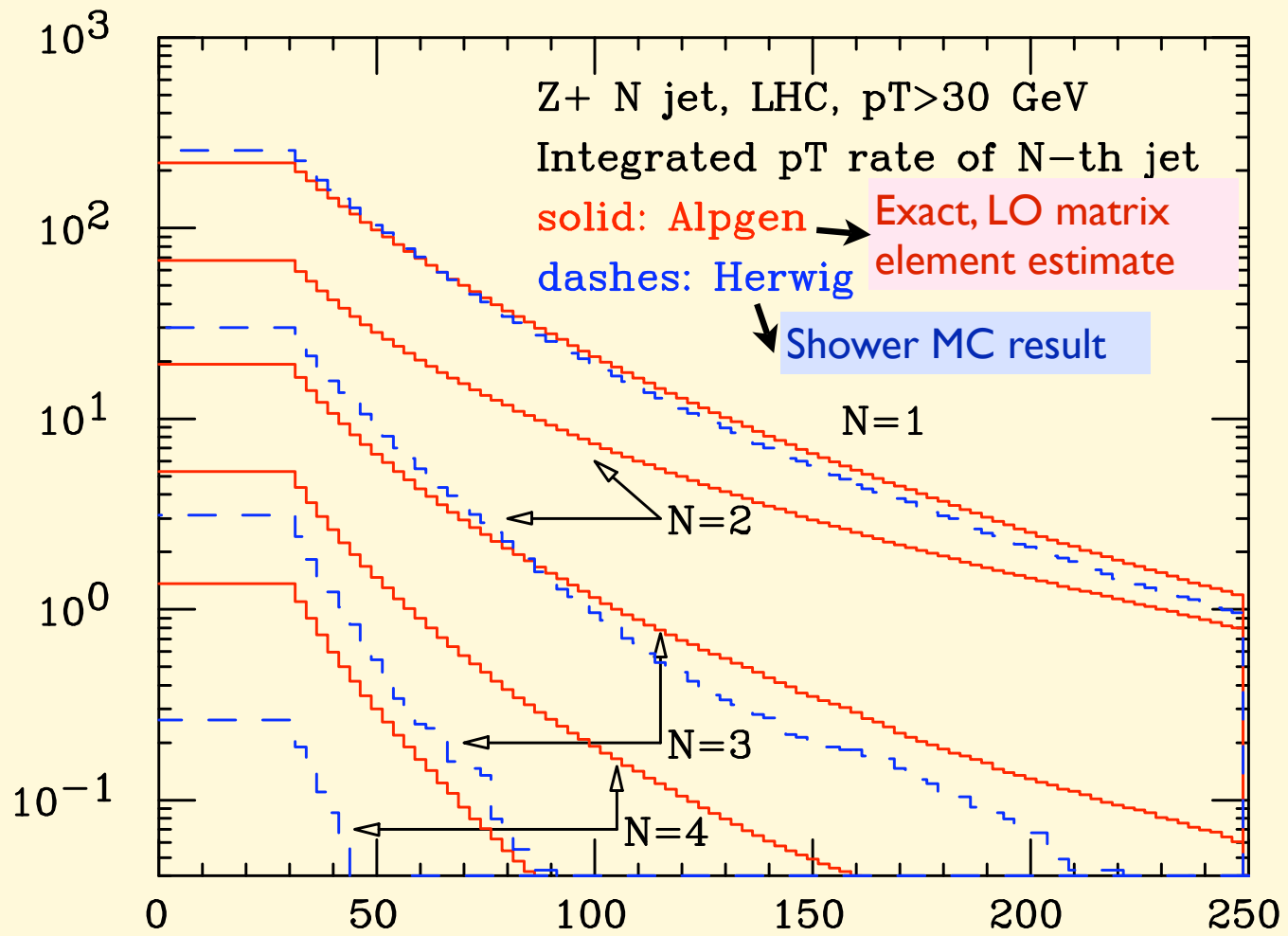
The obvious solution is to start the shower
from a higher-order process calculated at the
parton level with the exact LO matrix element:
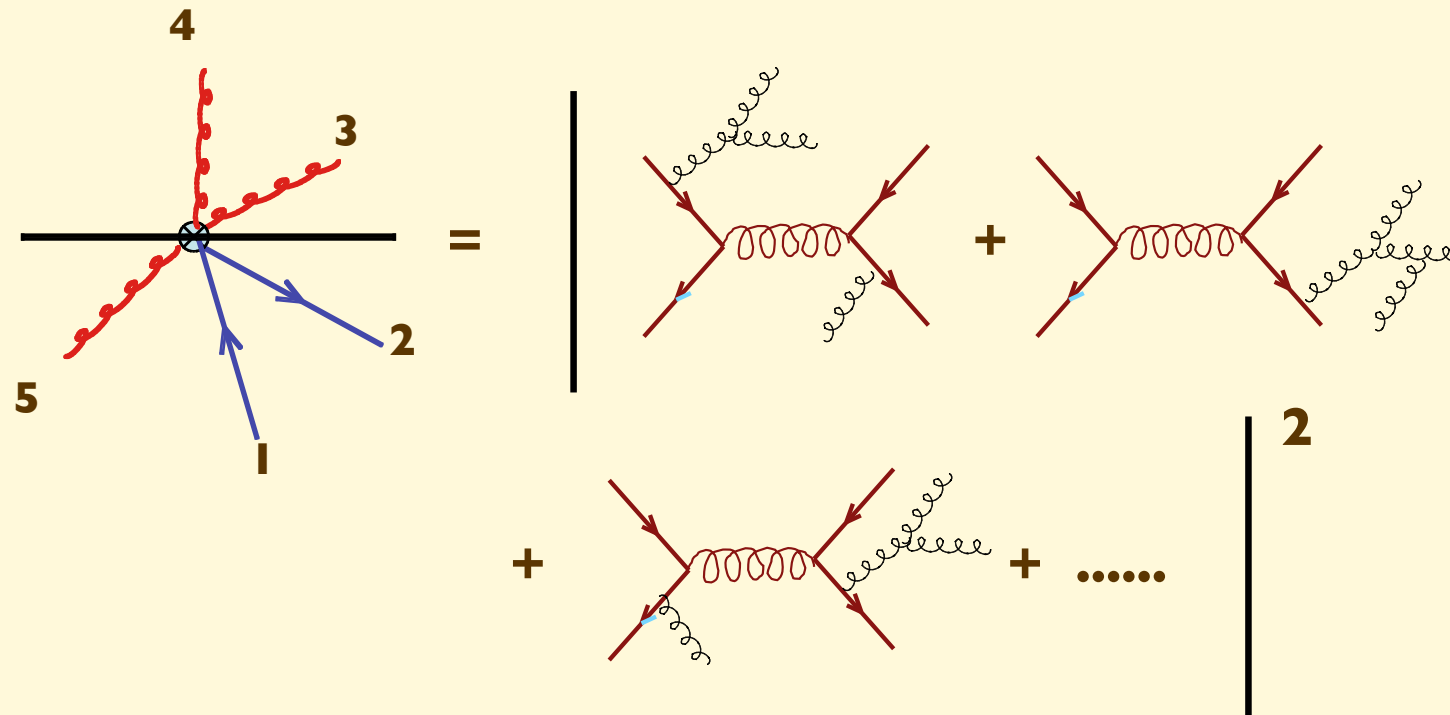


Each hard parton then undergoes the shower evolution according to the previous
prescription.

**This approach is also afflicted by difficulties:**



versus

with $P_{T1} \ll P_{T4} \ll P_{T2}, P_{T3}$

g2
g4 (from shower evolution)
g1 (from matrix element)
g3

g2
g1 (from shower evolution)
g4 (from matrix element)
g3
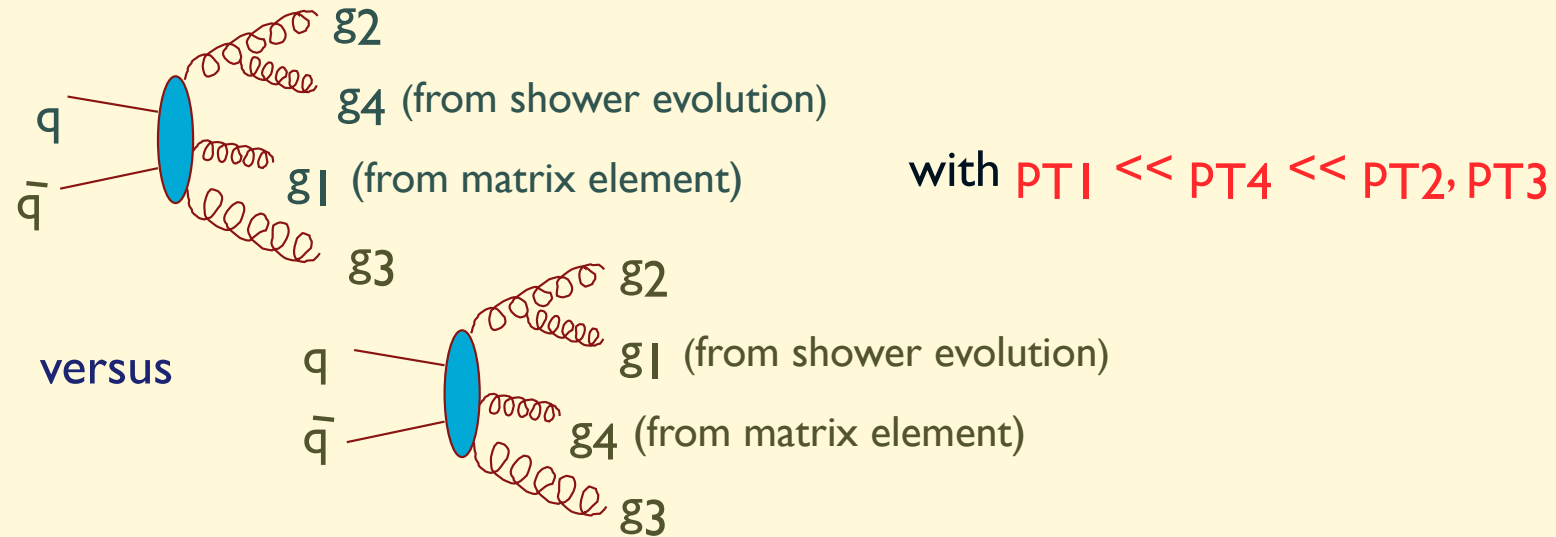
$\Rightarrow$ **double counting of the same phase-space points**

**Recent work started providing solutions to these problems, and new generations of MC codes successfully combine higher-order ME and shower evoloution** ("CKKW", "MLM matching")

# COMPLEMENTARITY OF THE 3 TOOLS

| | ME MC's | X-sect evaluators | Shower MC's |
|---|---|---|---|
| Final state description | Hard partons → jets. Describes geometry, correlations, etc | Limited access to final state structure | Full information available at the hadron level |
| Higher order effects: loop corrections | Hard to implement, require introduction of negative probabilities | Straighforward to implement, when available | Included as vertex corrections (Sudakov FF's) |
| Higher order effects: hard emissions | Included, up to high orders (multijets) | Straighforward to implement, when available | Approximate, incomplete phase space at large angle |

**Recent progress:**

MC@NLO for full 1-loop corrections

New algorithms to merge hard ME with showers

24

# Introduction to hadronic collisions: theoretical concepts and practical tools for the LHC

## Lecture 4

*Weizmann Institute & Technion Institute*
*Dec 27 2006 - Jan 1 2007*

**Michelangelo L. Mangano**
TH Unit, Physics Dept, CERN
michelangelo.mangano@cern.ch

# Ex: Gluino pair production



$\sigma[q\bar{q} \rightarrow \tilde{g}\,\tilde{g}]$

$L[q\bar{q}]$

$\sigma[pp \rightarrow \tilde{g}\,\tilde{g}]$
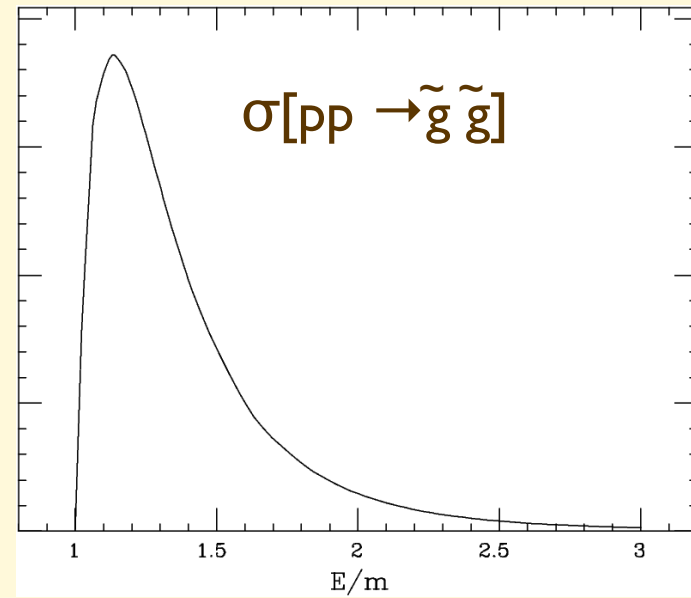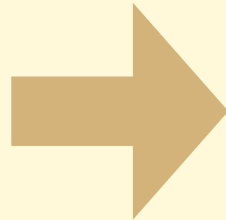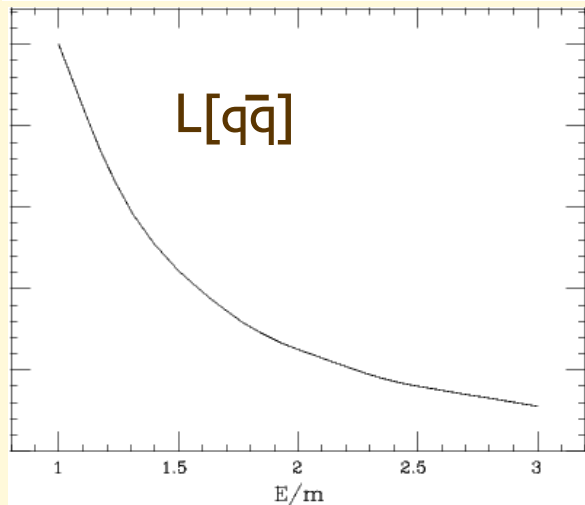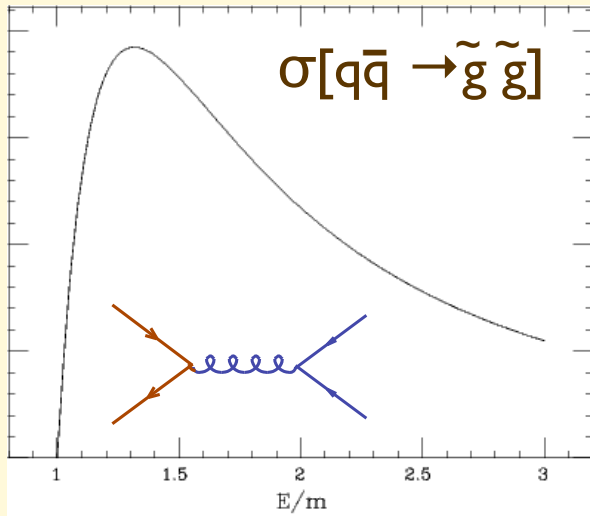
⇒ **slow gluinos,  β~0.5**

# Gluino final states



$\tilde{g}$
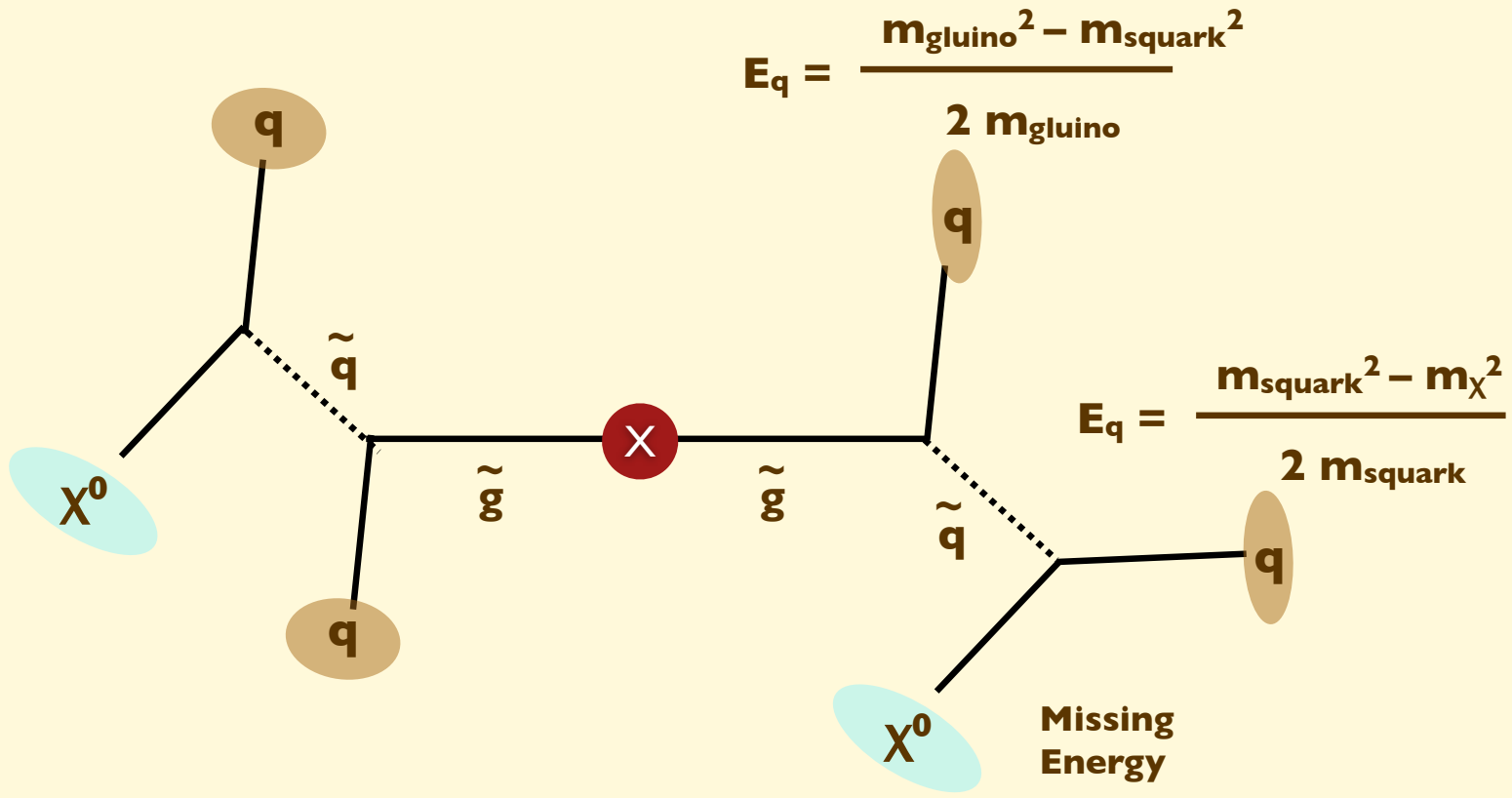
q jet

$\tilde{q}$

q jet

$X^0$ Missing Energy

$\tilde{g}$

q jet

$\tilde{q}$

$X^0{}_2$

q jet

$Z^0$

f

$\bar{f}$

$X^0$

Missing Energy

$\tilde{g}$

q jet

$\tilde{q}$

q jet

$X^\pm$

$W^\pm$

f

f'

$X^0$ Missing Energy

$\tilde{g} \rightarrow \geq 2$ jet $+$ MET $+ \geq 0\ \ell^\pm$

3

**Typical analysis cuts (ATLAS):**

$\geq$4jets, $E_T$>50 GeV      leading jet $E_T$>100 GeV

no lepton with $E_T$>20 GeV

MissET> max(100, 0.2 $M_{eff}$)

$M_{eff}$ = MET + $\sum_{i=1,..,4}$ $E_T^i$

Transverse sphericity > 0.2
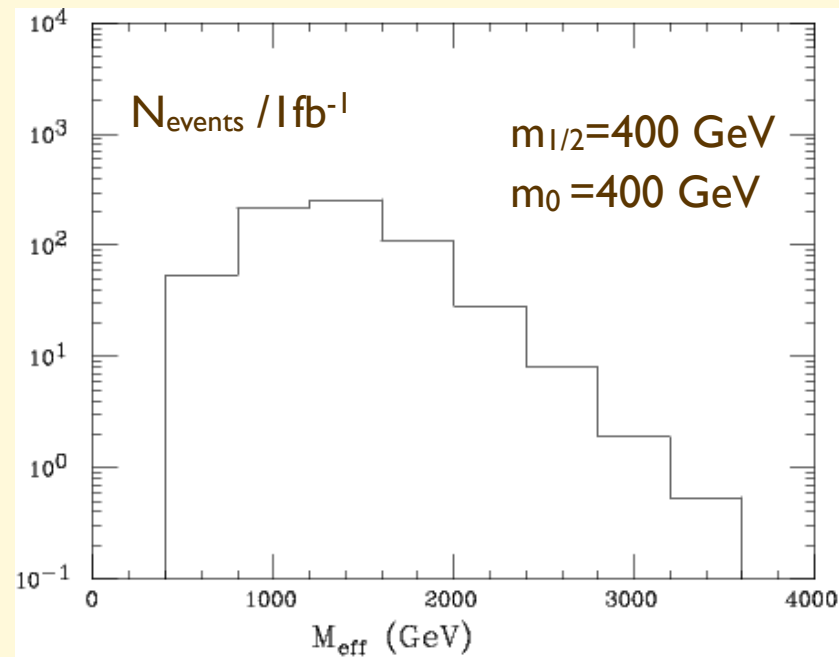
# SM Backgrounds

**Missing energy ⇒ νs ⇒ W/Z production**

**"Irreducible":** individual events cannot be distinguished from the signal

    **Z+4jets, Z→ νν**

**"Reducible":** individual events feature properties which distinguish them from the signal, but these can only be exploited with limited efficiency

  **W+3jets, W→ τν, τ→hadrons (jet)**

τ jet has low multiplicity, and originates from a displaced vertex, because of τs lifetime

  **W+4jets, W→ e/μ ν, lepton undetected**

e/μ can be detected, but cannot be vetoed with 100% efficiency, else the signal would be killed as well (e /μ may come from π conversions or decays)

  **tt → W+jets, with W→ leptons as above**

In addition to the above, top decays have b's, but these cannot be detected and vetoed with 100% efficiency

**"Instrumental":** individual events resemble the signal because of instrumental "effects" (namely instrumental deficiencies)

**Multijets**　　　　The missing ET may originate from several sources:

Mismeasurement of the energy of individual jets

Incomplete coverage in rapidity (forward jets undetected)

Accidental extra deposits of energy (cosmic rays on time, beam backgrounds, , electronic noise, etc.etc.etc.)



QCD, without MET cuts

SUSY

$M_{eff}$ (GeV)
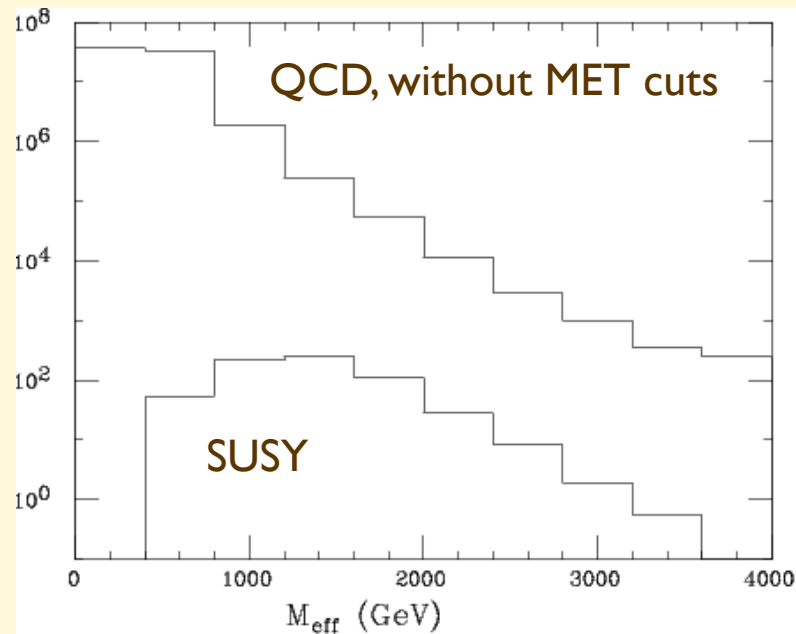
It is sufficient that these effects leave a permille fraction of the QCD rate for the signal to be washed away!

# Z(→νν) + jets

## 1. Shower MC vs Matrix element results



Z+ N jet, LHC, pT>30 GeV
Integrated pT rate of N−th jet
solid: Alpgen → Exact, LO matrix element estimate
dashes: Herwig → Shower MC result

N=1
N=2
N=3
N=4

# Z(→νν) + jets
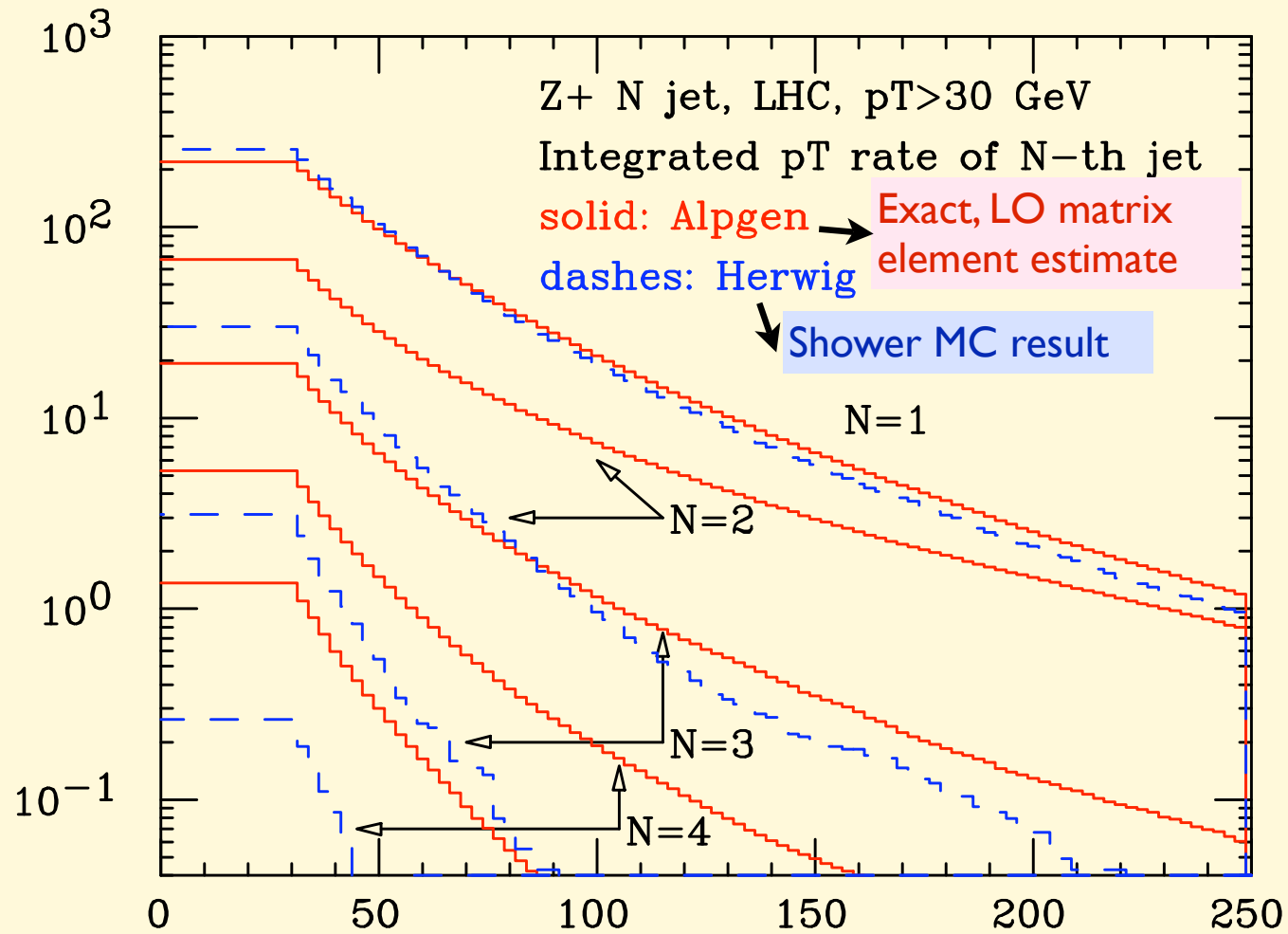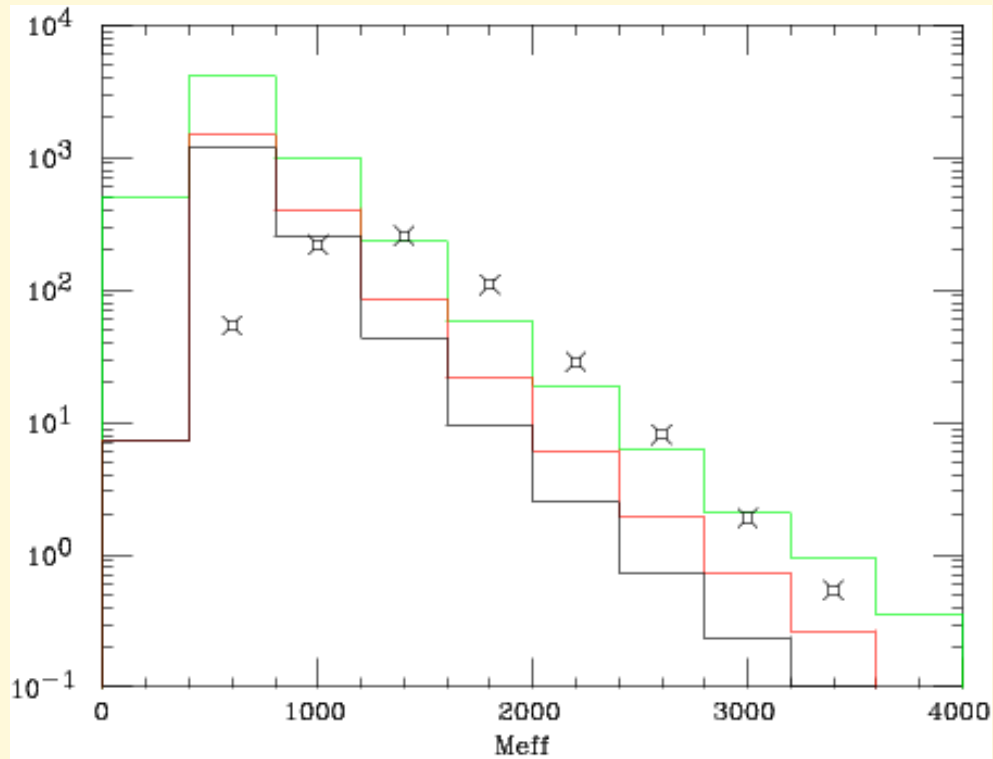
# Normalizing the bg rate using data ...

Use Z->ee + multijets, apply same cuts as MET analysis but replace MET with ET(e⁺e⁻)

Extract $Z \rightarrow \nu\nu$ bg using, bin-by-bin:
$(Z \rightarrow \nu\nu) = (Z \rightarrow ee)\ B(Z \rightarrow \nu\nu)/B(Z \rightarrow ee)$

Assume that the SUSY signal is of the same size as the bg, and evaluate the luminosity required to determine the Z->nunu bg with an accuracy such that:

$$N_{susy} > 3\ \text{sigma}$$

where

$\text{sigma} = \text{sqrt}[\ N(Z \rightarrow ee)\ ] * B(Z \rightarrow \nu\nu)/B(Z \rightarrow ee)$
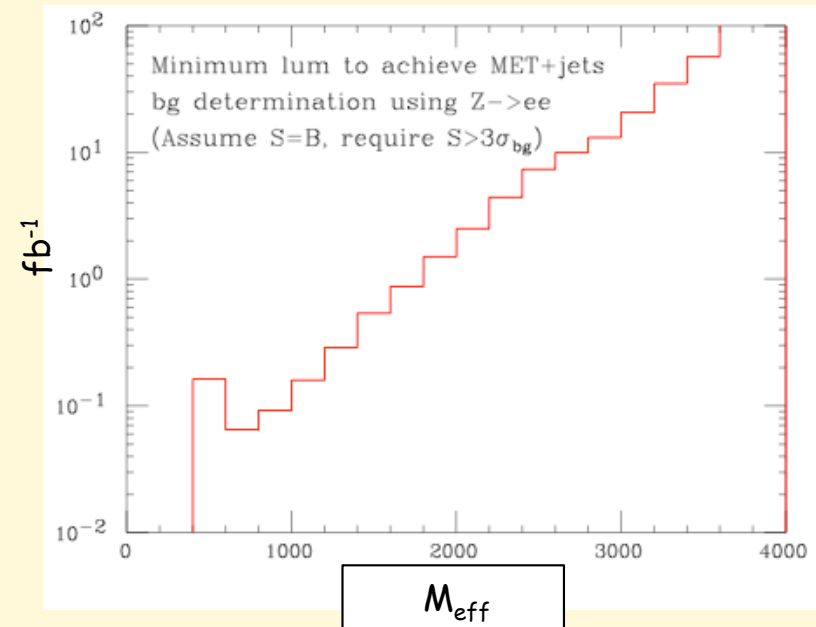


=> several hundred pb⁻¹ are required. They are sufficient if we believe in the MC shape (and only need to fix the overall normalization). Much ore is needed if we want to keep the search completely MC independent

# W(→lν) +4 jets
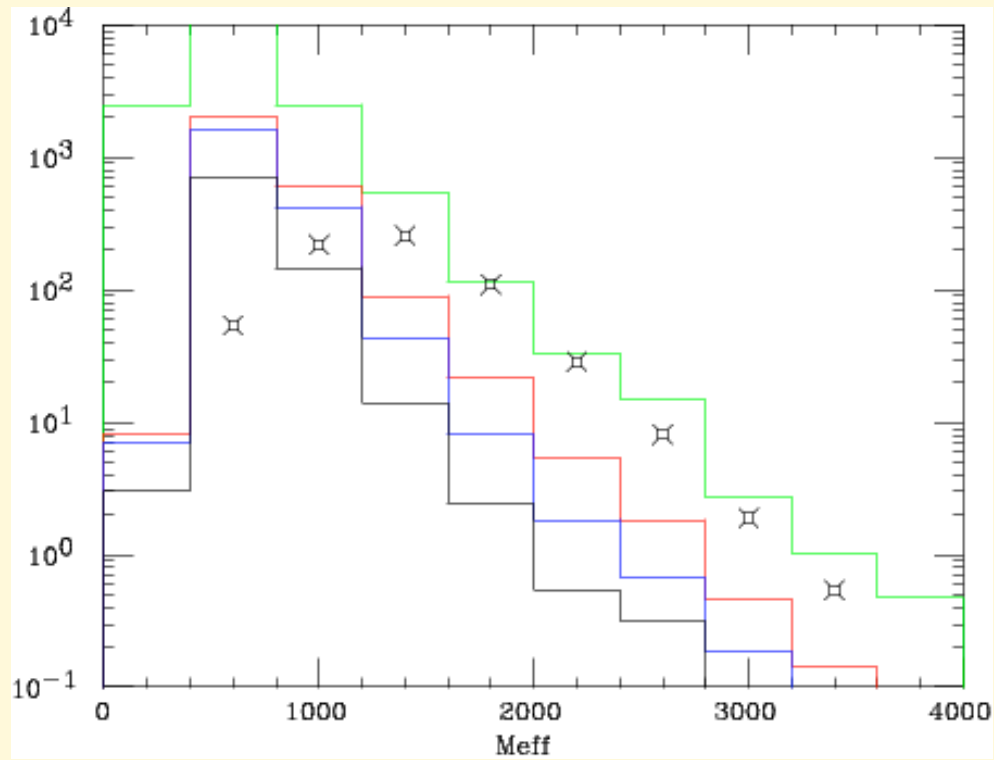


Jet cuts only

+ MET cut

+ ST cut

+ pt$_{lept}$<20

SUSY

# W(→tau-jet ν) + jets



W+3 jets

W+4 jets
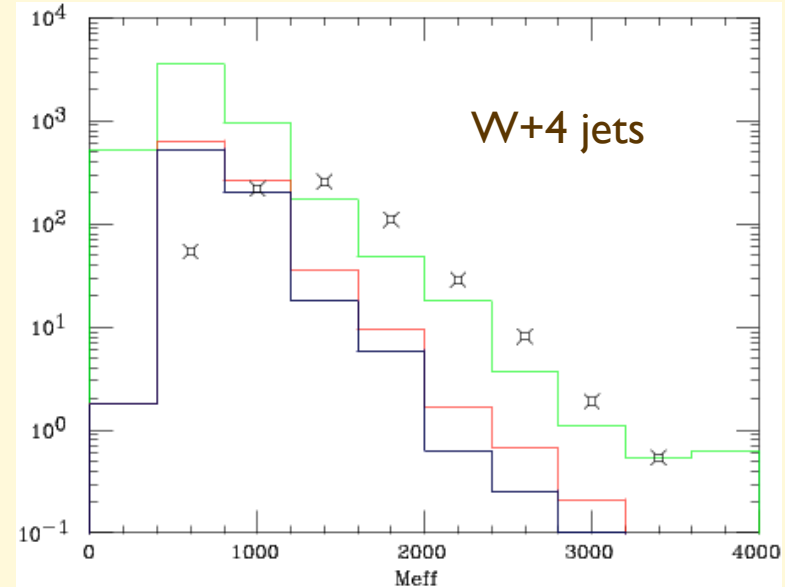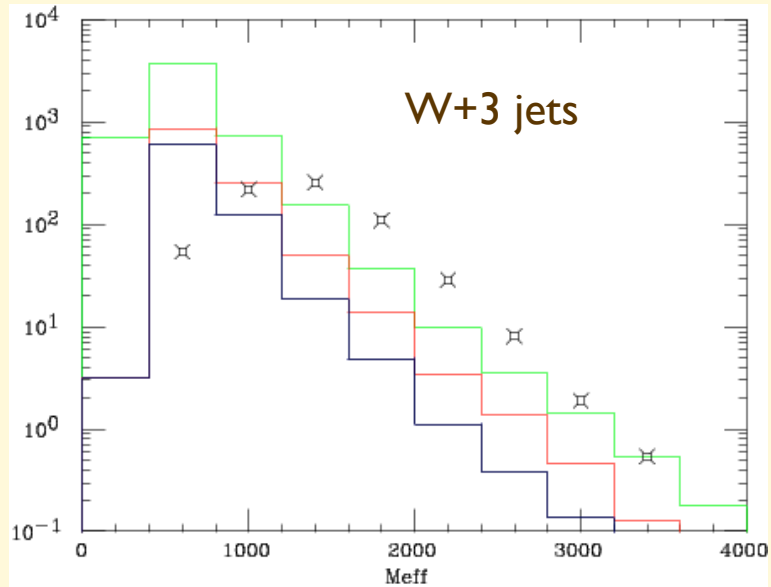
| | |
|---|---|
| —— (light green) | Jet cuts only |
| —— (red) | + MET cut |
| —— (blue) | + ST cut |
| —— (black) | + pt$_{lept}$<20 |
| ⋈ | SUSY |

# Top final states

# Top final states



**Rest frame**
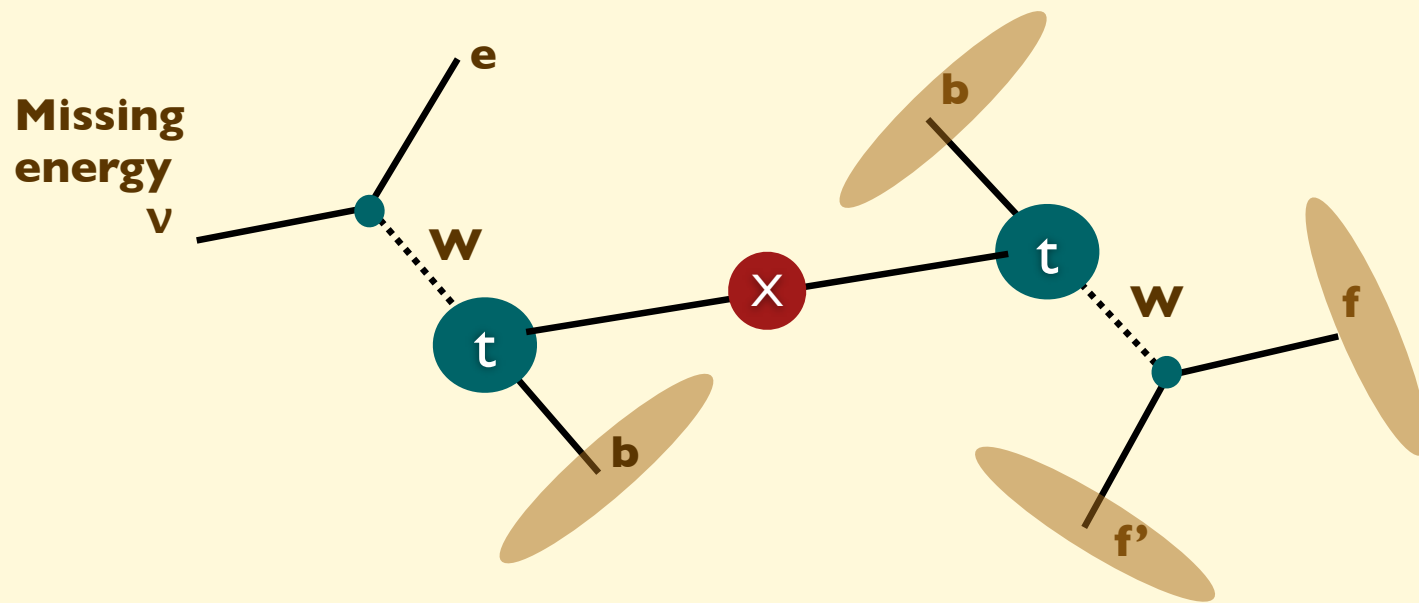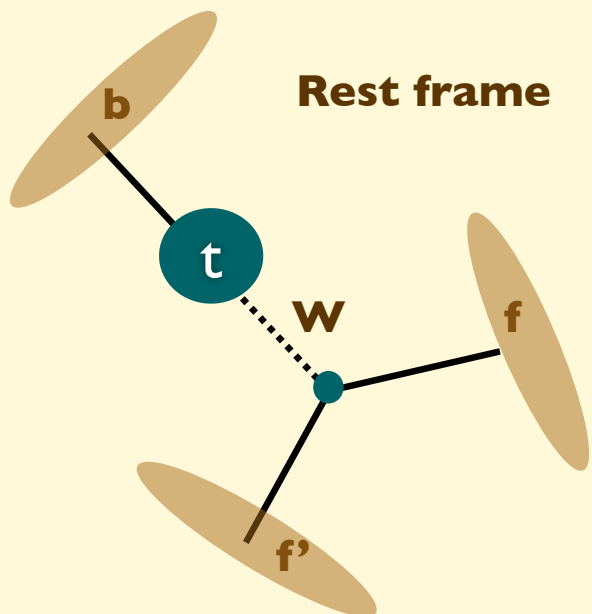
$$p_b = \frac{m_{top}^2 - m_W^2}{2\,m_{top}}$$

$$p_f^{max} = \frac{m_W}{2}\,\frac{m_{top}^2 + m_W^2}{2\,m_{top}\,m_W}$$

**Boosting the top ...**
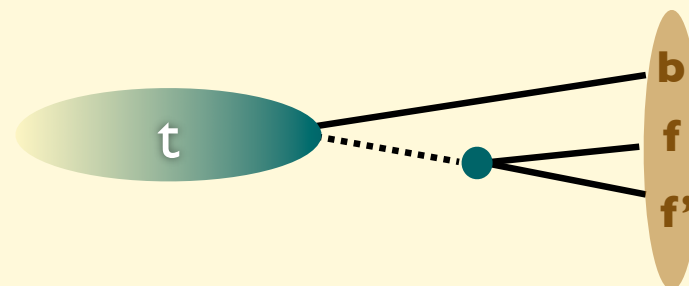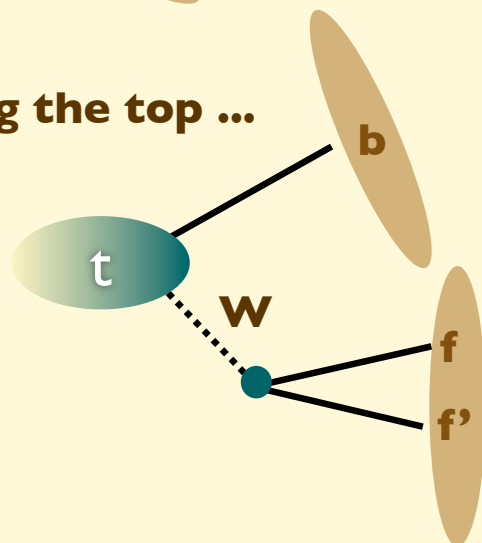
# Top final states
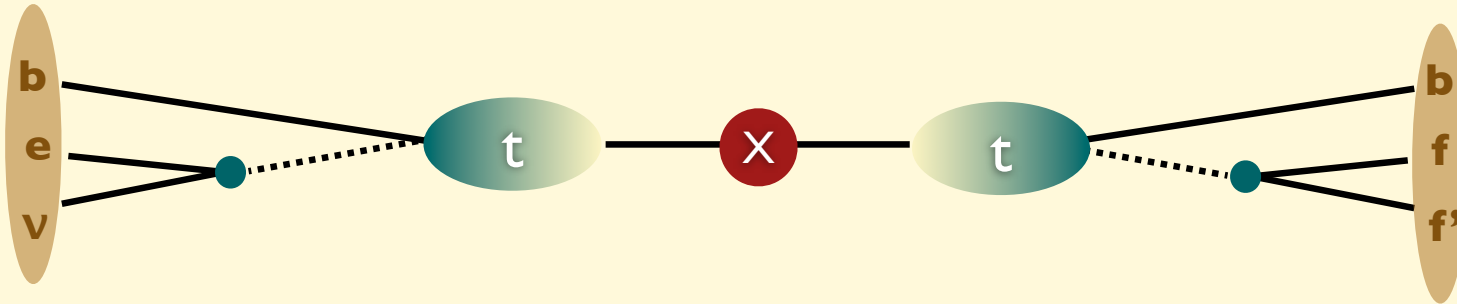


Large Meff leads to highly collimated final states

Sphericity and multi-jet cuts very effective against
the leading-order t-tbar contribution!

tt+1 jet

tt+2 jets

tt+3 jets
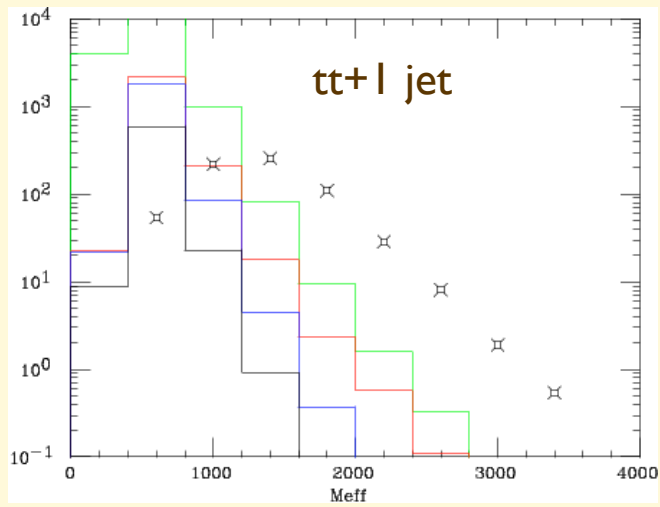
Jet cuts only

+ MET cut

+ ST cut

+ $pt_{lept}<20$

SUSY
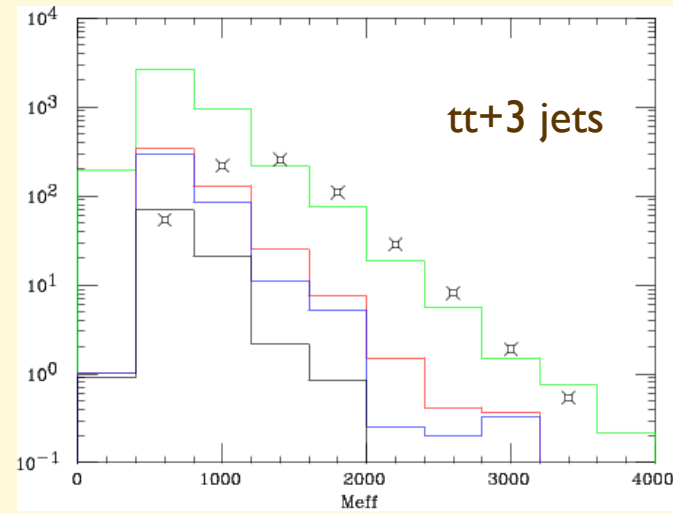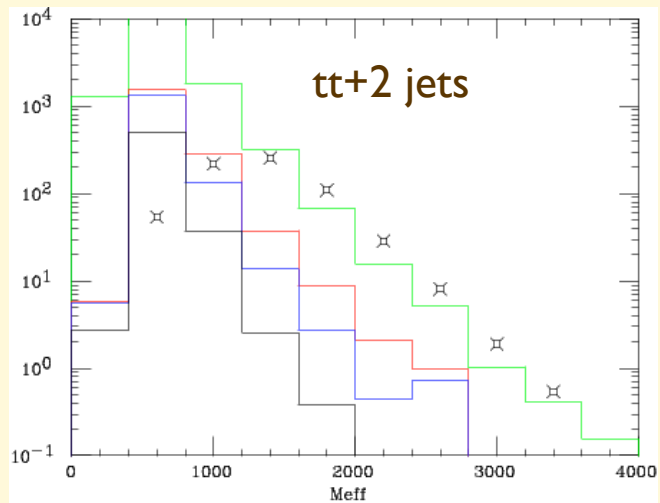
All jet multiplicities contribute at approximately the same level!!

**Instrumental sources of missET: incomplete calorimeter η coverage**



Undetected jet ⇒ missing ET

$\eta_{max}$
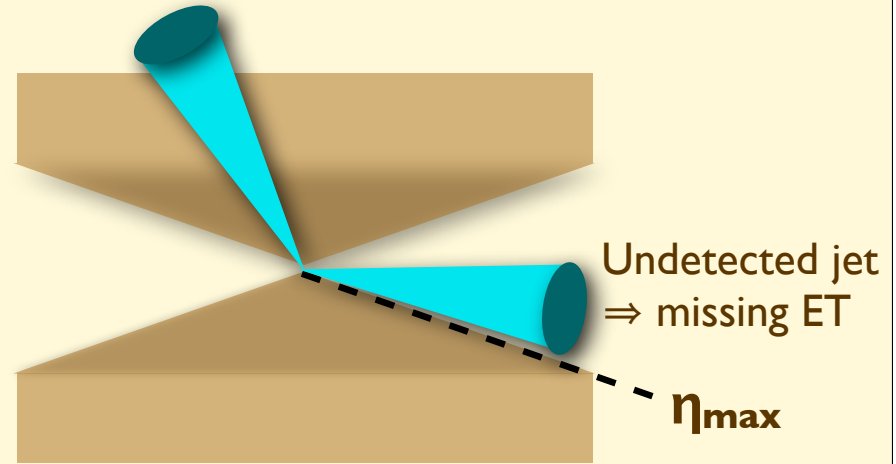
$\sigma$(jet-jet with MET> $E_{T0}$) / $\sigma$(pp→X)



$\eta_{max}$=3

$\eta_{max}$=4

$\eta_{max}$=5

$E_{T0}$ (GeV)
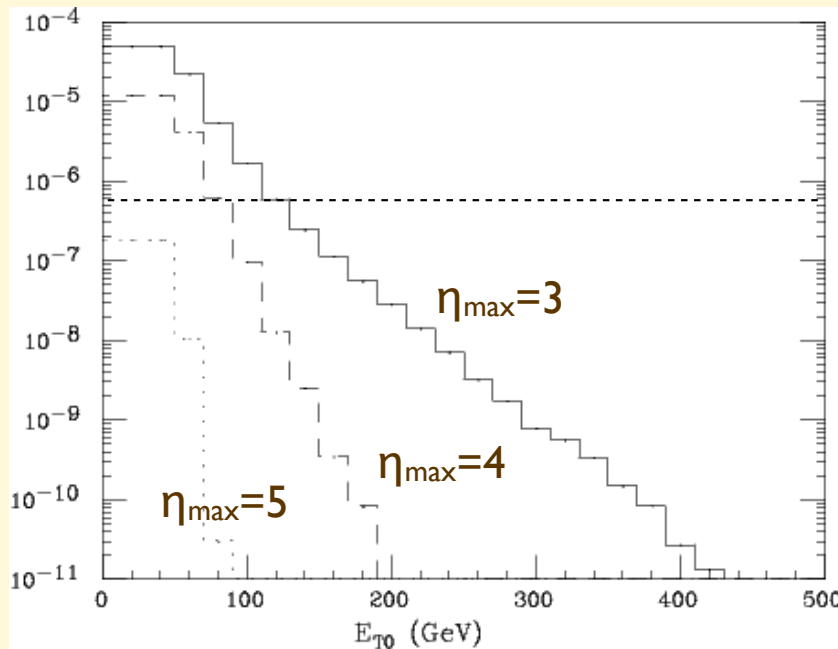
cfr:
$\sigma$(W→lν)/$\sigma$(pp→X) ≈ 6 x $10^{-7}$

**NB:**
At L=$10^{34}$ cm$^{-2}$ s$^{-1}$,
⟨N(pp collisions)⟩ ≈ 20

⇒ **probability 20x larger**

# Instrumental sources of missET:
## jet energy resolution
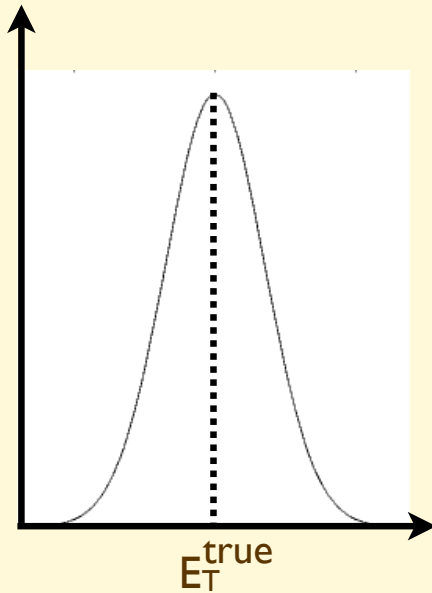


$$\mathrm{Prob}[p_T] \propto \exp{-\frac{(p_T - p_T^{\mathrm{true}})^2}{\sigma^2}}$$

$$\sigma = C\sqrt{E_T^{\mathrm{true}}/\mathrm{GeV}}, \quad C = O(1)$$
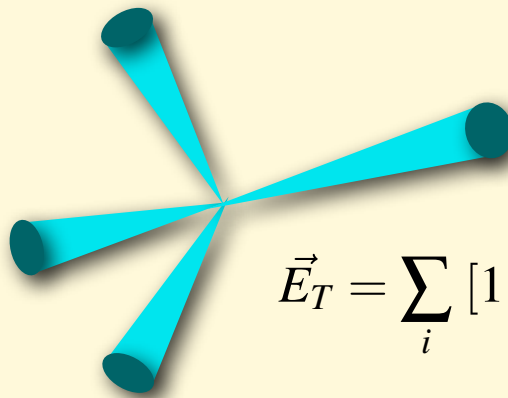
$$\vec{E}_T = \sum_i [1 + \delta_i]\, \vec{p}_{T,i}^{\,\mathrm{true}} = \sum_i \delta_i\, \vec{p}_{T,i}^{\,\mathrm{true}}$$

$$\langle |\vec{E}_T|^2 \rangle = \sum_{i,j} \langle \delta_i \delta_j \rangle\, \vec{p}_{T,i} \cdot \vec{p}_{T,j} \qquad \langle \delta_i \delta_j \rangle = \frac{C^2}{p_{T,i}} \delta_{ij}$$

$$\langle \mathrm{MET} \rangle = C\sqrt{\sum_i p_{T,i}}$$

18

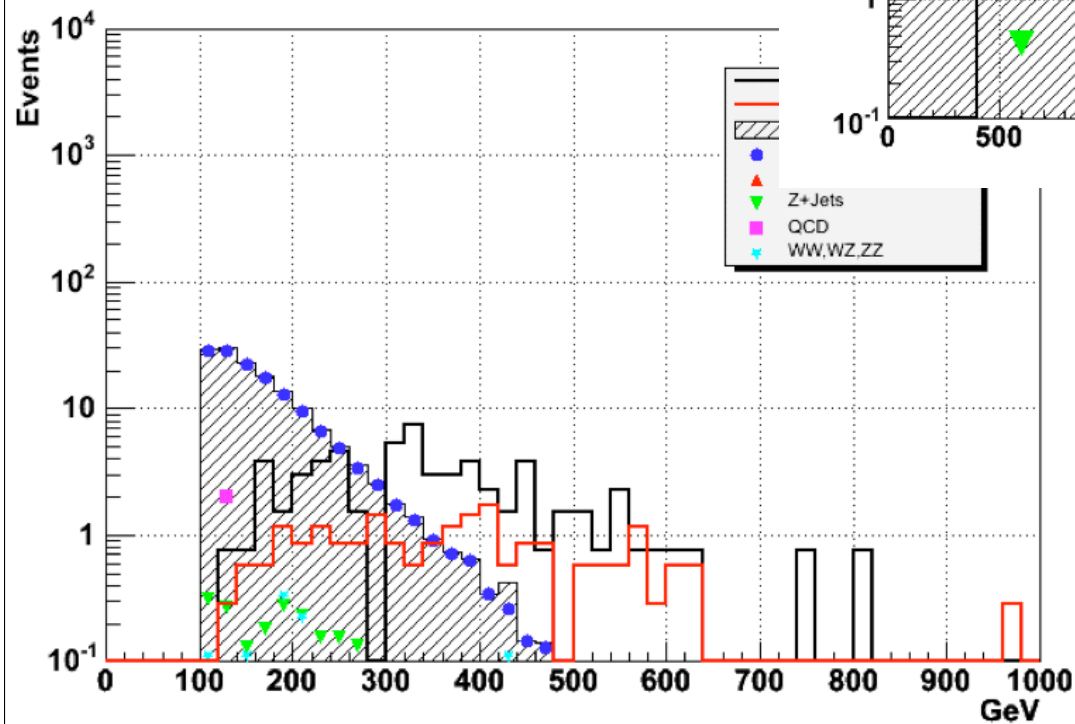# Overall result, after the complete detector simulation, etc....
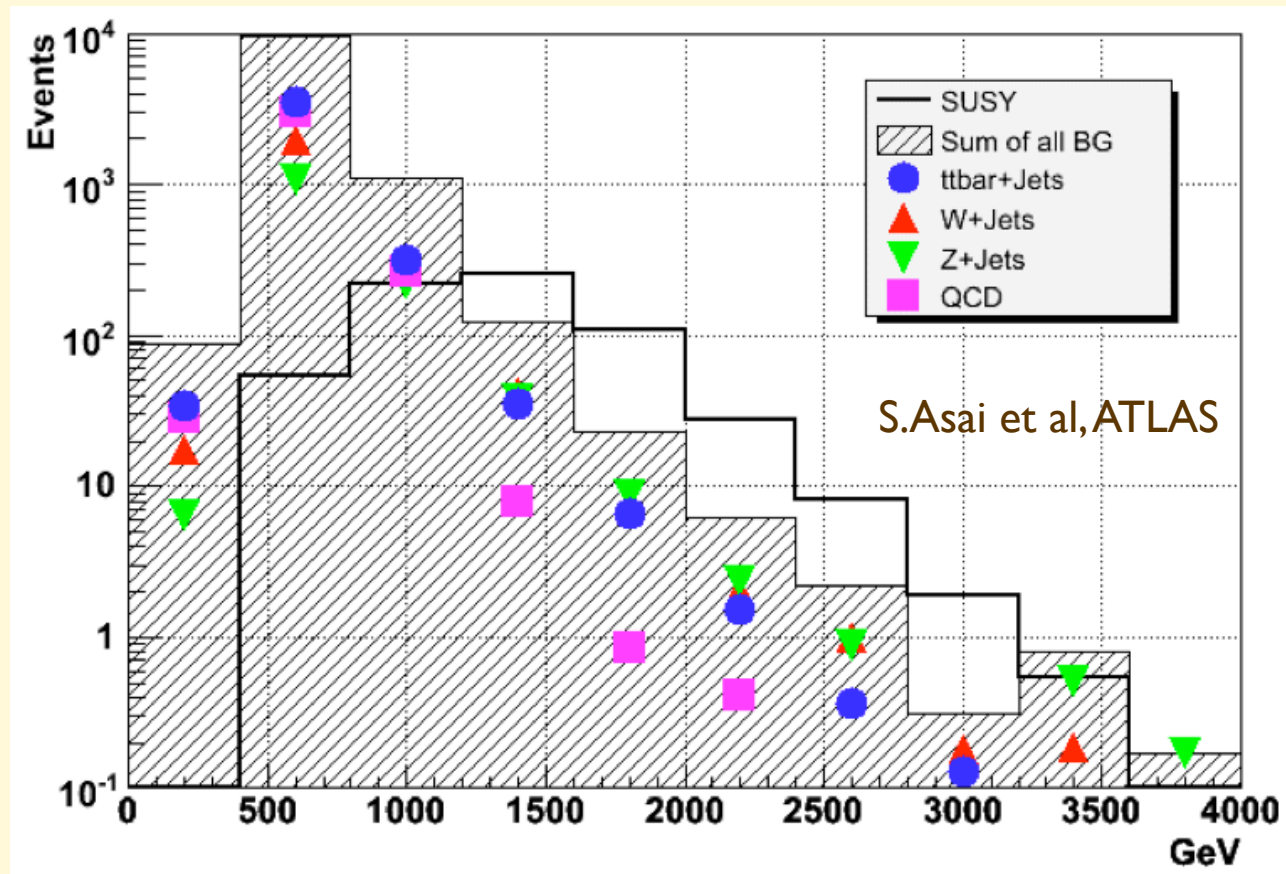


S.Asai et al, ATLAS

# Adding leptons ...

S. Asai et al, ATLAS
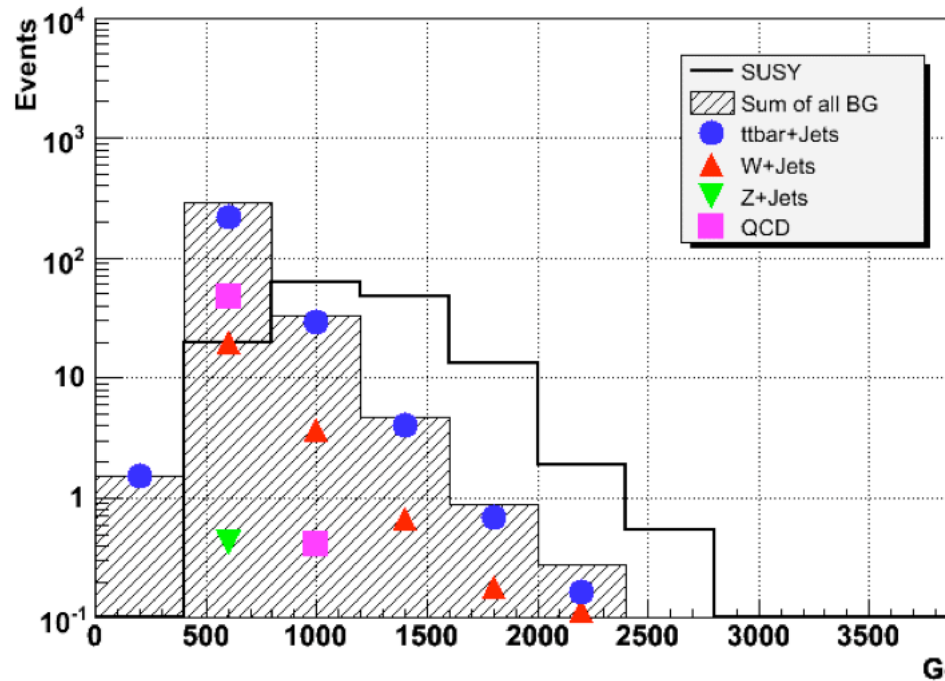
# Some properties of rates for multijet final states

# Multijet rates

| σ [μb] | N jet=2 | N jet=3 | N jet=4 | N jet=5 |
|---|---|---|---|---|
| $E_T^{jet}$ >20 GeV | 350 | 19 | 2.6 | 0.35 |
| $E_T^{jet}$ >50 GeV | 12.7 | 0.45 | 0.045 | 0.004 |
| $E_T^{jet}$ >100 GeV | 0.85 | 0.021 | 0.0015 | 0.0001 |



σ(3)/σ(2)     σ(4)/σ(3)     σ(5)/σ(4)

0.054   0.035   0.025
0.130   0.100   0.071
0.130   0.090   0.067

■ ET>20   ■ ET>50   ■ ET>100
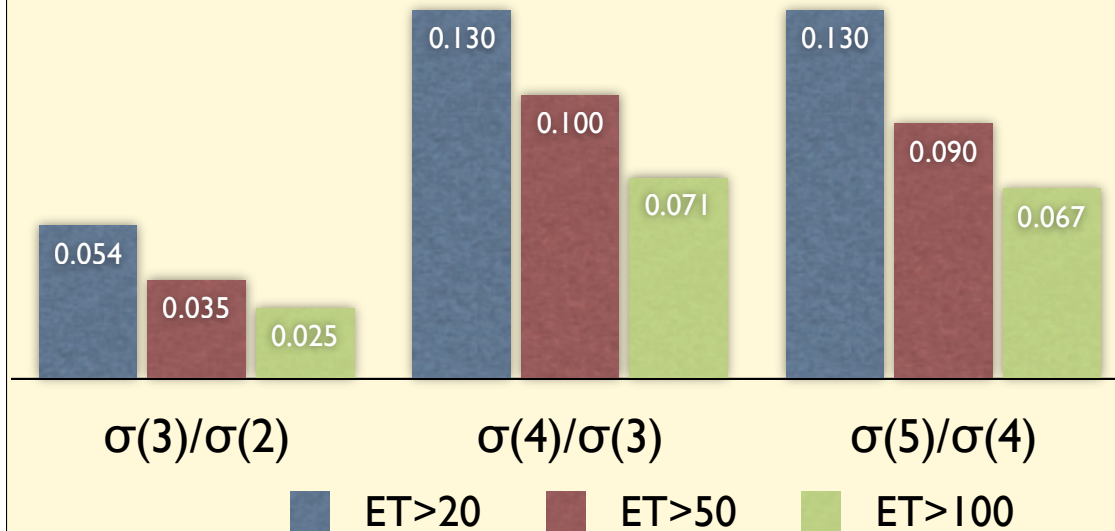
- The higher the jet $E_T$ threshold, the harder to emit an extra jet

- When several jets are already present, however, emission of an additional one is less suppressed

22

# Multijet rates, vs √s, with $E_T^{jet}$ > 20 GeV

| σ [μb] | N jet=2 | N jet=3 | N jet=4 | N jet=5 |
|---|---|---|---|---|
| √s > 100 GeV | 75 | 17.3 | 2.6 | 0.37 |
| √s > 500 GeV | 0.27 | 0.47 | 0.30 | 0.13 |
| √s > 1000 GeV | 0.012 | 0.021 | 0.022 | 0.031 |
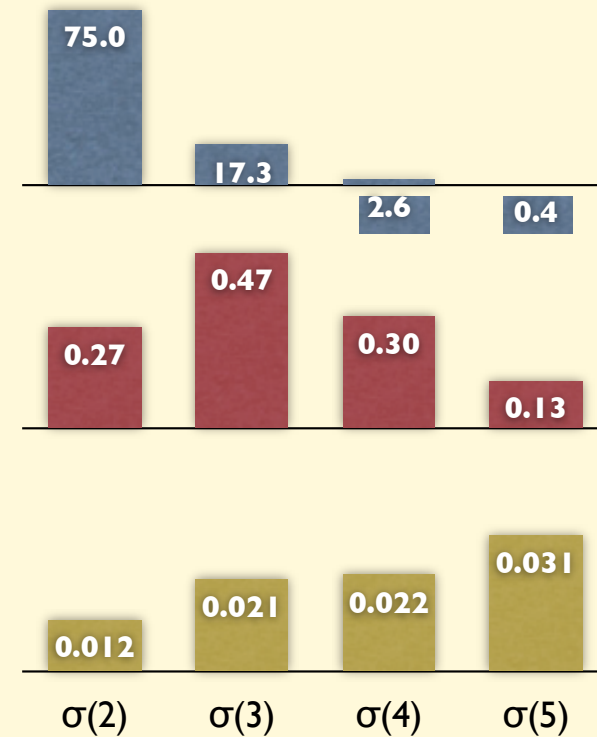
**High mass final states are dominated by multijet configurations**



23

# W+Multijet rates

| σ×B(W→eν)[pb] | N jet=1 | N jet=2 | N jet=3 | N jet=4 | N jet=5 | N jet=6 |
|:---:|:---:|:---:|:---:|:---:|:---:|:---:|
| LHC | 3400 | 1130 | 340 | 100 | 28 | 7 |
| Tevatron | 230 | 37 | 5.7 | 0.75 | 0.08 | 0.009 |

$E_T$(jets) > 20 GeV , $|\eta|$<2.5 , $\Delta R$>0.7
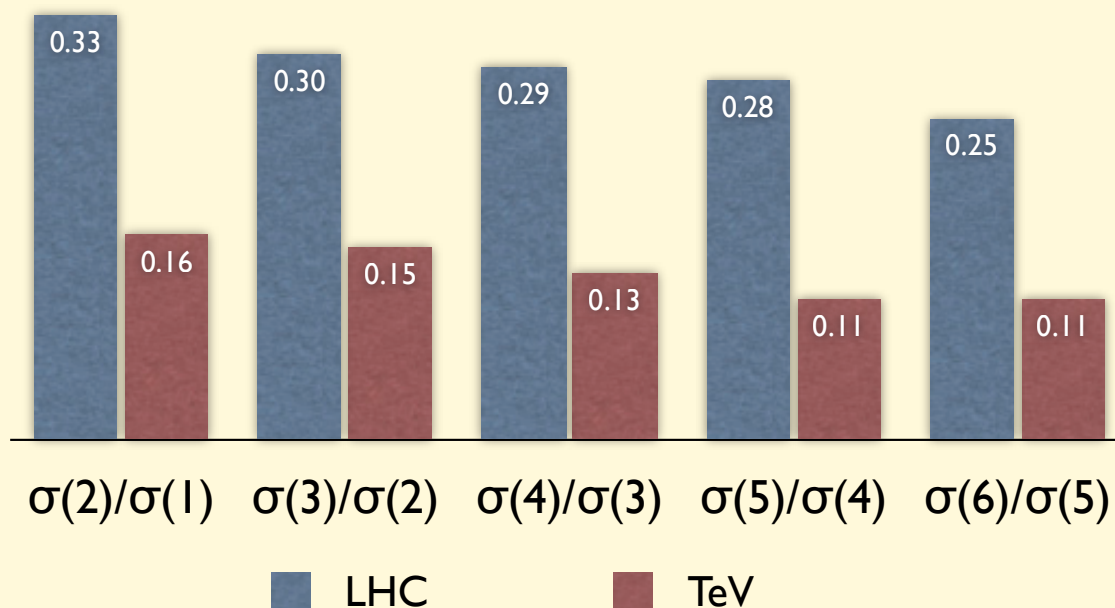


- Ratios almost constant over a large range of multiplicities
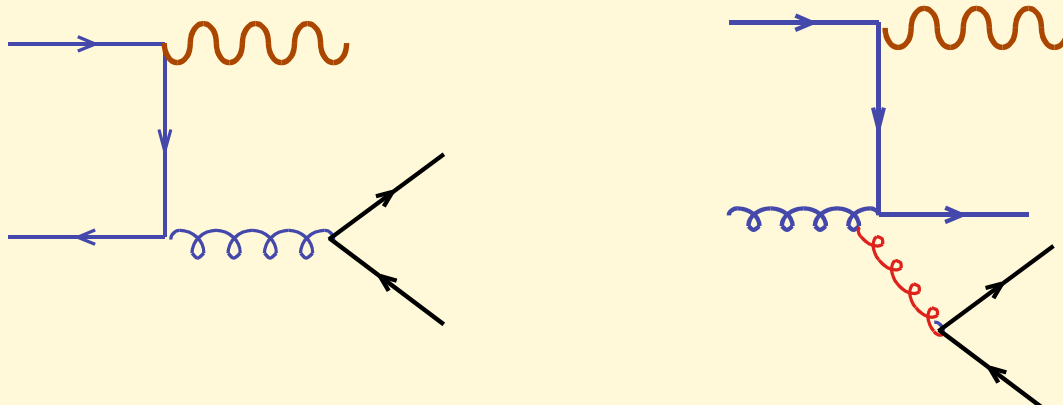
- $O(\alpha_s)$ at Tevatron, but much bigger at LHC

# Wbb+jets rates



σ([W→lν] bb + N jets)[pb] , LHC
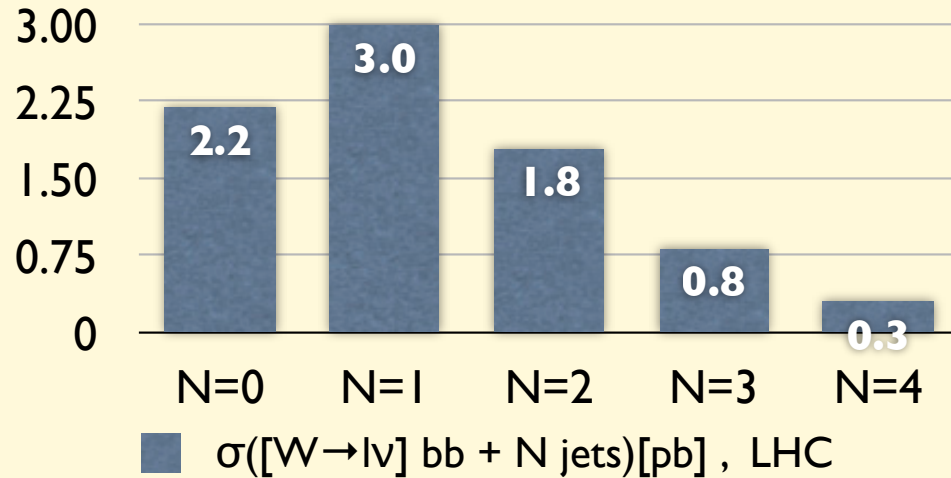
**Pattern of multiplicity distribution very different than in W+jets!**

**In pp collisions (contrary to the Tevatron, p-pbar) :**

$N_{jet}=0 \propto \alpha_s^2$ x Lum(q qbar)  ≈  $N_{jet}=1 \propto \alpha_s^3$ x Lum(q g)

**Beware of naive $\alpha_s$ power counting!!**

# Leptons

Experimentally, electrons, muons and taus are entirely different objects. Their identification requires different components of the detector, different techniques, and is subject to different backgrounds.
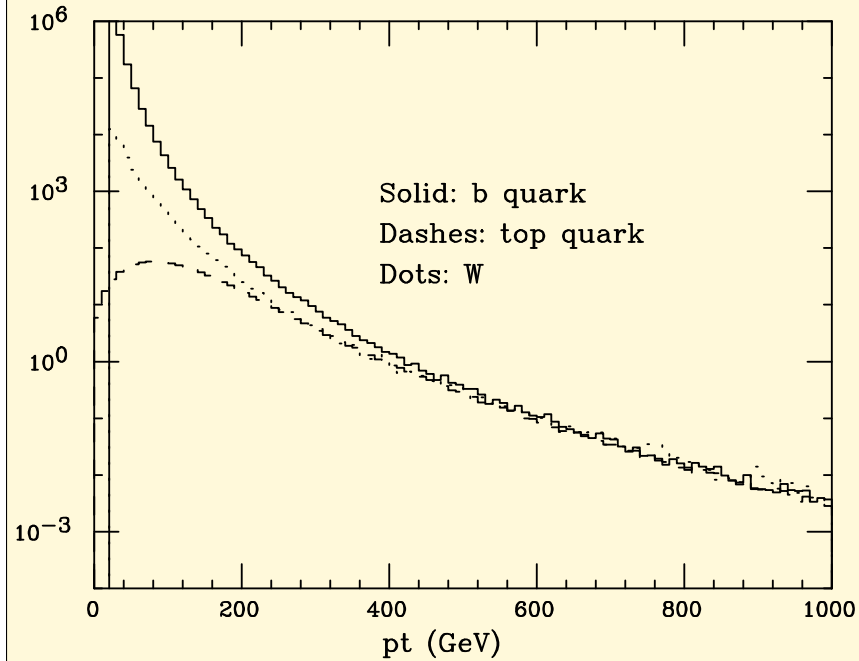
As seen from a theorists, all leptons are produced the same. Nevertheless there is a large variety of possible production mechanisms, each one of them leading to different overall properties of the final state. When considering leptons as a signal for new physics, it is important to have a clear picture of their irreducible SM sources

# Single lepton

**Sources of single high-pt leptons:**

- $W \rightarrow e/\mu + \nu$

- $Z \rightarrow \tau\tau \rightarrow e/\mu + X$

- $b \rightarrow e/\mu + X$

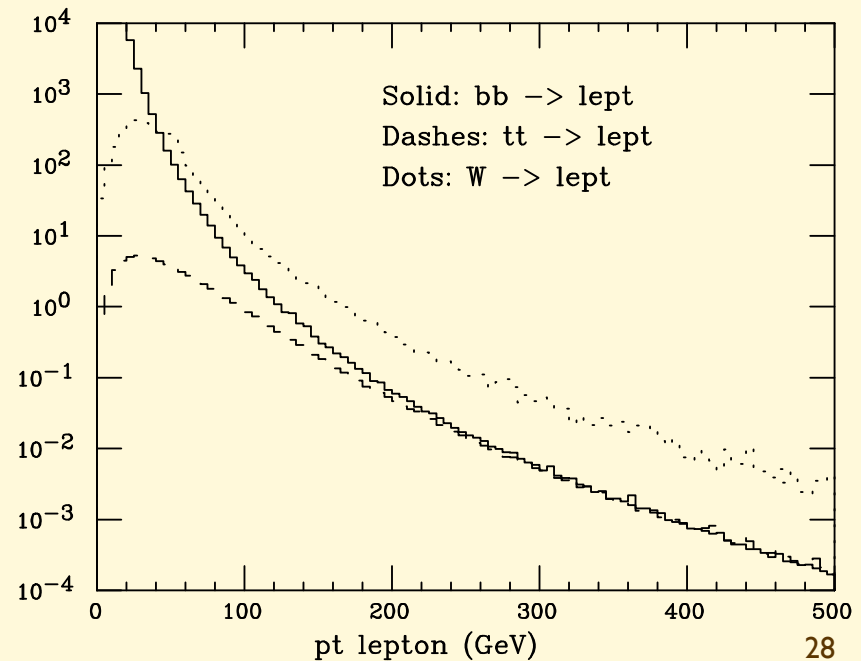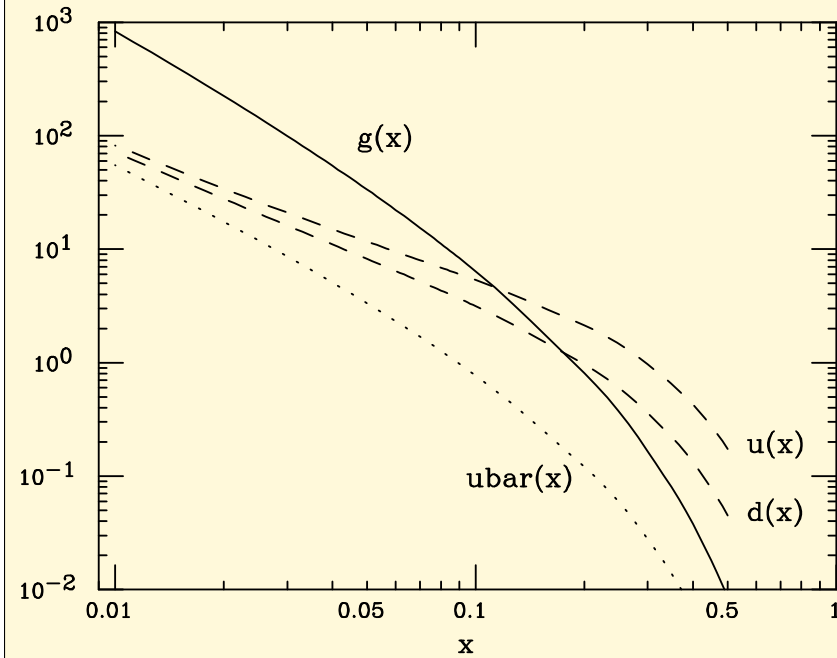- $t \rightarrow Wb \rightarrow e/\mu + \nu + b$

# Differential Rates

Solid: b quark
Dashes: top quark
Dots: W

$10^6$

$10^3$

$10^0$

$10^{-3}$

0    200    400    600    800    1000
pt (GeV)

- At large pt b and t production ~ equal !

- At large pt, W and heavy quark production ~ equal!

*W → lepton is a 2-body decay, b/t → lepton is 3-body: lepton takes a larger fraction of momentum in W decay => harder spectrum, larger rate at higher pt in W production

*The global features of the event accompanying the lepton will clearly be very different in each case. Which of the three processes will dominate in a given analisys, will therefore depend on the details
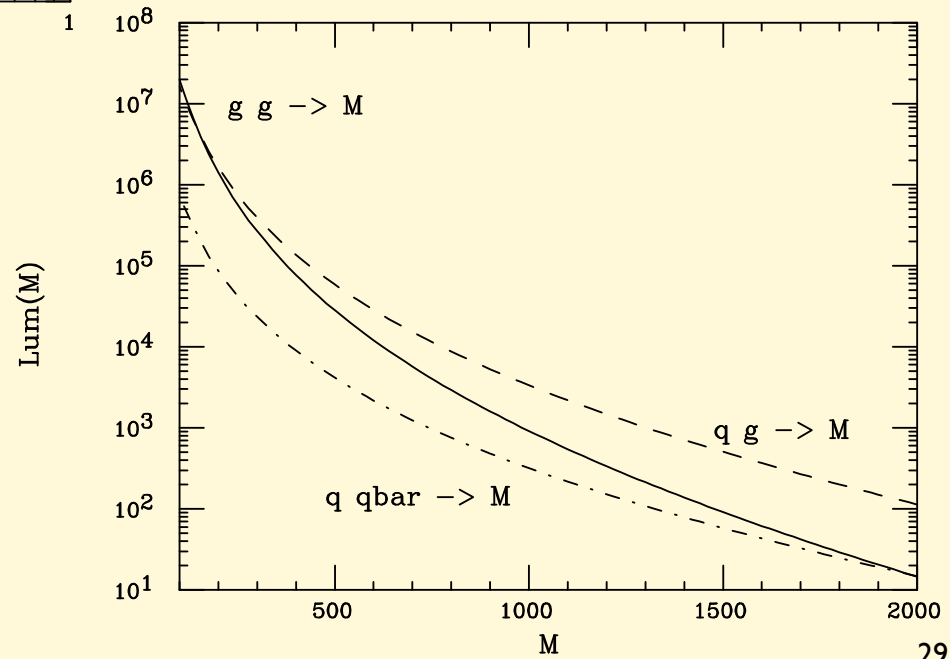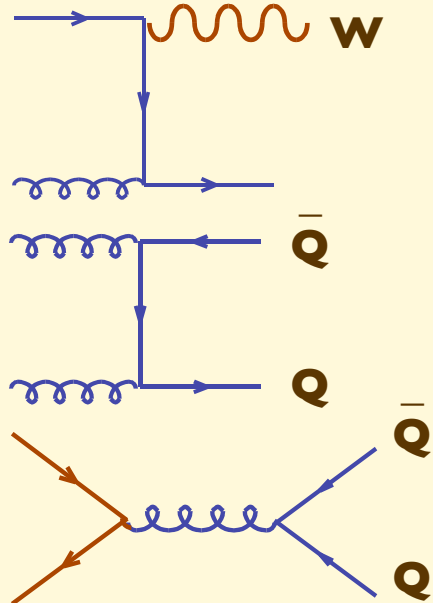
Solid: bb −> lept
Dashes: tt −> lept
Dots: W −> lept

$10^4$

$10^3$

$10^2$

$10^1$

$10^0$

$10^{-1}$

$10^{-2}$

$10^{-3}$

$10^{-4}$

$d\sigma/dpt$ (pb/5 GeV)

0    100    200    300    400    500
pt lepton (GeV)

28

**How come Q and W spectra are comparable at large Et?**

The LO processes for QQ production are weighted by the gg or qqbar luminsity, which drops at large mass much more rapidly than L(qg)

$$\frac{\bar{Q} \; Q}{W} = \frac{C_F \alpha_s}{1/2 \times \alpha_w} \times \left(\frac{N}{N^2 - 1}\right) \times \frac{1}{1/2} \times F(s \leftrightarrow u)$$

Quark colour charge

Initial state colour averages

~1/3 at 90°

Quark weak charge

V-A, only L-handed quarks

$$\approx \frac{\alpha_s}{\alpha_W} \sim 3$$

**Dileptons**

| WW | tt | Z |
|---|---|---|
| 75pb | 500pb | 50nb |
| 2l+MET, no jets | 2l+MET, jets, b's | 2l, m(ll)=mZ, no MET, no jets |

Dilepton production dominated by top pairs!

**Trileptons**

| WWW | ttW | ZW |
|---|---|---|
| 130fb | 500fb | 28pb |

ttW ~ $10^{-3}$ tt => trilepton contribution from tt, with 3rd lepton form b→l decay, important => require isolation!

**Quadrileptons**

| WWWW | tttt | ZWW |
|---|---|---|
| 0.6fb | 12fb | 100fb |

ZWWW=0.7fb

# Ratios

| W/Z | WW / WZ | WWW / WWZ | WWWW / WWWZ |
|:---:|:---:|:---:|:---:|
| 3 | 2.5 | 1.3 | 1 |

Ratio determined by couplings to quarks, u/d asymmetry of proton → Ratio determined by couplings among W/Z, SU(2) invariance

| WW/W | WWW / WW | WWWW / WWW | |
|:---:|:---:|:---:|:---:|
| .5E-3 | 2E-3 | 5e-3 | |
| ZW / W | ZWW / WW | ZWWW / WWW | $1W \sim 10^{-3}$ |
| .5E-3 | 4E-3 | 7e-3 | |

# Top production and bgs
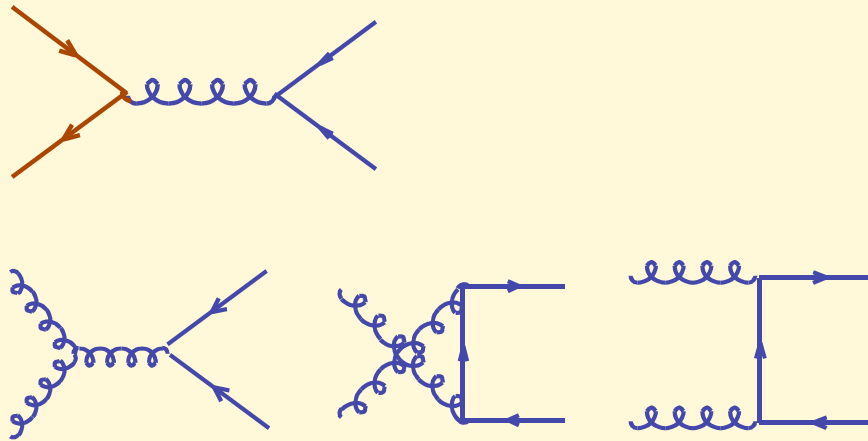


| | σ(tt) [pb] | σ(W+X) | σ(W+bbX) [ptb>20 GeV] | σ(W+bbjj X) [ptb,ptj >20 GeV] |
|---|---|---|---|---|
| Tevatron | 6 | 20 x 10³ | 3 | 0.16 |
| LHC | 800 | 160 x 10³ | 20 | 16 |
| Increase | x 100 | x 10 | x 10 | x 100 |

Missing $E_T > 20$ GeV

1 lepton $P_T > 20$ GeV

4 jets(R=0.4) $P_T > 40$ GeV

No b-tagging required



$N_{top} = 1279 \pm 81$

$\sigma(m_{top}) = 15.82 \pm 0.$

$N_W = 565 \pm 10$

$\sigma(m_W) = 7.57 \pm$
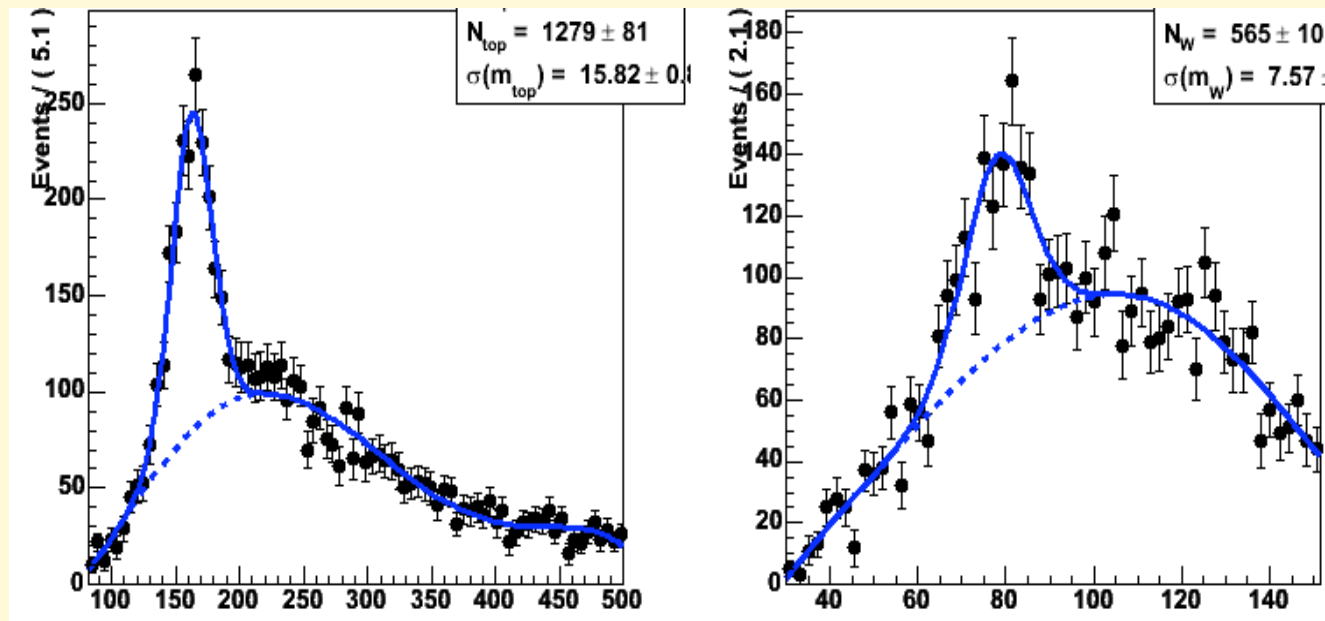
The signal is clearly visible over the background, even without b tagging

# tt cross-section
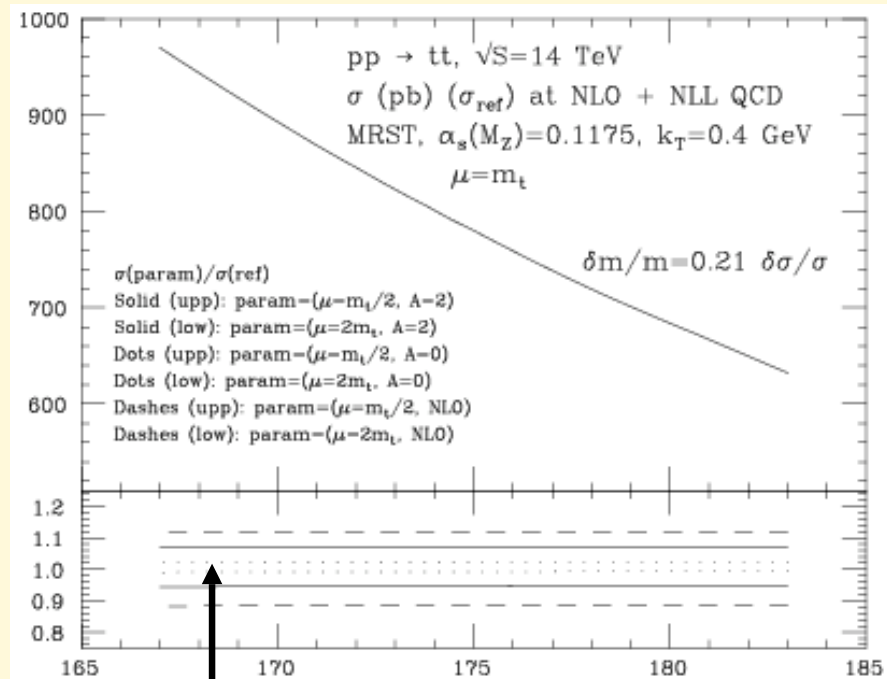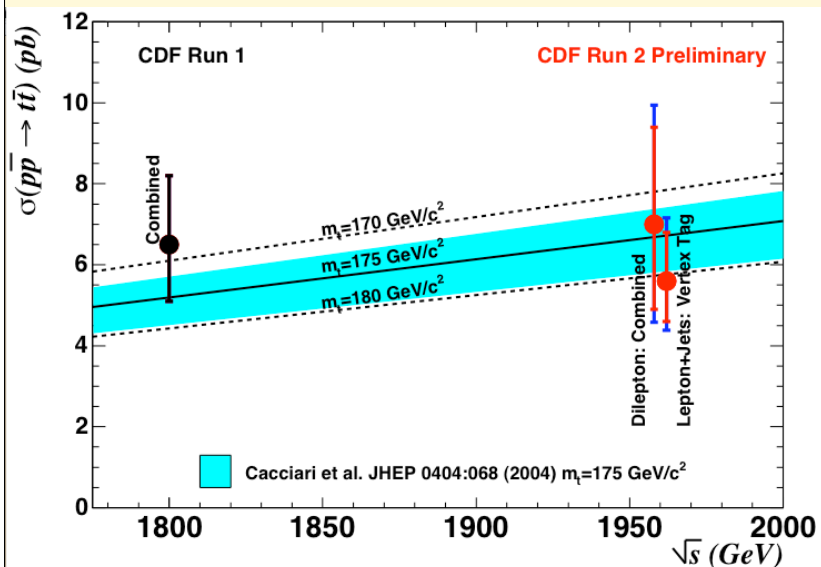


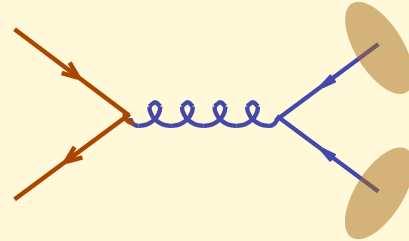$$\sigma_{tt}^{\text{FNAL}} = 6.5\text{pb} \, (1 \pm 5\%_{\text{scale}} \pm 7\%_{\text{PDF}})$$

$$\sigma_{tt}^{\text{LHC}} = 840\text{pb} \, (1 \pm 5\%_{\text{scale}} \pm 3\%_{\text{PDF}})$$

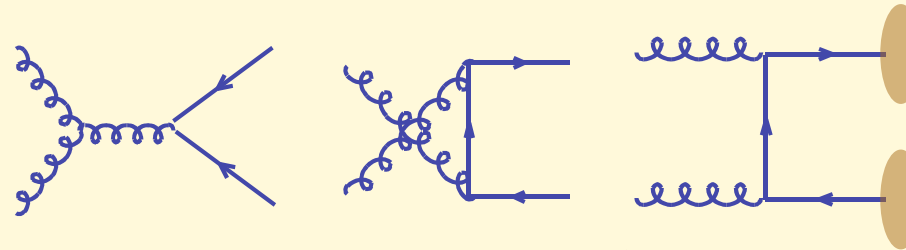Scale unc: $\pm 12\%_{\text{NLO}} => \pm 5\%_{\text{NLO+NLL}})$

$$\Delta\sigma = \pm 6\% => \Delta m = \pm 2 \text{ GeV}$$

# b jets

$O(\alpha_S^2)\ L_{q\ qbar}$

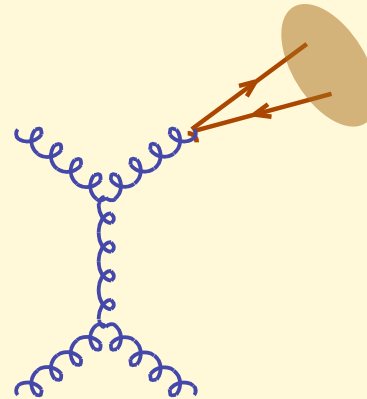$O(\alpha_S^2)\ L_{gg}$
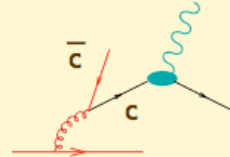
$O(\alpha_S^2)\ L_{gg} \times \alpha_S\ Log\ (Q/mb)$

Asymptotically in Q, the probability of finding a b quark inside a gluon jet is 1 !

* Single b-jet in the event.
* b momentum only a fraction of the jet energy => soft muons

36

From Lecture 1:

## Example: charm in the proton

$$\frac{dc(x,Q)}{dt} = \frac{\alpha_s}{2\pi} \int_x^1 \frac{dy}{y} g(y,Q) P_{qg}\left(\frac{x}{y}\right)$$

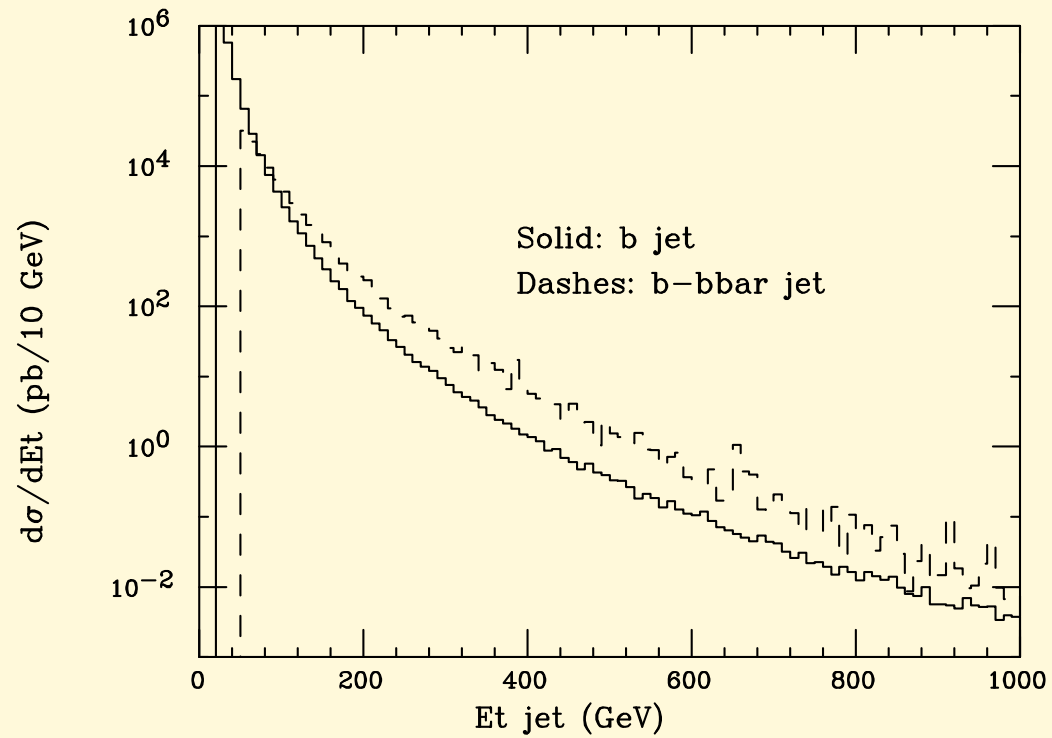Assuming a typical behaviour of the gluon density: $g(x,Q) \sim A/x$

and using $\quad P_{qg}(x) = \frac{1}{2}\left[x^2 + (1-x)^2\right]$ we get:

$$\frac{dc(x,Q)}{dt} = \frac{\alpha_s}{2\pi} \int_x^1 \frac{dy}{y} g(x/y,Q) P_{qg}(y) = \frac{\alpha_s}{2\pi} \int_x^1 dy \frac{A}{x} \frac{1}{2}[y^2 + (1-y)^2] = \frac{\alpha_s}{6\pi} \frac{A}{x}$$

and therefore:

$$c(x,Q) \sim \frac{\alpha_s}{6\pi} \log\left(\frac{Q^2}{m_c^2}\right) g(x,Q)$$

If $g(x) = \delta(1-x) \Rightarrow \int dx\ c(x) = \dfrac{\alpha_s}{6\pi} \log\left(\dfrac{Q^2}{m_c^2}\right)$

While the rate at high ET is dominated by b-bbar jets, triggers selecting high-pT b quarks (e.g. a trigger on the muon pT) will select b-jets.